Supporting Information for

Reductive Electrophotocatalysis: Merging Electricity and Light to Achieve Extreme Reduction Potentials

Hyunwoo Kim[†], Hyungjun Kim[‡], Tristan H. Lambert*[†], and Song Lin*[†]

[†]Department of Chemistry and Chemical Biology, Cornell University, Ithaca, New York 14853, United States

[‡]Department of Chemistry, Incheon National University, 119 Academy-ro, Yeonsu-gu, Incheon 22012, Republic of Korea

Correspondence to: tristan.lambert@cornell.edu, songlin@cornell.edu

Table of Contents

Section 1. General Information

All reactions were performed in oven-dried two-neck glass tubes unless otherwise noted. The tubes were fitted with a rubber septum and a threaded Teflon cap with airtight, electrical feed-throughs. The reactions were conducted under a nitrogen atmosphere. Flash chromatography was performed using silica gel 60 (230-400 mesh) from SiliCycle. Commercial reagents were purchased from Sigma Aldrich, Alfa Aesar, Acros, TCI, AK Scientific, and Oakwood and used as received with the following exceptions: toluene, dichloromethane, tetrahydrofuran, diethyl ether, and acetonitrile were dried by passing through columns of activated alumina; dimethylformamide was dried by passing through columns of activated molecular sieves. Triethylamine were distilled from CaH_2 at 760 torr. 4-Chloro-*N*,*N*-dimethylaniline,[1] methyl (4-bromobenzoyl)-*L*-leucinate[2], tert-butyl 3-[2-(4-bromobenzamido)-3-methoxy-3-oxopropyl]-1*H*-indole-1-carboxylate[3] and methyl 2-[1-(4-chlorobenzoyl)-5-methoxy-2-methyl-1*H*-indol-3-yl]acetate[4] were synthesized by the previously reported procedures (starting materials for **14**, **17**, **18** and **19**, respectively). Proton nuclear magnetic resonance (^{1}H NMR) spectra and carbon nuclear magnetic resonance (^{13}C NMR) spectra were recorded on Mercury-300 (300 MHz), Inova-400 (400 MHz) and Inova-500 (500 MHz) spectrometers. Chemical shifts for protons are reported in parts per million downfield from tetramethylsilane and are referenced to residual protium in the NMR solvent ($CHCl_3$ = δ 7.26). Chemical shifts for carbon are reported in parts per million downfield from tetramethylsilane and are referenced to the carbon resonances of the solvent ($CDCl_3$ = δ 77.0). Data are represented as follows: chemical shift, multiplicity (br. s = broad, s = singlet, d = doublet, t = triplet, q = quartet, m = multiplet), coupling constants in Hertz (Hz), integration. Infrared (IR) spectra of the newly synthesized compounds were obtained using a Bruker Hyperion Tensor 27 FTIR spectrometer. Cyclic voltammetry data were measured with a BASi Epsilon potentiostat. The mass spectral (MS) data were obtained on a Thermo Fisher Scientific Exactive series DART Mass Spectrometer. All UV Vis spectra were measured on a Agilent Cary-60 spectrophotometer. Enantiomeric excesses were determined by chiral HPLC of isolated material using a SHIMADZU system with CHIRALPAK® columns.

Electrolysis experiments were performed using a BASi EC Epsilon potentiostat/galvanostat or a DC power supply. Carbon Felt was purchased from Fuel Cell Store. The carbon was cut into 1 x 0.5 x 0.6 cm^3 pieces before use, and was connected to electrical feed-through on the Teflon cap of the electrochemical cell via a piece of graphite (2B pencil lead, 2 mm in diameter). The zinc plate was cut into 1 x 0.5 x 0.02 cm^3 and was connected to electrical feed-through on the Teflon cap of the electrochemical cell via a piece of graphite (2B pencil lead, 2 mm in diameter). $Ag/AgNO_3$ reference electrodes were obtained from CH Instruments and stored in an acetonitrile solution with 0.01 M $AgNO_3$ and 0.1 M $TBAClO_4$ before use. Potential was calibrated to that of saturated calomel electrode (SCE). Blue LEDs (Westinghouse Lighting 3315100, 15 W) used in this study were purchased from amazon.com.

Abbreviations: Boc—*tert*-butyl carbamate, ^{n}Bu—*n*-butyl, ^{t}Bu—*tert*-butyl, DCM—dichloromethane, DMSO—dimethyl sulfoxide, MeCN—acetonitrile, MeOH—methanol, NEt_3—triethylamine, ^{i}Pr—isopropyl, TBA—tetrabutylammonium.

Section 2. General Procedure for Electrophotocatalytic Reduction of Aryl Halides

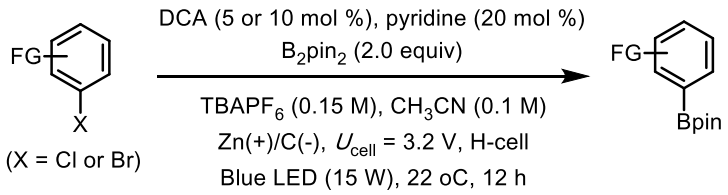

Method A: An oven-dried, 10 mL H-type divided cell with glass frit was equipped with a stir bar respectively, aryl halides (0.4 mmol), 9,10-dicyanoanthracene (0.02 mmol, 4.6 mg or 0.04 mmol, 9.1 mg), B_2pin_2 (0.8 mmol, 203.2 mg) and $^nBu_4PF_6$ (0.6 mmol, 232.5 mg) were added into cathode chamber while the anodic chamber was added with $^nBu_4PF_6$ (0.6 mmol, 232.5 mg). The divided cell was equipped with carbon felt cathode and Zn plate anode. A balloon filled nitrogen (1 atm.) was connected to the divided cell and purged three times. Then 4.0 mL of MeCN was added to the anodic chamber and cathodic chamber respectively. Subsequently, pyridine (0.08 mmol, 6.4 μL) was added to cathodic chamber. Then electrolysis system was stirred at a constant cell potential of 3.2 V at 22 ^oC for 12 h, under irradiation of blue LEDs (15 W x 2). An electric fan was used to maintain the reaction temperature. When the reaction was finished, the reaction mixture of both chamber was washed and collected with dichloromethane (10.0 mL x 3). The pure product was obtained by flash column chromatography on silica gel (hexane: ethyl acetate).

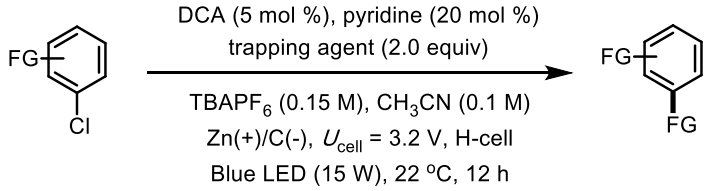

Method B: An oven-dried, 10 mL H-type divided cell with glass frit was equipped with a stir bar respectively, aryl halides (0.4 mmol), 9,10-dicyanoanthracene (0.02 mmol, 4.6 mg or 0.04 mmol, 9.1 mg), and $^nBu_4PF_6$ (0.6 mmol, 232.5 mg) were added into cathode chamber while the anodic chamber was added with $^nBu_4PF_6$ (0.6 mmol, 232.5 mg). The divided cell was equipped with carbon felt cathode and Zn plate anode. A balloon filled nitrogen (1 atm.) was connected to the divided cell and purged three times. Then 4.0 mL of MeCN was added to the anodic chamber and cathodic chamber respectively. Subsequently, Sn_2Me_6 (0.08 mmol, 6.4 μL) was added to cathodic chamber. Then electrolysis system was stirred at a constant cell potential of 3.2 V at 22 ^oC for 12 h, under irradiation of blue LEDs (15 W x 2). An electric fan was used to maintain the reaction temperature. When the reaction was finished, the reaction mixture of both chamber was washed and collected with dichloromethane (10.0 mL x 3). A mixture of the product and a trace of inseparable residue was obtained by flash column chromatography on silica gel (hexane: ethyl acetate).

Method C: An oven-dried, 10 mL H-type divided cell with glass frit was equipped with a stir bar respectively, aryl halides (0.4 mmol), 9,10-dicyanoanthracene (0.02 mmol, 4.6 mg or 0.04 mmol, 9.1 mg) and $^{n}Bu_4PF_6$ (0.6 mmol, 232.5 mg) were added into cathode chamber while the anodic chamber was added with $^{n}Bu_4PF_6$ (0.6 mmol, 232.5 mg). The divided cell was equipped with carbon felt cathode and Zn plate anode. A balloon filled nitrogen (1 atm.) was connected to the divided cell and purged three times. Then 4.0 mL of MeCN was added to the anodic chamber and cathodic chamber respectively. Subsequently, (hetero)arene (0.80 mmol, 20 equiv.) was added to cathodic chamber. Then electrolysis system was stirred at a constant cell potential of 3.2 V at 22 ^{o}C for 12 h, under irradiation of blue LEDs (15 W x 2). An electric fan was used to maintain the reaction temperature. When the reaction was finished, the reaction mixture of both chamber was washed and collected with dichloromethane (10.0 mL x 3). The pure product was obtained by flash column chromatography on silica gel (hexane: ethyl acetate).

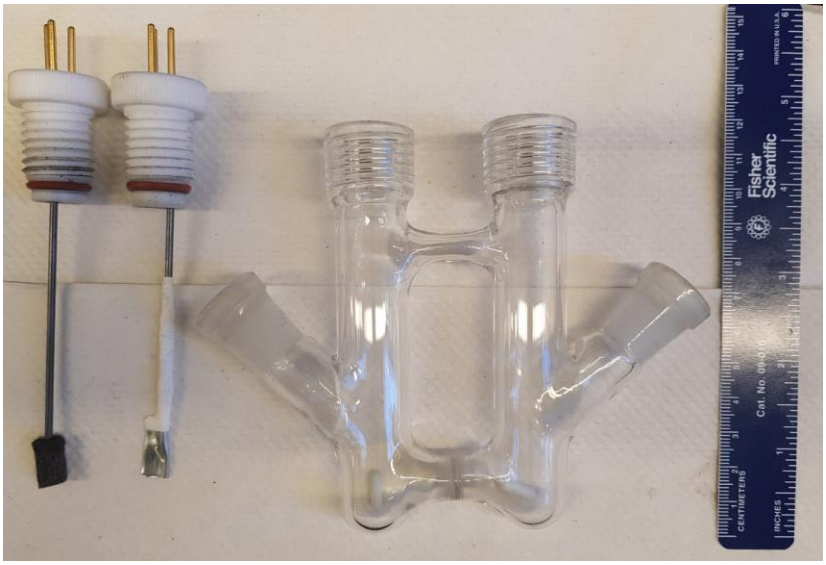

Figure S1. Preparation of Electrodes and H-type Divided Cell

Figure S2. Setup for Reductive Electrophotocatalysis: Before Light On (Left), After Light On (Right)

Section 3. Quantum Chemical Simulations

Frontier molecular orbitals (FMOs) of DCA

It is highly important to understand photophysical behavior of electrophoto-catalyst, 9,10-dicyanoanthracene (DCA). Neutral DCA molecules accept one electron from external source to get reduced, and are excited by irradiation of blue light. To get deeper chemical insights into these processes, we performed quantum chemical simulations to visualize the shape of frontier molecular orbitals (FMOs), to obtain one-electron FMOs' energies, and to reveal the transition character during absorption. Geometry optimizations for neutral DCA and negatively charged DCA were carried out with ωB97X-D and basis sets of 6-31G* in gas phase. Spatial distribution of FMOs were described at the same level of theory used in the optimizations. The acetonitrile solvent medium environment was modeled by SMD approach for FMOs visualization and orbital energy estimation. The spatial distribution of FMOs was visualized with IQMol. Electron transition character of absorption was investigated with time-dependent DFT (TDDFT) approach. TDDFT single-point energy calculations employing the same functional and the same basis sets were performed on the optimized DCA anion geometry to describe the electronic structure of excited DCA anion. All quantum chemical simulations were conducted with Q-Chem 5.0.

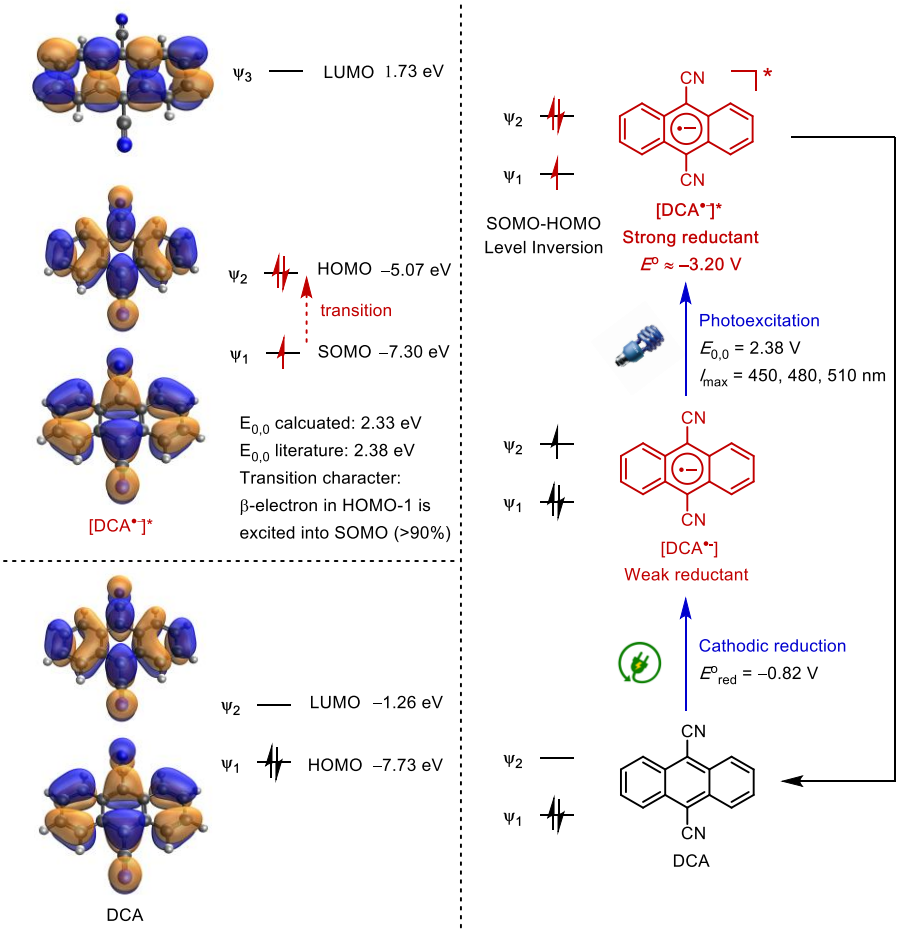

Figure S3. DFT Calculations on the FMOs of DCA and DCA anion.

Reduction potential of aryl-halides

We performed quantum chemical simulations to predict electrochemical properties of selected aryl-halides that the reduction potential are not reported in the precedent literature (**S5** to **S11**, **Scheme S1**). Reduction potential (E) could be estimated from the Gibbs free energy change during the reduction:

$$E(\text{V vs. SCE}) = -\frac{\Delta G}{nF} - E(\text{SCE})$$

where ΔG is the Gibbs free energy difference between neutral and anionic aryl-halide species, n is the number of electrons involved (n=1 in this study), and F is Faraday constant of 23.06 kcal/mol. Experimental reduction potentials were reported with respect to the reference electrode, standard calomel electrode (SCE) in this study. All calculated reduction potential was referenced to the absolute reduction potential of SCE in acetonitrile—4.641 V.

Geometries of neutral and anionic aryl-halides were optimized with B3LYP functional. Except bromine atom which was described by LANL2DZ effective core potentials (ECPs) and corresponding basis sets, all other light atoms were illustrated with 6-31G*. Frequency calculations were performed to estimate thermodynamic contributions (enthalpy and entropy terms—H and S, respectively, **Table S1**) at the same level of theory used in the geometry optimizations. Electronic energy was refined with the larger basis sets, 6-311++G** for the light atoms, and uncontracted LANL2DZ basis sets for the Br atom. During all quantum chemical simulations associated to reduction potential estimation, the acetonitrile solvent medium environment was modeled by SMD approach. All quantum chemical simulations were conducted with Q-Chem 5.0. Free energy value for a substrate in which the C–Cl bond breaking spontaneously occurs upon single-electron reduction (**S12**) was also calculated for whole reaction step including C–Cl bond scission.

Reduction potentials estimated from the quantum chemical simulations were underestimated compared to the reported ones (**S1** to **S4**, **Scheme S1**). Notably, the close examinations revealed that the deviation is systematic downshift. The raw calculation results could be improved by simple correction based on linear relationship between the theoretical estimations and experimentally measured ones. Linear regression between calculations and experiments yielded $E(\text{Expt.}) = 1.0053 \times E(\text{Calc.}) + 0.3205$ with R^2 value of 0.9835. We reported both raw and corrected reduction potential via linear regression.

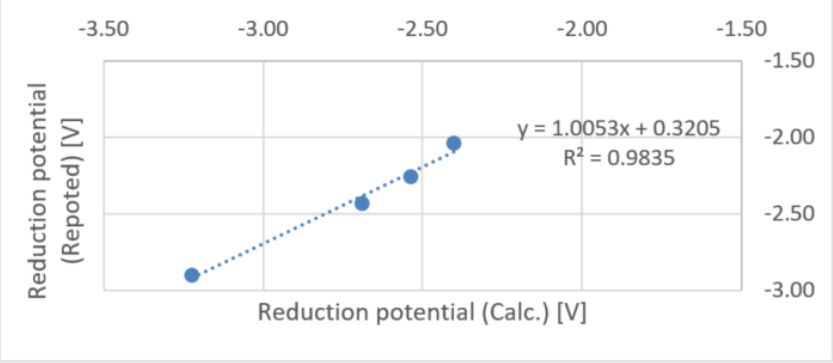

Figure S4. Correction of reduction potential by linear regression between calculated and reported reduction potentials (**S1** to **S4** in **Scheme S1**).

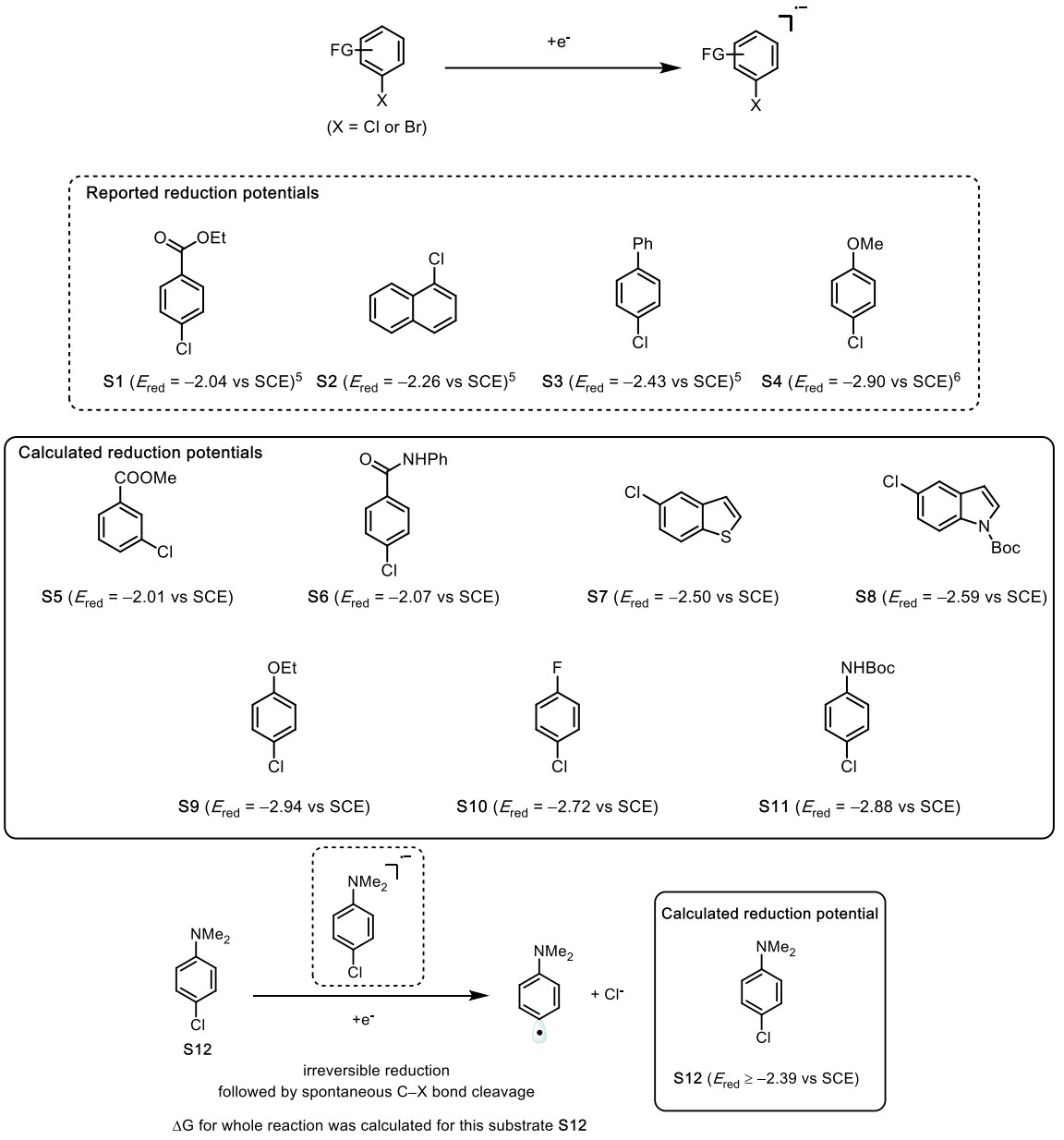

Scheme S1. Calculated reduction potentials of aryl halides. (E_{red} of aryl halides are corrected according to the linear calibration curve shown on **Figure S4**)

	Neutral Aryl Halides				Aryl Halides Anions (Reduced Form)				
#	X	*E (Electronic E)*	*H (Enthalpy)*	*S (Entropy)*	**G (Free E)**	*E (Electronic E)*	*H (Enthalpy)*	*S (Entropy)*	**G (Free E)**
S1	Cl	-959.2247619	109.747	107.411	-959.1009	-959.3027822	107.587	109.033	-959.18314
S2	Cl	-845.6237727	92.382	89.042	-845.51886	-845.6955109	89.521	91.167	-845.59617
S3	Cl	-923.0619999	115.19	100.466	-922.92617	-923.1276852	112.578	104.4	-922.99788
S4	Cl	-806.5019079	83.469	89.011	-806.41118	-806.5450748	79.515	94.441	-806.46323
S5	Cl	-919.8930313	91.087	100.217	-919.79549	-919.9741047	88.739	101.143	-919.88075
S6	Cl	-1091.82019	134.178	118.422	-1091.6626	-1091.897824	131.862	122.05	-1091.7457
S7	Cl	-1166.392889	71.152	88.174	-1166.3214	-1166.452152	68.049	95.366	-1166.389
S8	Cl	-1169.481587	165.608	127.883	-1169.2784	-1169.539308	162.477	130.875	-1169.3426
S9	Cl	-845.833197	102.158	96.378	-845.71619	-845.8758959	98.264	101.529	-845.76754
S10	Cl	-791.2115334	56.625	80.673	-791.15963	-791.2626279	52.737	85.378	-791.21915
S11	Cl	-1093.262194	157.682	126.927	-1093.0712	-1093.306315	153.484	132.343	-1093.1246
S12	Cl	-378.8889269	109.885	101.272	-378.76193	-365.6360618	107.191	90.029	-378.83333

#	Raw Red Potential (vs. SCE)	Corrected Red Potential (vs. SCE)	Reported Red Potential (vs. SCE
S1	-2.40	-2.10	-2.04
S2	-2.54	-2.23	-2.26
S3	-2.69	-2.38	-2.43
S4	-3.22	-2.92	-2.9
S5	-2.32	-2.01	
S6	-2.38	-2.07	
S7	-2.80	-2.50	
S8	-2.90	-2.59	
S9	-3.24	-2.94	
S10	-3.02	-2.72	
S11	-3.19	-2.88	
S12	-2.70	-2.39	

Table S1. Frequency calculation data

Section 4. Procedure of Miyaura Borylation

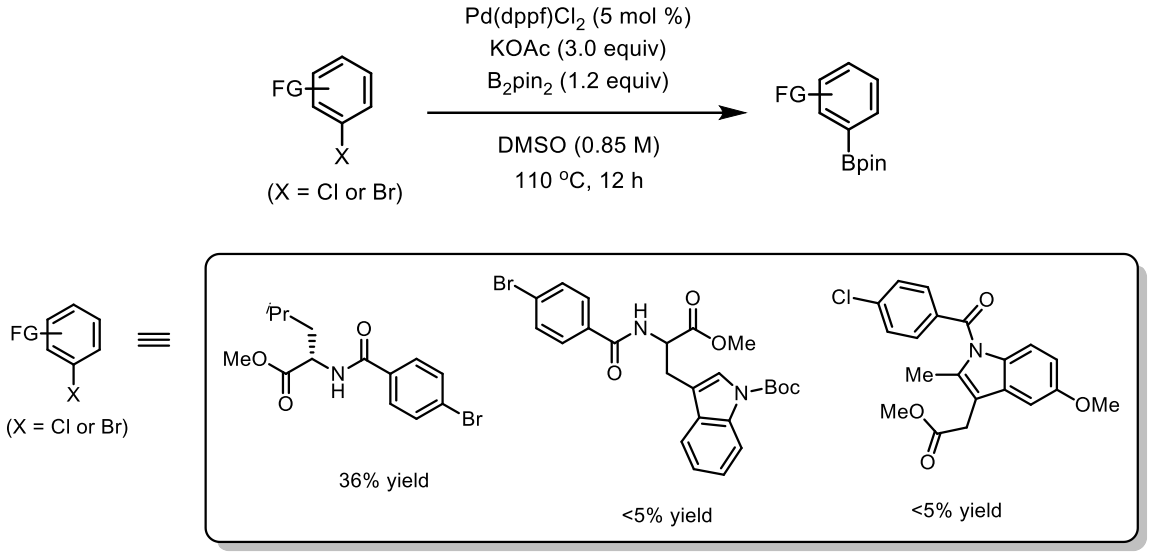

The aryl halide (0.25 mmol, 1.0 equiv) was weighed in a sealed tube, followed by bis(pinacolato)diboron (64 mg, 1.2 equiv), potassium acetate (74 mg, 3.0 equiv), $Pd(dppf)Cl_2$ (5 mol%). The tube was evacuated and backfilled three times with N_2 and C Then, the reaction mixture was heated at 110 °C for 12 h. The crude mixture was cooled to room temperature, filtered through a short pad of Celite, washed with EtOAc (50 mL) and the solvents were removed under reduced pressure. The crude product was then purified by flash column chromatography.

Section 5. Procedures of Mechanistic Studies

1. Controlled Potential Electrolysis

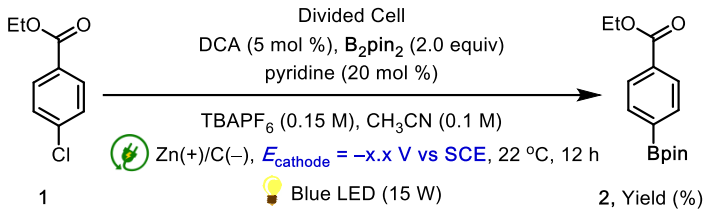

An identical procedure was followed as described in **Method A** with the exception that the reaction was carried out under controlled cathodic potential (indicated in the graph below) with a non-aqueous reference electrode on the cathode chamber. When the reaction was finished, the reaction mixture of both chamber was washed and collected with dichloromethane (10.0 mL x 3). The yield of the product was determined by ^{1}H NMR by using CH_2Br_2 as an internal standard.

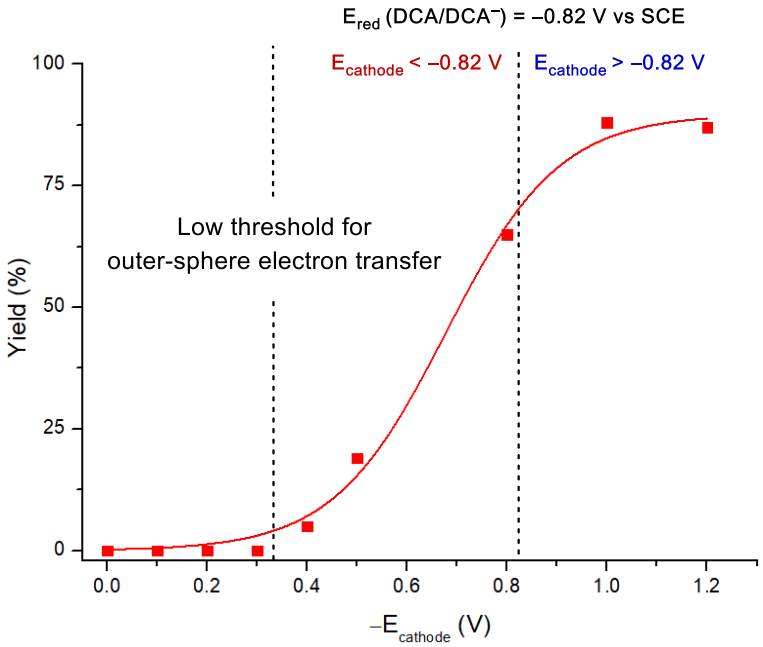

Figure S5. Controlled Potential Electrolysis with Respect to the Cathodic Potential

2. Faradaic Efficiency

1 was subjected to **Method A** with electrolysis (using a potentiostat) being terminated after 2F/mol of current had passed through the reaction medium. Faradaic efficiency was calculated to be **35%**.

3. Light/dark experiment

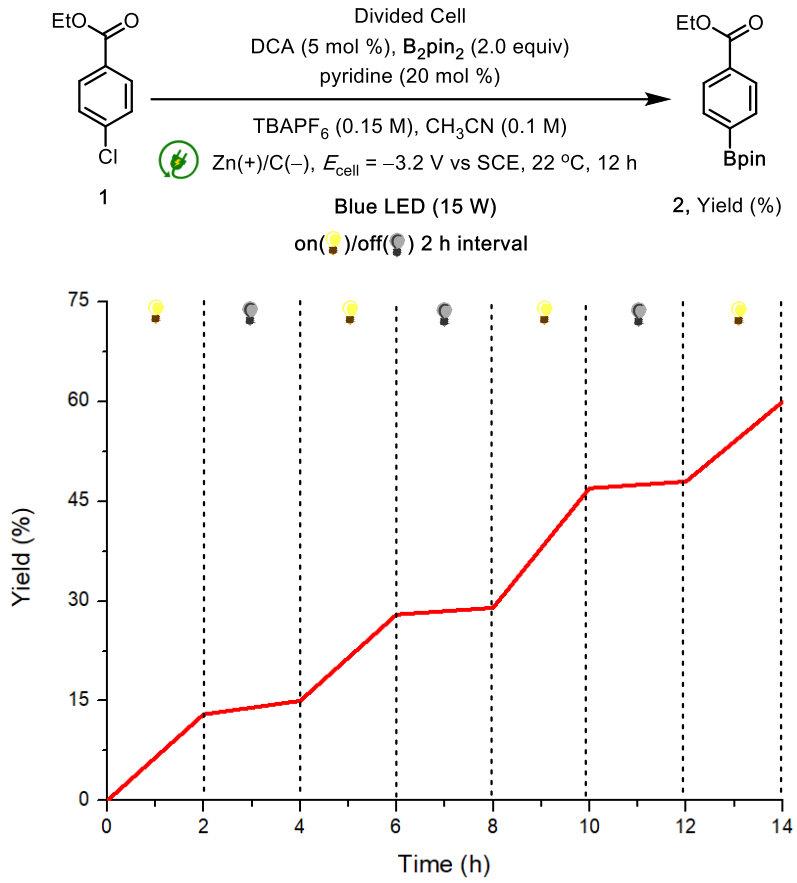

Figure S6. Light/Dark Experiment

1 was subjected to **Method A**. The reaction was alternatively irradiated with a 15 W blue LEDs and kept in the dark in 2 h intervals. Each dataset was obtained by multiple reaction setups. The reactions were terminated at the start and after each interval, passed through a silica plug, and diluted with $CDCl_3$. Yields of the **2** was determined by ^1H NMR and based on CH_2Br_2 as an internal standard.

4. Cyclic voltammetry data

Cyclic voltammogram of 9,10-dicyanoanthracene (DCA) at a glassy carbon electrode in 0.1 M $TBAPF_6$ in MeCN. Scan rate = 100 mV/s. The reversible oxidation/reduction traces for DCA is showcased below.

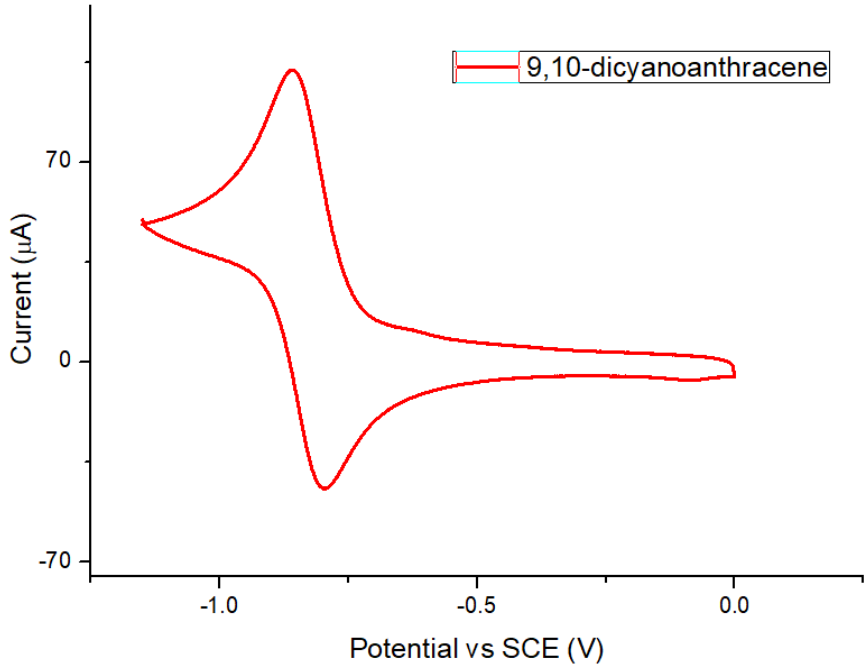

Figure S7. Cyclic Voltammogram of DCA

5. Control experiments without electricity

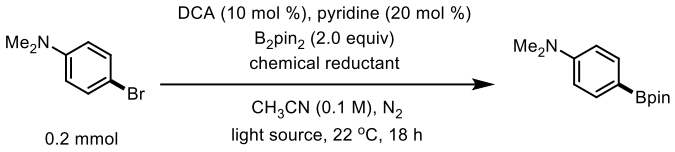

entry	chemical reductant	light source	yield (%)	recovered S.M. (%)	
1	NEt_3 (1.0 equiv)	CFLs (23 W)	n.r.	98%	E^o_{red} of chemical reductants ~ +0.9 V vs SCE
2	NEt_3 (1.0 equiv)	Blue LEDs (15 W)	n.r.	98%	
3	$NiPr_2Et$ (1.0 equiv)	CFLs (23 W)	n.r.	92%	
4	$NiPr_2Et$ (1.0 equiv)	Blue LEDs (15 W)	n.r.	98%	
5	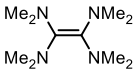 (1.0 equiv)	CFLs (23 W)	3%	97%	E^o_{red} of TDAE = –0.78 V vs SCE
6	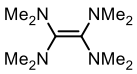 (1.0 equiv)	Blue LEDs (15 W)	4%	96%	

4-Bromo-*N*,*N*-dimethylaniline (40.0 mg, 0.2 mmol, 1.0 equiv.) and 9,10-dicyanoanthracene (4.6 mg, 0.02 mmol, 0.1 equiv.) and bis(pinacolato)diboron (64 mg, 1.2 equiv), were weighed in a vial (5 mL). The vial evacuated and backfilled three times with N_2. Then degassed MeCN (1.0 mL) was added followed by the addition of chemical reductants (1.0–2.0 equiv). The reaction was irradiated with an external light source at 22°C for 18 hours. The solvents were removed from the crude mixture under reduced pressure. The yield of the product and recovered starting material (S.M.) was determined by ^1H NMR by using CH_2Br_2 as an internal standard.

6. The Possibility for Donor-Acceptor Complex Formation

In order to investigate whether some electron-donor-acceptor (EDA) complex has been produced when chloroarenes were added, more UV-vis study was carried out. It is known that UV-vis spectrum of DCA anion has an absorption band that is responsible for fluorescence emission (450, 480 and 510, Figure **S8**).[5] Further studies revealed that the addition of 4-chloroanisole (**3**) did not change the absorption spectra of DCA anion (see Figure S4). Therefore, the formation of an EDA complex can be excluded.

(1) Experimental procedure for UV-Vis of DCA^{-}: An oven-dried, 10 mL H-type divided cell with glass frit was equipped with a stir bar respectively, 9,10-dicyanoanthracene (4 μmol, 0.9 mg) and $^{n}Bu_4PF_6$ (0.6 mmol, 232.5 mg) were added into cathode chamber while the anodic chamber was added with $^{n}Bu_4PF_6$ (0.6 mmol, 232.5 mg). The divided cell was equipped with carbon felt cathode and Zn plate anode. A balloon filled nitrogen (1 atm.) was connected to the divided cell and purged three times. Then 4.0 mL of MeCN was added to the anodic chamber and cathodic chamber respectively. Then electrolysis system was stirred at a constant cell potential of 3.2 V at 22 °C for 1 h. The resulting solution in the cathodic chamber was transferred to the cuvette with 1 cm optical path.

(2) Experimental procedure for UV-Vis of compound **3**: A 20 mL vial was charged with 4-chloroanisole **3** (0.6 mg, 4.0 μmol) and 4 mL MeCN in a glove box. The resulting solution was transferred to the cuvette with 1 cm optical path utilizing an oven-dried glass Pasteur pipette.

(3) Experimental procedure for UV-Vis of compound **3** and DCA^{-}: 4-Chloroanisole **3** (0.6 mg, 4.0 μmol) was added to the following solution obtained by procedure (1). The solution was transferred to the cuvette with 1 cm optical path utilizing an oven-dried glass Pasteur pipette.

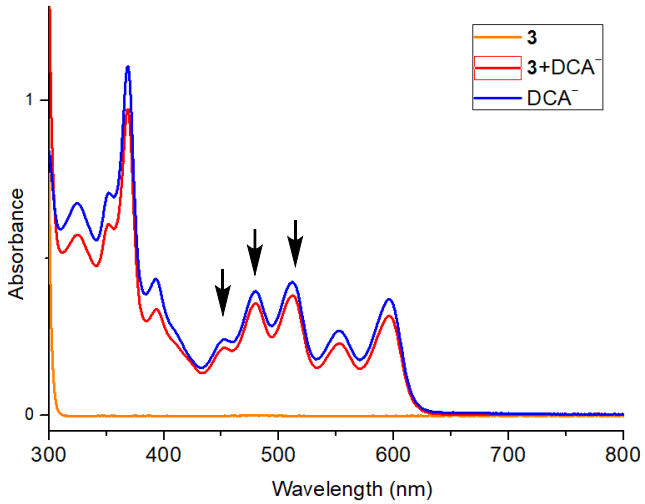

Figure S8. Orange Line: UV-vis spectrum of 1 mM 4-chloroanisole **3** in MeCN. Blue line: UV-vis spectrum of 1 mM DCA^{-} in MeCN. Red line: UV-vis spectrum of 1 mM 4-chloroanisole **3** and 1 mM DCA^{-} in MeCN.

Section 6. Spectral Data for Products

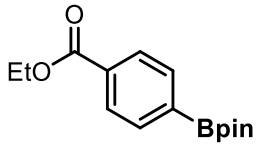

Ethyl 4-(4,4,5,5-tetramethyl-1,3,2-dioxaborolan-2-yl)benzoate (2). Followed Method A and purified using silica gel chromatography to give **2** as a colorless oil, 88% yield (97.2 mg) from chloroarene and 90% (99.4 mg) from bromoarene; ^{1}H NMR (500 MHz, $CDCl_3$) δ 8.04 (d, *J* = 8.3 Hz, 2H), 7.88 (d, *J* = 8.3 Hz, 2H), 4.40 (q, *J* = 7.1 Hz, 2H), 1.41 (t, *J* = 7.1 Hz, 3H), 1.37 (s, 12H); ^{13}C NMR (126 MHz, $CDCl_3$) δ 166.7, 134.6, 132.7, 128.6, 84.2, 61.0, 24.9, 14.3; ^{11}B NMR (160 MHz, $CDCl_3$) δ 30.62 ; MS (DART) exact mass calculated for [$C_{15}H_{22}BO_4^+$]: 277.1606, found 277.1621.

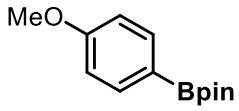

2-(4-Methoxyphenyl)-4,4,5,5-tetramethyl-1,3,2-dioxaborolane (4). Followed Method A and purified using silica gel chromatography to give **4** as a white solid, 53% yield (49.6 mg) from chloroarene and 68% (63.6 mg) from bromoarene. ^{1}H NMR (500 MHz, $CDCl_3$) δ 7.79 (d, *J* = 8.6 Hz, 2H), 6.92 (d, *J* = 8.6 Hz, 2H), 3.85 (s, 3H), 1.36 (s, 12H); ^{13}C NMR (126 MHz, $CDCl_3$) δ 162.2, 136.5, 113.3, 83.6, 55.1, 24.9; ^{11}B NMR (160 MHz, $CDCl_3$) δ 30.94; MS (DART) exact mass calculated for [$C_{13}H_{20}BO_3^+$]: 235.1500, found 235.1510.

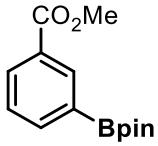

Methyl 3-(4,4,5,5-tetramethyl-1,3,2-dioxaborolan-2-yl)benzoate (5). Followed Method A and purified using silica gel chromatography to give **5** as a white solid, 65% yield (68.1 mg) from chloroarene and 60% (62.9 mg) from bromoarene; ^{1}H NMR (500 MHz, $CDCl_3$) δ 8.44 (s, 1H), 8.10 (d, *J* = 7.8 Hz, 1H), 7.96 (d, *J* = 7.4 Hz, 1H), 7.42 (t, *J* = 7.6 Hz, 1H), 3.89 (s, 3H), 1.33 (s, 12H); ^{13}C NMR (126 MHz, $CDCl_3$) δ 167.2, 139.2, 135.8, 132.3, 129.6, 127.8, 84.1, 52.0, 24.9; ^{11}B NMR (160 MHz, $CDCl_3$) δ 30.60; MS (DART) exact mass calculated for [$C_{14}H_{20}BO_4^+$]: 263.1449, found 263.1465.

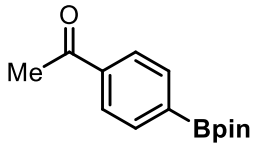

1-[4-(4,4,5,5-Tetramethyl-1,3,2-dioxaborolan-2-yl)phenyl]ethan-1-one (6). Followed Method A and purified using silica gel chromatography to give 59.1 mg (60% yield) of **6** as a white solid from bromoarene; ^{1}H NMR (500 MHz, $CDCl_3$) δ 7.91 (d, *J* = 8.2 Hz, 2H), 7.87 (d, *J* = 8.2 Hz, 2H), 2.60 (s, 3H), 1.34 (s, 12H); ^{13}C NMR (126 MHz, $CDCl_3$) δ 198.5, 139.0, 134.9, 127.3, 84.2, 24.9; ^{11}B NMR (160 MHz, $CDCl_3$) δ 30.78 ; MS (DART) exact mass calculated for [$C_{14}H_{20}BO_3^+$]: 247.1500, found 247.1515.

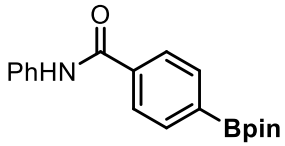

***N*-Phenyl-4-(4,4,5,5-tetramethyl-1,3,2-dioxaborolan-2-yl)benzamide (7)**. Followed Method A and purified using silica gel chromatography to give **7** as a white solid, 55% yield (71.1 mg) from chloroarene and 70% (90.5 mg) from bromoarene; ^{1}H NMR (500 MHz, $CDCl_3$) δ 8.04 (s, 1H), 7.92 (d, *J* = 7.9 Hz, 2H), 7.86 (d, *J* = 7.9 Hz, 2H), 7.66 (d, *J* = 7.9 Hz, 2H), 7.37 (t, *J* = 7.8 Hz, 2H), 7.16 (t, *J* = 7.4 Hz, 1H), 1.39 (s, 12H); ^{13}C NMR (126 MHz, $CDCl_3$) δ 165.8, 137.9, 137.2, 135.1, 129.1, 126.2, 124.6, 120.3, 84.2, 24.9; ^{11}B NMR (160 MHz, $CDCl_3$) δ 30.95; MS (DART) exact mass calculated for [$C_{19}H_{23}BNO_3^+$]: 324.1766, found 324.1780.

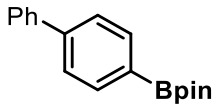

2-[(1,1'-Biphenyl)-4-yl]-4,4,5,5-tetramethyl-1,3,2-dioxaborolane (8). Followed Method A and purified using silica gel chromatography to give **8** as a white solid, 60% yield (67.2 mg) from chloroarene and 71% (79.5 mg) from bromoarene; ^{1}H NMR (500 MHz, $CDCl_3$) δ 7.93 (d, *J* = 7.9 Hz, 2H), 7.69 – 7.61 (m, 4H), 7.48 (t, *J* = 7.6 Hz, 2H), 7.39 (t, *J* = 7.3 Hz, 1H), 1.40 (s, 12H); ^{13}C NMR (126 MHz, $CDCl_3$) δ 143.9, 141.1, 135.3, 128.8, 127.6, 127.3, 126.5, 83.9, 24.9; ^{11}B NMR (160 MHz, $CDCl_3$) δ 30.96; MS (DART) exact mass calculated for [$C_{18}H_{22}BO_2^+$]: 281.1707, found 281.1734.

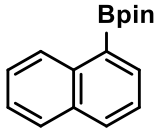

4,4,5,5-Tetramethyl-2-(naphthalen-1-yl)-1,3,2-dioxaborolane (9). Followed Method A and purified using silica gel chromatography to give **9** as a white solid, 60% yield (61.0 mg) from chloroarene and 82% (83.3 mg) from bromoarene; ^{1}H NMR (500 MHz, $CDCl_3$) δ 8.78 (d, *J* = 8.4 Hz, 1H), 8.09 (d, *J* = 6.8 Hz, 1H), 7.93 (d, *J* = 8.2 Hz, 1H), 7.83 (d, *J* = 8.0 Hz, 1H), 7.54 (t, *J* = 7.6 Hz, 1H), 7.47 (t, *J* = 7.5 Hz, 2H), 1.43 (s, 12H); ^{13}C NMR (126 MHz, $CDCl_3$) δ 137.0, 135.7, 133.2, 131.7, 128.5, 128.4, 126.4, 125.5, 125.0, 83.8, 25.0; ^{11}B NMR (160 MHz, $CDCl_3$) δ 31.56; MS (DART) exact mass calculated for [$C_{16}H_{20}BO_2^+$]: 255.1435, found 255.1430.

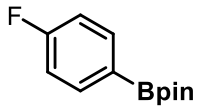

2-(4-Fluorophenyl)-4,4,5,5-tetramethyl-1,3,2-dioxaborolane (10). Followed Method A and purified using silica gel chromatography to give **10** as a white solid, 67% yield (59.5 mg) from chloroarene and 76% (67.5 mg) from bromoarene; ^{1}H NMR (500 MHz, $CDCl_3$) δ 7.86 – 7.71 (m, 2H), 7.03 (t, *J* = 8.9 Hz, 2H), 1.32 (s, 12H); ^{13}C NMR (126 MHz, $CDCl_3$) δ 165.1 (d, *J* = 250.3 Hz), 137.0 (d, *J* = 8.2 Hz), 114.9 (d, *J* = 20.2 Hz), 83.9, 24.9; ^{11}B NMR (160 MHz, $CDCl_3$) δ 30.54; ^{19}F NMR (376 MHz, $CDCl_3$) δ -97.87; MS (DART) exact mass calculated for [$C_{12}H_{17}BFO_2^+$]: 223.1300, found 223.1300.

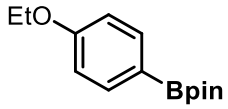

2-(4-Ethoxyphenyl)-4,4,5,5-tetramethyl-1,3,2-dioxaborolane (11). Followed Method A and purified using silica gel chromatography to give **11** as a white solid, 34% yield (33.7 mg) from chloroarene and 58% (57.5 mg) from bromoarene; ^{1}H NMR (500 MHz, $CDCl_3$) δ 7.76 (d, *J* = 8.6 Hz, 2H), 6.91 (d, *J* = 8.6 Hz, 2H), 4.08 (q, *J* = 7.0 Hz, 2H), 1.44 (t, *J* = 7.0 Hz, 3H), 1.36 (s, 12H). ^{13}C NMR (126 MHz, $CDCl_3$) δ 161.6, 136.5, 113.8, 83.5, 63.2, 24.9, 14.8; ^{11}B NMR (160 MHz, $CDCl_3$) δ 30.90; MS (DART) exact mass calculated for [$C_{14}H_{22}BO_3^+$]: 249.1657, found 249.1670.

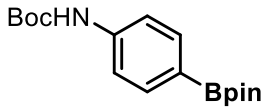

***tert*-Butyl [4-(4,4,5,5-tetramethyl-1,3,2-dioxaborolan-2-yl)phenyl]carbamate (12)**. Followed Method A and purified using silica gel chromatography to give **2k** as a mixture of white solids (mixture with B_2Pin_2), and the yield was determined by ^{1}H NMR spectra with CH_2Br_2 as an internal standard. ^{1}H NMR peaks were referenced by authentic spectral data of precedent literature[6]; ^{1}H NMR (500 MHz, $CDCl_3$) 7.72 (d, J = 8.2 Hz, 2H), 7.35 (d, J = 8.0 Hz, 2H), 6.57 (s, 1H), 4.93 (s, 3H), 1.51 (s, 9H), 1.33 (s, 12H); MS (DART) exact mass calculated for [$C_{17}H_{27}BNO_4^+$]: 320.2028, found 320.2040.

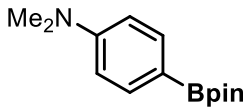

***N*,*N*-Dimethyl-4-(4,4,5,5-tetramethyl-1,3,2-dioxaborolan-2-yl)aniline (13)**. Followed Method A and purified using silica gel chromatography to give **2l** as a white solid, 32% yield (31.6 mg) from chloroarene and 54% (53.4 mg) from bromoarene; ^{1}H NMR (500 MHz, $CDCl_3$) δ 7.72 (d, J = 8.8 Hz, 2H), 6.72 (d, J = 8.8 Hz, 2H), 3.01 (s, 6H), 1.36 (s, 12H); ^{13}C NMR (126 MHz, $CDCl_3$) δ 152.6, 136.2, 111.3, 83.2, 40.1, 24.9; ^{11}B NMR (160 MHz, $CDCl_3$) δ 30.74; MS (DART) exact mass calculated for [$C_{14}H_{23}BNO_2^+$]: 248.1816, found 248.1833.

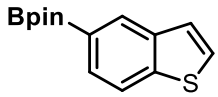

2-(Benzo[*b*]thiophen-5-yl)-4,4,5,5-tetramethyl-1,3,2-dioxaborolane (14). Followed Method A and purified using silica gel chromatography to give **14** as a white solid, 21% yield (21.9 mg) from chloroarene and 65% (67.6 mg) from bromoarene; ^{1}H NMR (500 MHz, $CDCl_3$) δ 8.30 (s, 1H), 7.88 (d, J = 8.1 Hz, 1H), 7.74 (d, J = 8.1 Hz, 1H), 7.40 (d, J = 5.4 Hz, 1H), 7.34 (d, J = 5.4 Hz, 1H), 1.36 (s, 12H); ^{13}C NMR (126 MHz, $CDCl_3$) δ 142.7, 139.2, 130.8, 129.7, 126.0, 124.2, 121.9, 83.9, 24.9; ^{11}B NMR (160 MHz, $CDCl_3$) δ 31.11; MS (DART) exact mass calculated for [$C_{14}H_{18}BO_2S^+$]: 261.1115, found 261.1131.

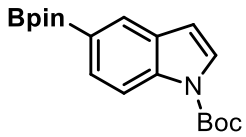

***tert*-Butyl 5-(4,4,5,5-tetramethyl-1,3,2-dioxaborolan-2-yl)-1*H*-indole-1-carboxylate (15)**. Followed Method A and purified using silica gel chromatography to give **15** as a white solid, 21% yield (23.3 mg) from chloroarene and 46% (63.1 mg) from bromoarene. ^{1}H NMR (500 MHz, $CDCl_3$) δ 8.12 (d, *J* = 7.6 Hz, 1H), 8.04 (s, 1H), 7.74 (d, *J* = 8.3 Hz, 1H), 7.55 (d, *J* = 3.7 Hz, 1H), 6.55 (d, *J* = 3.7 Hz, 1H), 1.65 (s, 9H), 1.35 (s, 12H); ^{13}C NMR (126 MHz, $CDCl_3$) δ 149.7, 137.3, 130.6, 130.2, 128.3, 125.9, 114.5, 107.6, 83.8, 83.7, 28.2, 24.9; ^{11}B NMR (160 MHz, $CDCl_3$) δ 31.03 ; MS (DART) exact mass calculated for [$C_{19}H_{27}BNO_4^+$]: 344.2028, found 344.2046.

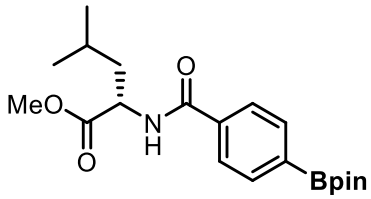

Methyl [4-(4,4,5,5-tetramethyl-1,3,2-dioxaborolan-2-yl)benzoyl]-*L*-leucinate (16). Followed Method A and purified using silica gel chromatography to give 112.6 mg (75%) of **16** as a white solid. IR (Film): 3308, 2956, 2920, 2851, 1754, 1636, 1539, 1360, 1142, 1082 cm^{-1}; ^{1}H NMR (500 MHz, $CDCl_3$) δ 7.86 (d, *J* = 7.7 Hz, 2H), 7.77 (d, *J* = 7.6 Hz, 2H), 6.57 (d, *J* = 8.3 Hz, 1H), 4.86 (td, *J* = 8.3, 4.6 Hz, 1H), 3.76 (s, 3H), 1.78 – 1.64 (m, 3H), 1.35 (s, 12H), 0.98 (dd, *J* = 9.4, 5.8 Hz, 6H); ^{13}C NMR (126 MHz, $CDCl_3$) δ 173.7, 167.0, 136.1, 135.0, 126.2, 84.2, 52.4, 51.2, 42.0, 25.0, 24.9, 24.9, 22.8, 22.1; ^{11}B NMR (160 MHz, $CDCl_3$) δ 30.57; MS (DART) exact mass calculated for [$C_{20}H_{31}BNO_5^+$]: 376.2290, found 376.2315. Enantiomeric excess was determined by HPLC (>99% ee, IA, nHexane/EtOH= 95/5, 1.0 mL/min).

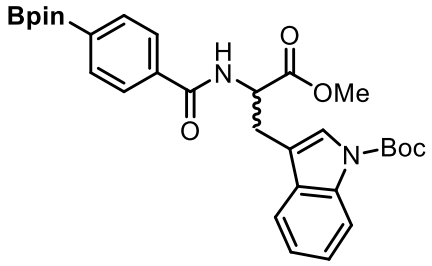

***tert*-Butyl 3-{3-methoxy-3-oxo-2-[4-(4,4,5,5-tetramethyl-1,3,2-dioxaborolan-2-yl)benzamido]propyl}-1*H*-indole-1-carboxylate (17)**. Followed Method A and purified using silica gel chromatography to give 160.1 mg (73%) of **17** as a white solid. IR (Film): 3325, 2978, 2926, 2853, 1731, 1646, 1525, 1453, 1357, 1143, 1085 cm^{-1}; ^{1}H NMR (500 MHz, $CDCl_3$) δ 8.11 (s, 1H), 7.83 (d, *J* = 7.6 Hz, 2H), 7.68 (d, *J* = 7.7 Hz, 2H), 7.49 (d, *J* = 7.7 Hz, 1H), 7.39 (s, 1H), 7.30 (t, *J* = 7.6 Hz, 1H), 7.17 (t, *J* = 7.4 Hz, 1H), 6.75 (d, *J* = 7.2 Hz, 1H), 5.15 (q, *J* = 5.5 Hz, 1H), 3.73 (s, 3H), 3.39 (qd, *J* = 14.7, 5.2 Hz, 2H), 1.64 (s, 9H), 1.35 (s, 12H); ^{13}C NMR (126 MHz, $CDCl_3$) δ 172.1, 166.9, 149.5, 136.0, 135.3, 135.0, 130.6, 126.2, 124.6, 124.2, 122.7, 118.9, 115.3, 114.9, 84.2, 83.7, 53.2, 52.6, 28.2, 27.4, 24.9; ^{11}B NMR (160 MHz, $CDCl_3$) δ 31.05; MS (DART) exact mass calculated for [$C_{30}H_{38}BN_2O_7^+$]: 549.2767 , found 549.2800.

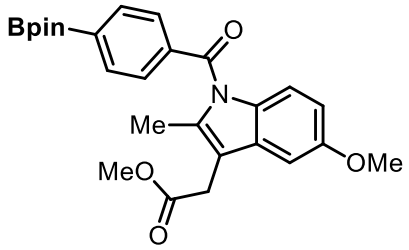

Methyl 2-{5-methoxy-2-methyl-1-[4-(4,4,5,5-tetramethyl-1,3,2-dioxaborolan-2-yl)benzoyl]-1*H*-indol-3-yl}acetate (18). Followed Method A and purified using silica gel chromatography to give 64.8 mg (35%) of **18** as a white solid. IR (Film): 2977, 2925, 2852, 1737, 1681, 1609, 1477, 1353, 1317, 1222, 1142, 1087 cm^{-1}; ^{1}H NMR (500 MHz, $CDCl_3$) δ 7.93 (d, *J* = 7.6 Hz, 2H), 7.71 (d, *J* = 7.7 Hz, 2H), 6.97 (d, *J* = 2.6 Hz, 1H), 6.90 (d, *J* = 9.0 Hz, 1H), 6.67 (dd, *J* = 9.0, 2.5 Hz, 1H), 3.86 (s, 3H), 3.72 (s, 3H), 3.69 (s, 2H), 2.38 (s, 3H), 1.40 (s, 12H); ^{13}C NMR (126 MHz, $CDCl_3$) δ 171.4, 169.5, 156.0, 137.9, 136.1, 135.0, 130.9, 130.6, 128.7, 115.2, 112.4, 111.6, 101.2, 84.3, 55.7, 52.2, 30.2, 24.9, 13.4; ^{11}B NMR (160 MHz, $CDCl_3$) δ 30.73; MS (DART) exact mass calculated for [$C_{26}H_{31}BNO_6^+$]: 464.2239, found 464.2270.

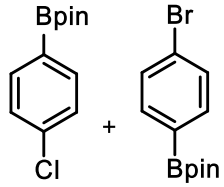

20 21

(20:21 = 17:1)

2-(4-Chlorophenyl)-4,4,5,5-tetramethyl-1,3,2-dioxaborolane (20) and **2-(4-bromophenyl)-4,4,5,5-tetramethyl-1,3,2-dioxaborolane (21)**. Followed Method A and purified using silica gel chromatography to give 44.3 mg of **20** and **21** as a mixture, product ratio (**20**:**21**) was determined to be 17:1 (50%:3%) by ^{1}H NMR spectra. ^{1}H NMR peaks were referenced by authentic spectral data of precedent literature.[6] ; **2h** (major): ^{1}H NMR (500 MHz, $CDCl_3$) δ 7.75 (d, *J* = 8.3 Hz, 2H), 7.37 (d, *J* = 8.3 Hz, 2H), 1.36 (s, 12H); ^{13}C NMR (126 MHz, $CDCl_3$) δ 137.5, 136.1, 128.0, 84.0, 24.9; ^{11}B NMR (160 MHz, $CDCl_3$) δ 30.70; MS (DART) exact mass calculated for [$C_{12}H_{17}BClO_2^+$]: 239.1005, found 239.1019; **2h'** (minor): ^{1}H NMR (500 MHz, $CDCl_3$) δ 7.68 (d, *J* = 8.2 Hz, 2H), 7.53 (d, *J* = 8.2 Hz, 2H), 1.36 (s, 12H); ^{13}C NMR (126 MHz, $CDCl_3$) δ 136.3, 134.8, 131.0, 84.0, 24.9; ^{11}B NMR (160 MHz, $CDCl_3$) δ 30.70; MS (DART) exact mass calculated for [$C_{12}H_{17}BBrO_2^+$]: 283.0499, found 283.0490.

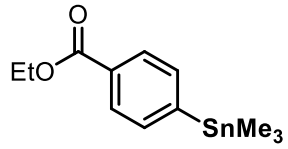

Ethyl 4-(trimethylstannyl)benzoate (22). Followed Method B and the yield was determined by 1H NMR integration using CH_2Br_2 (14.0 μL, 0.2 mmol) as an internal standard. ^{1}H and ^{13}C NMR data were referenced by authentic spectral data of precedent literature[7]; ^{1}H NMR (500 MHz, $CDCl_3$) δ 7.98 (d, *J* = 7.9 Hz, 2H), 7.58 (d, *J* = 8.1 Hz, 2H), 4.92 (s, 2H), 4.38 (d, *J* = 7.1 Hz, 2H), 1.39 (d, *J* = 7.1 Hz, 3H), 0.32 (s, 9H).; ^{13}C NMR (126 MHz, $CDCl_3$) δ ^{13}C NMR (126 MHz, $CDCl_3$) δ 166.9, 149.5, 135.8, 128.5, 60.9, 14.4, -9.5; MS (DART) exact mass calculated for [$C_{12}H_{19}O_2Sn^+$]: 315.0402, found 315.0420.

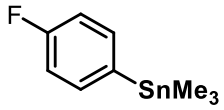

(4-Fluorophenyl)trimethylstannane (23). Followed Method B and the yield was determined by 1H NMR integration using CH_2Br_2 (28.0 μL, 0.4 mmol) as an internal standard. ^{1}H, ^{13}C and ^{19}F NMR data were referenced by authentic spectral data of precedent literature[7]; ^{1}H NMR (500 MHz, $CDCl_3$) δ 7.48 – 7.44 (m, 2H), 7.08 – 7.05 (m, 2H), 4.94 (s, 3H), 0.31 – 0.30 (m, 9H); ^{13}C NMR (126 MHz, $CDCl_3$) δ 163.4 (d, *J* = 246.6 Hz), 137.3 (d, *J* = 6.7 Hz), 137.1 (d, *J* = 4.1 Hz), 115.2 (d, *J* = 19.1 Hz), -9.4; ^{19}F NMR (376 MHz, $CDCl_3$) δ -113.32; MS (DART) exact mass calculated for [$C_9H_{14}FSn^+$]: 261.0096, found 261.0080.

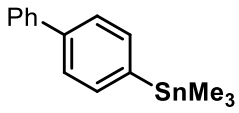

(1,1'-Biphenyl)-4-yltrimethylstannane (24). Followed Method B and the yield was determined by 1H NMR integration using CH_2Br_2 (14.0 μL, 0.2 mmol) as an internal standard. ^{1}H and ^{13}C NMR data were referenced by authentic spectral data of precedent literature[7]; ^{1}H NMR (500 MHz, $CDCl_3$) ^{1}H NMR (500 MHz, $CDCl_3$) δ 7.70 – 7.67 (m, 6H), 7.65 – 7.57 (m, 2H), 7.42 (m, 1H), 0.43 (s, 9H); ^{13}C NMR (126 MHz, $CDCl_3$) δ 141.2, 141.1, 141.0, 136.2, 128.7, 127.2, 127.1, 126.7, 18.9, -9.5; MS (DART) exact mass calculated for [$C_{15}H_{19}Sn^+$]: 319.0503, found 319.0489.

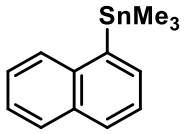

Trimethyl(naphthalen-1-yl)stannane (25). Followed Method B and the yield was determined by 1H NMR integration using CH_2Br_2 (14.0 μL, 0.2 mmol) as an internal standard. ^{1}H and ^{13}C NMR data were referenced by authentic spectral data of precedent literature[7]; ^{1}H NMR (500 MHz, $CDCl_3$) δ 7.92 – 7.89 (m, 3H), 7.73 (d, *J* = 6.5 Hz, 1H), 7.48 – 7.52 (m, 3H), 0.52 (s, 9H).; ^{13}C NMR (126 MHz, $CDCl_3$) δ 142.5, 138.5, 134.6, 133.6, 129.8, 129.0, 128.7, 125.8, 125.4, 125.3, 18.9, -8.4; MS (DART) exact mass calculated for [$C_{13}H_{17}Sn^+$]: 293.0347, found 293.0330.

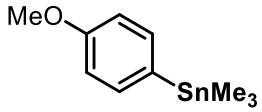

(4-methoxyphenyl)trimethylstannane (26). Followed Method B and the yield was determined by 1H NMR integration using CH_2Br_2 (14.0 μL, 0.2 mmol) as an internal standard. ^{1}H and ^{13}C NMR data were referenced by authentic spectral data of precedent literature[7]; ^{1}H NMR (500 MHz, $CDCl_3$) δ 7.46 (d, *J* = 8.4 Hz, 2H), 6.98 (d, *J* = 8.4 Hz, 2H), 4.96 (s, 2H), 3.85 (s, 3H), 0.32 (s, 9H); ^{13}C NMR (126 MHz, $CDCl_3$) δ 159.9, 136.9, 132.4, 114.0, 55.0, -9.5; MS (DART) exact mass calculated for [$C_{10}H_{17}OSn^+$]: 273.0296, found 273.0310.

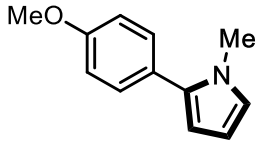

2-(4-Methoxyphenyl)-1-methyl-1*H*-pyrrole (27). Followed Method C and purified using silica gel chromatography to give 68.2 mg (91%) of **27** as a pale yellow solid. ^{1}H NMR (500 MHz, $CDCl_3$) δ 7.33 (d, *J* = 8.6 Hz, 2H), 6.95 (d, *J* = 8.6 Hz, 2H), 6.70 (s, 1H), 6.18 (d, *J* = 14.2 Hz, 2H), 3.85 (s, 3H), 3.64 (s, 3H); ^{13}C NMR (126 MHz, $CDCl_3$) δ 158.7, 134.4, 130.1, 126.0, 123.0, 113.8, 108.0, 107.6, 55.3, 34.9; MS (DART) exact mass calculated for [$C_{12}H_{14}NO^+$]: 188.1070, found 188.1081.

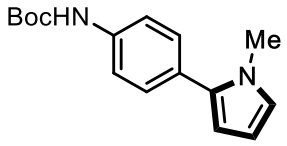

***tert*-Butyl [4-(1-methyl-1H-pyrrol-2-yl)phenyl]carbamate (28)**. Followed Method C and purified using silica gel chromatography to give 66.5 mg (61%) of **28** as a white solid. IR (Film): 3330, 2976, 2921, 2851, 1697, 1587, 1512, 1366, 1230, 1154 cm^{-1}; ^{1}H NMR (500 MHz, $CDCl_3$) δ 7.39 (d, *J* = 8.4 Hz, 2H), 7.32 (d, *J* = 8.6 Hz, 2H), 6.69 (t, *J* = 2.3 Hz, 1H), 6.52 (s, 1H), 6.18 (dd, *J* = 2.2, 1.1 Hz, 2H), 3.63 (s, 3H), 1.54 (s, 9H); ^{13}C NMR (126 MHz, $CDCl_3$) δ 152.8, 137.1, 134.2, 129.3, 128.2, 123.3, 118.5, 108.3, 107.7, 80.7, 35.0, 28.4; MS (DART) exact mass calculated for [$C_{16}H_{21}N_2O_2^+$]: 273.1598, found 273.1614.

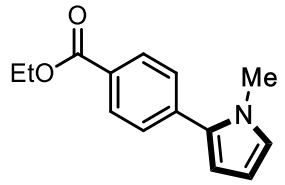

Ethyl 4-(1-methyl-1*H*-pyrrol-2-yl)benzoate (29). Followed Method C and purified using silica gel chromatography to give xx.x mg (xx%) of **29** as a white solid. ^{1}H NMR (500 MHz, $CDCl_3$) δ 8.10 (d, *J* = 8.4 Hz, 2H), 7.50 (d, *J* = 8.3 Hz, 2H), 6.79 (t, *J* = 2.2 Hz, 1H), 6.37 (dd, *J* = 3.7, 1.9 Hz, 1H), 6.29 – 6.21 (m, 1H), 4.42 (q, *J* = 7.1 Hz, 2H), 3.74 (s, 3H), 1.44 (t, *J* = 7.1 Hz, 3H); ^{13}C NMR (126 MHz, $CDCl_3$) δ 166.5, 137.7, 133.6, 129.7, 128.3, 127.9, 125.1, 110.0, 108.3, 61.0, 35.4, 14.4; MS (DART) exact mass calculated for [$C_{14}H_{16}NO_2^+$]: 230.1176, found 230.1186.

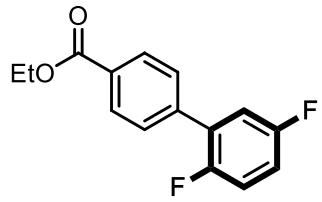

Ethyl 2',5'-difluoro-(1,1'-biphenyl)-4-carboxylate (30). Followed Method C and purified using silica gel chromatography to give 36.7 mg (34%) of **xx** as a white solid. ^{1}H NMR (500 MHz, $CDCl_3$) δ 8.12 (d, *J* = 8.4 Hz, 2H), 7.60 (d, *J* = 8.2 Hz, 2H), 7.19 – 7.10 (m, 2H), 7.04 (ddt, *J* = 9.1, 7.2, 3.5 Hz, 1H), 4.41 (q, *J* = 7.1 Hz, 2H), 1.42 (t, *J* = 7.2 Hz, 3H); ^{13}C NMR (126 MHz, $CDCl_3$) δ 166.3, 158.8 (dd, *J* = 242.9, 2.5 Hz), 155.72 (dd, *J* = 244.8, 2.5 Hz), 139.2, 130.1, 129.8, 129.3 (dd, *J* = 15.8, 7.9 Hz), 128.9 (d, *J* = 3.4 Hz), 117.4 (dd, *J* = 25.7, 8.7 Hz), 116.9 (dd, *J* = 24.5, 3.5 Hz), 116.0 (dd, *J* = 24.0, 8.6 Hz), 61.1, 14.4; ^{19}F NMR (376 MHz, $cdcl_3$) δ -118.7, -123.6; MS (DART) exact mass calculated for [$C_{15}H_{13}F_2O_2^+$]: 263.0878, found 263.0894.

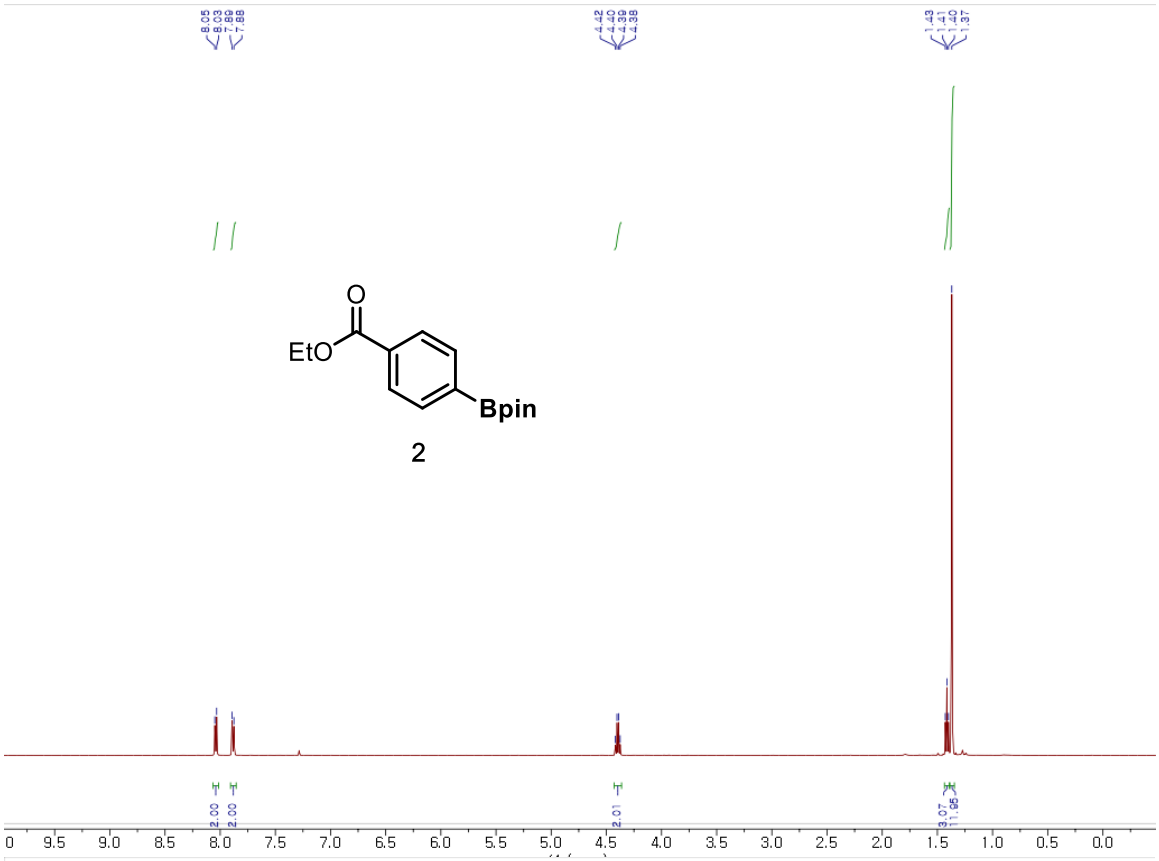
EtO
Bpin
2

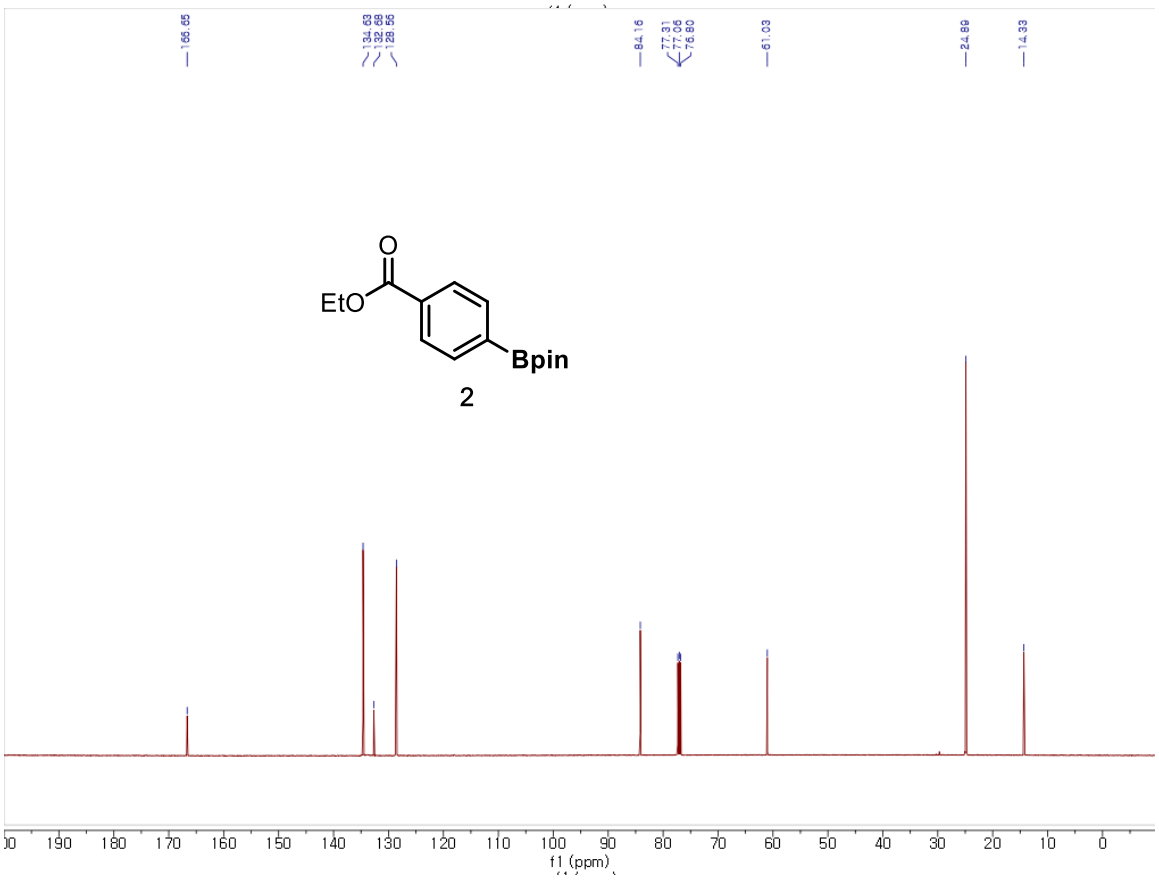
EtO
Bpin
2
f1 (ppm)

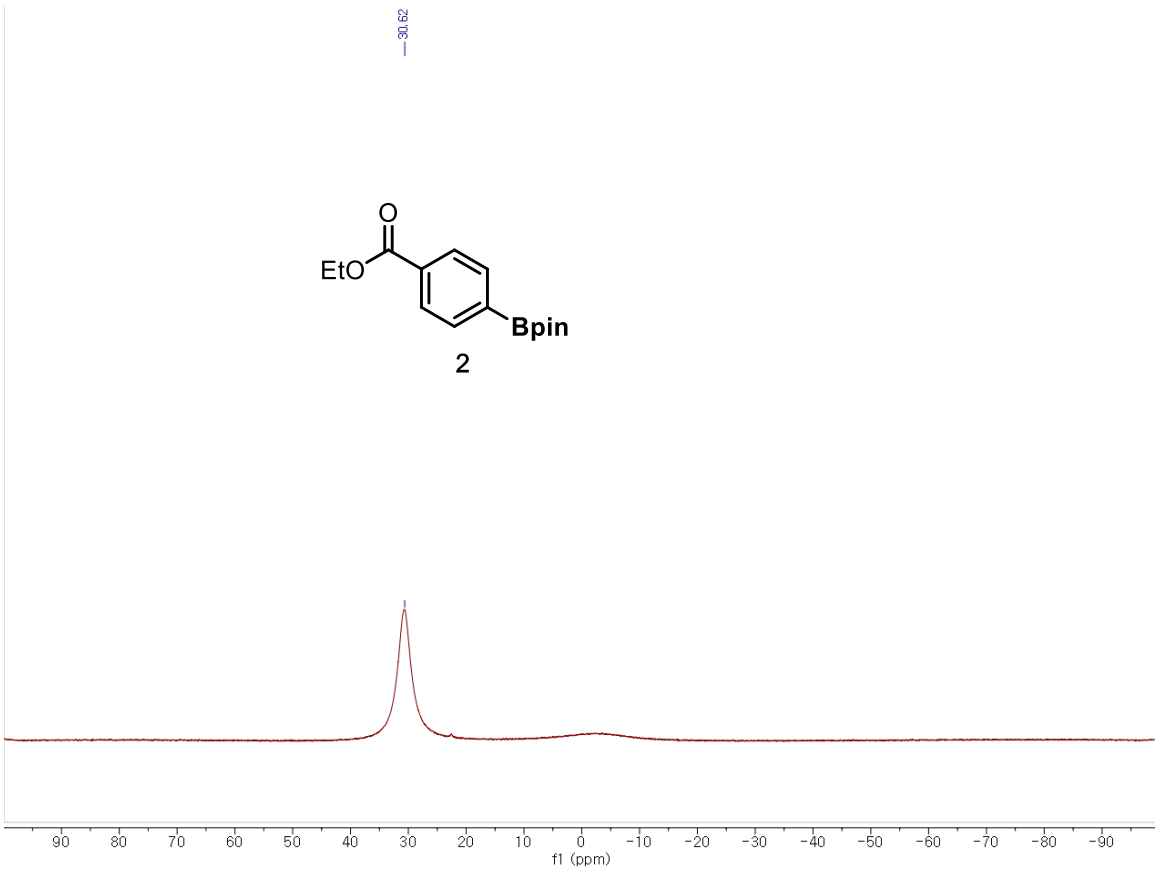
30.62
O
EtO
Bpin
2
90
80
70
60
50
40
30
20
10
0
-10
-20
-30
-40
-50
-60
-70
-80
-90
f1 (ppm)

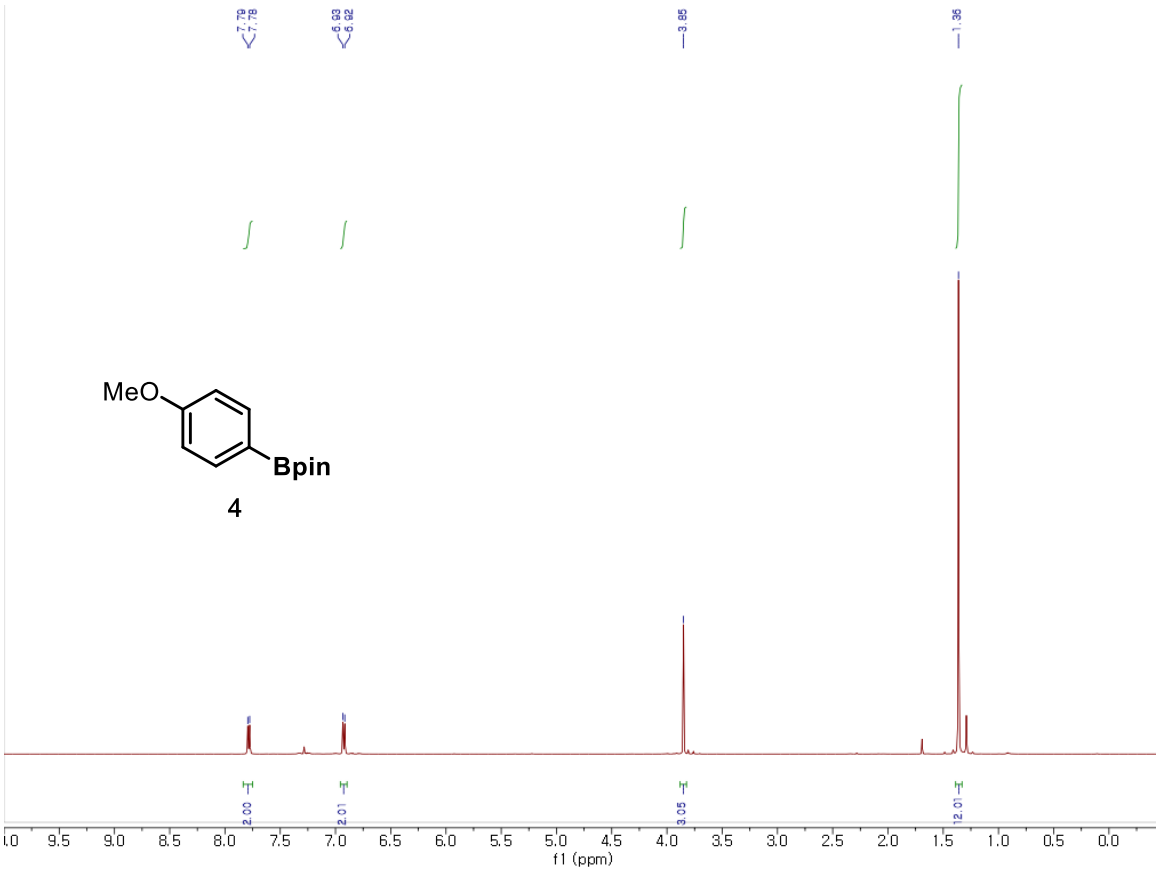
7.79
7.78
6.83
6.82
3.85
1.36
MeO
Bpin
4
2.00
2.01
3.05
12.01
f1 (ppm)

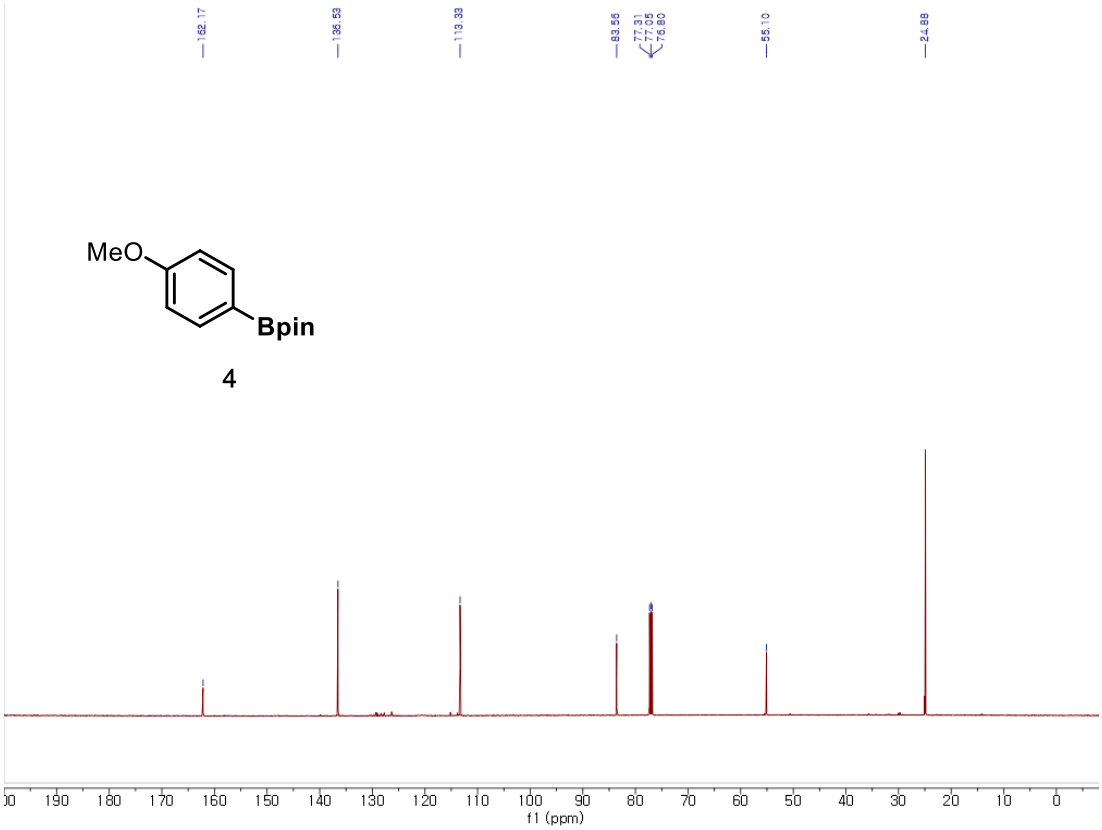
162.17
136.53
113.33
83.56
77.31
77.05
76.80
55.10
24.88
MeO
Bpin
4
f1 (ppm)

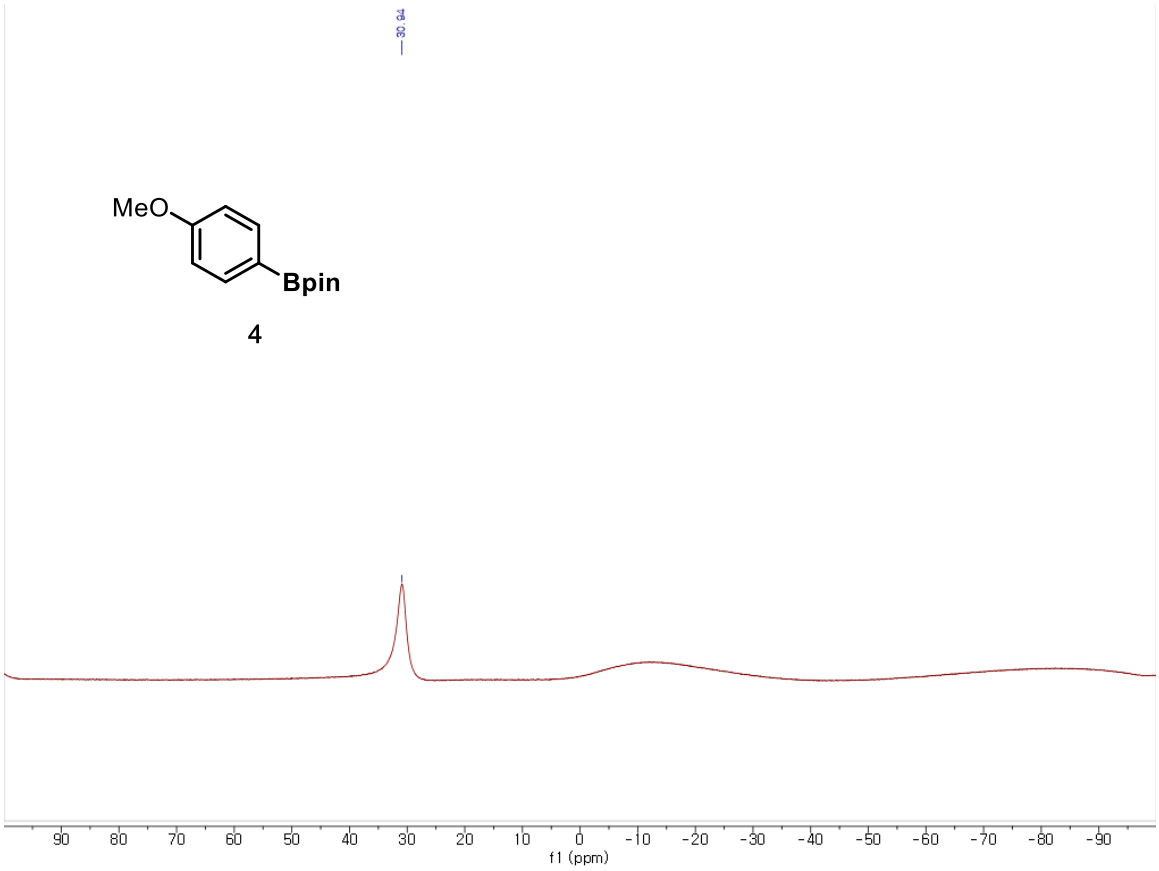
30.64
MeO
Bpin
4
90 80 70 60 50 40 30 20 10 0 -10 -20 -30 -40 -50 -60 -70 -80 -90
f1 (ppm)

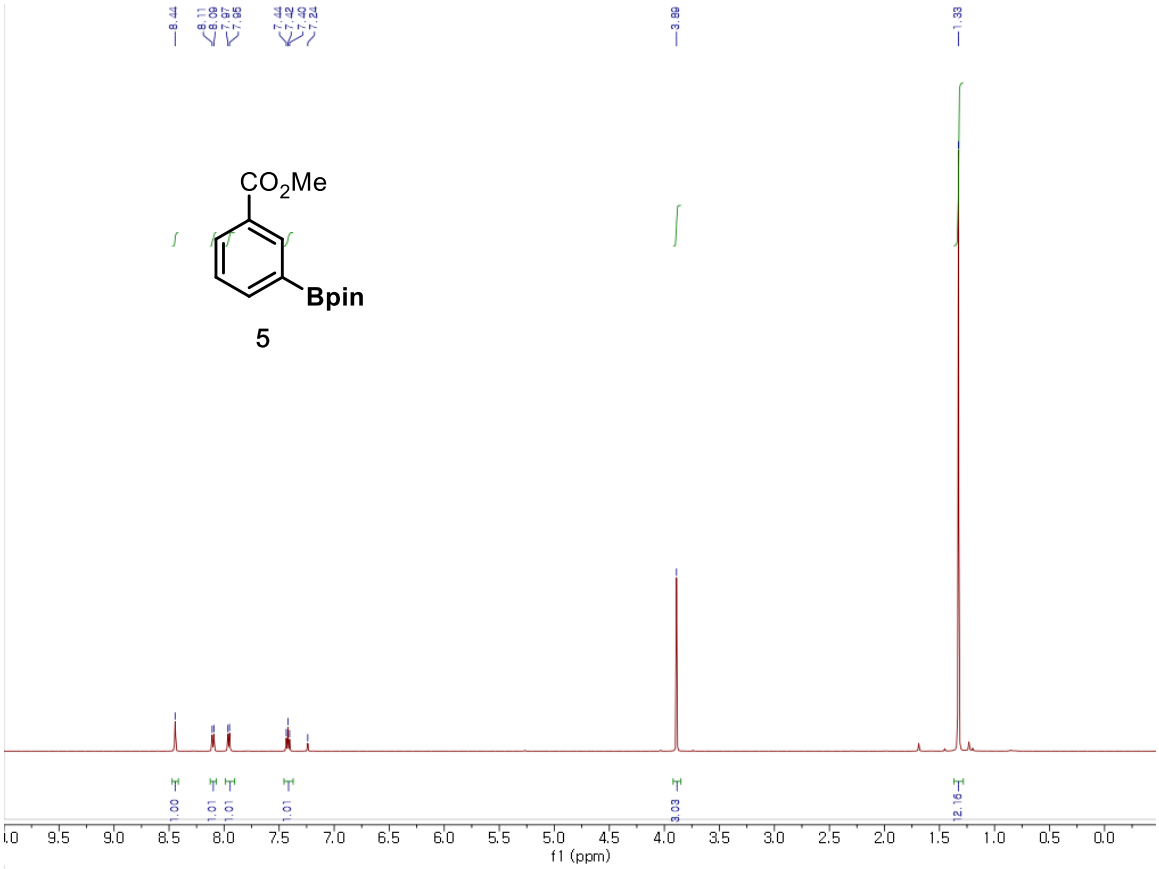
8.44
8.11
8.09
7.87
7.85
7.44
7.42
7.40
7.24
3.99
1.33
CO2Me
Bpin
5
1.00
1.01
1.01
1.01
3.03
12.16
f1 (ppm)

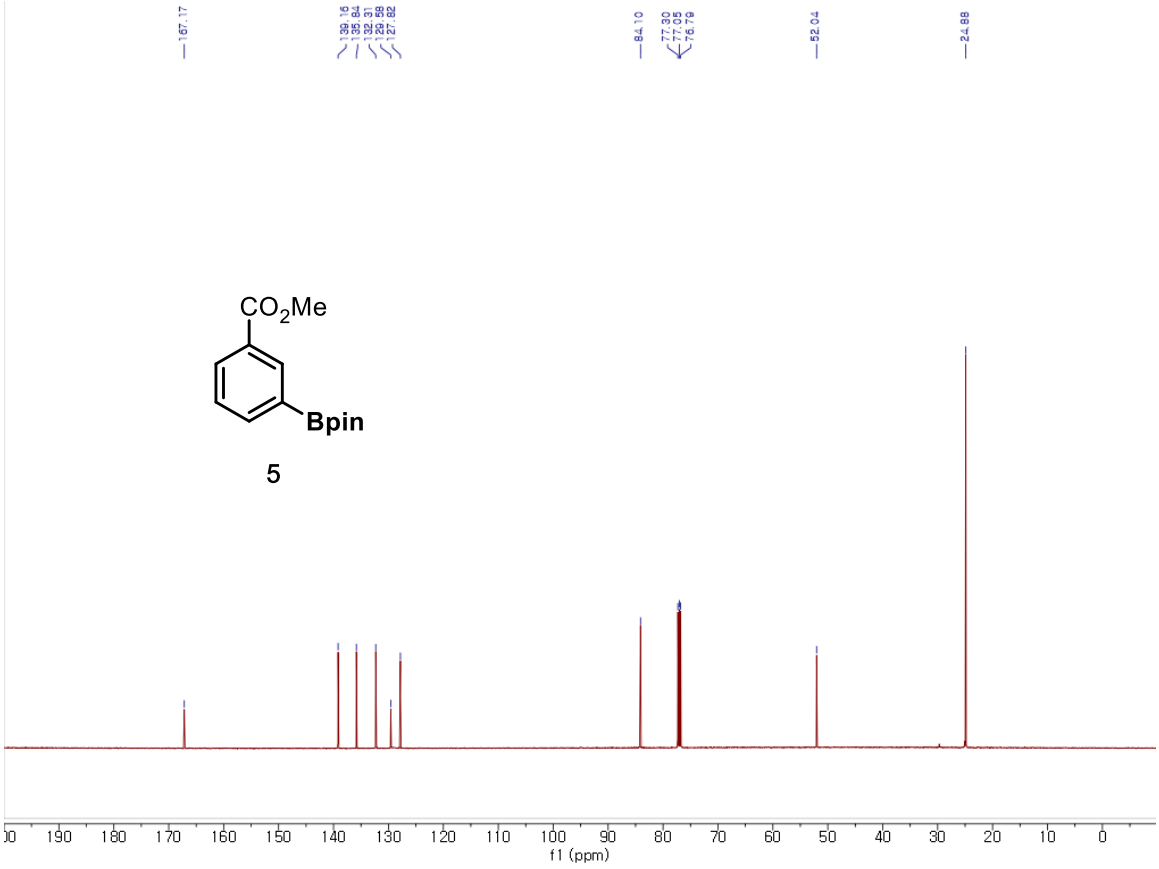
167.17
139.16
136.84
132.91
129.58
127.82
84.10
77.30
77.05
76.79
52.04
24.88
CO2Me
Bpin
5
f1 (ppm)

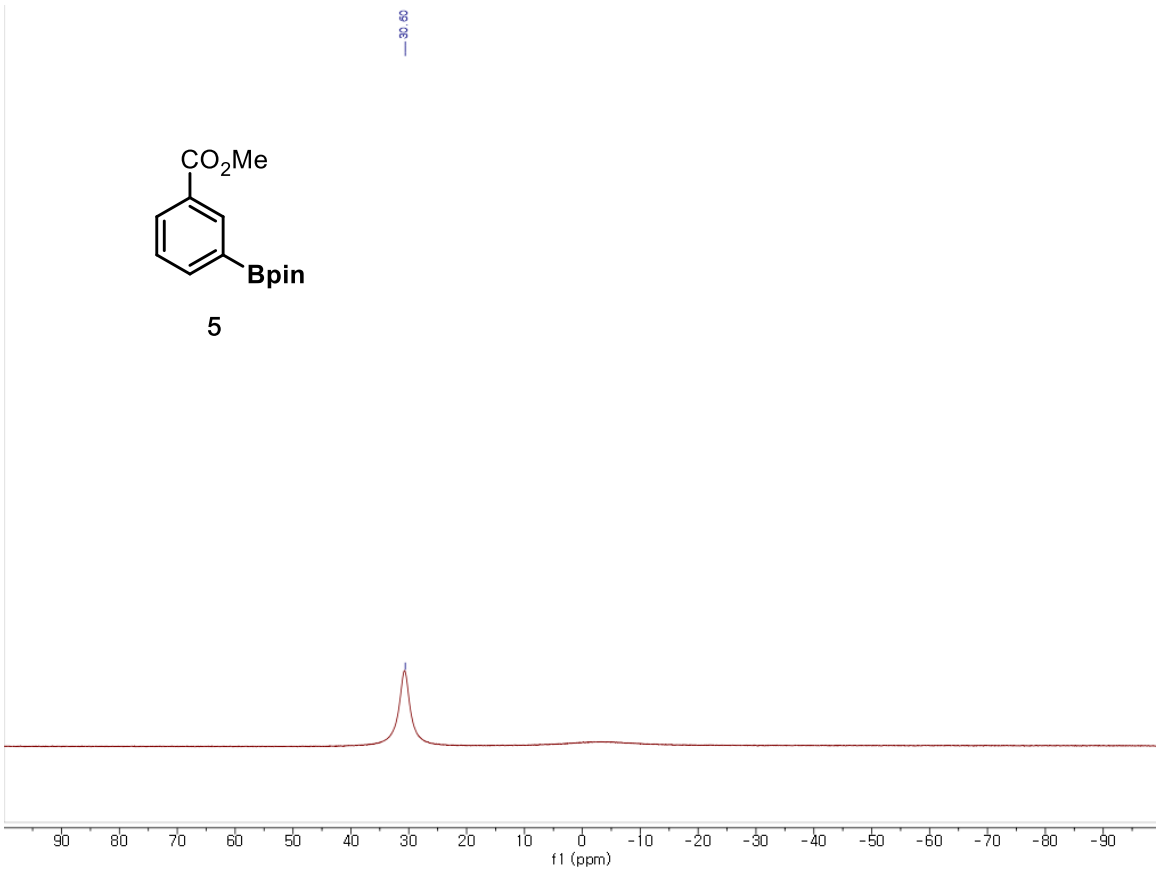
30.60
CO2Me
Bpin
5
90
80
70
60
50
40
30
20
10
0
-10
-20
-30
-40
-50
-60
-70
-80
-90
f1 (ppm)

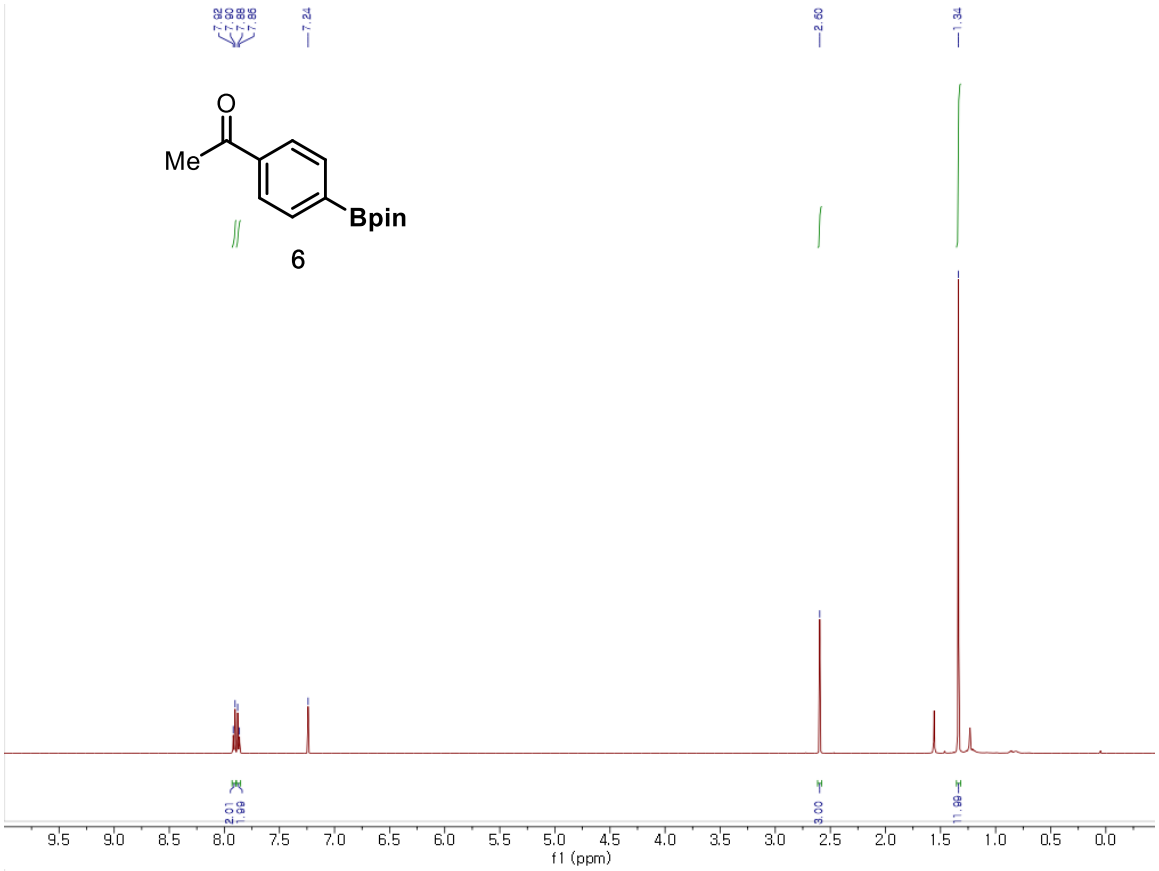
7.92
7.90
7.88
7.88
7.24
2.60
1.34
O
Me
Bpin
6
2.01
1.99
3.00
11.99
9.5 9.0 8.5 8.0 7.5 7.0 6.5 6.0 5.5 5.0 4.5 4.0 3.5 3.0 2.5 2.0 1.5 1.0 0.5 0.0
f1 (ppm)

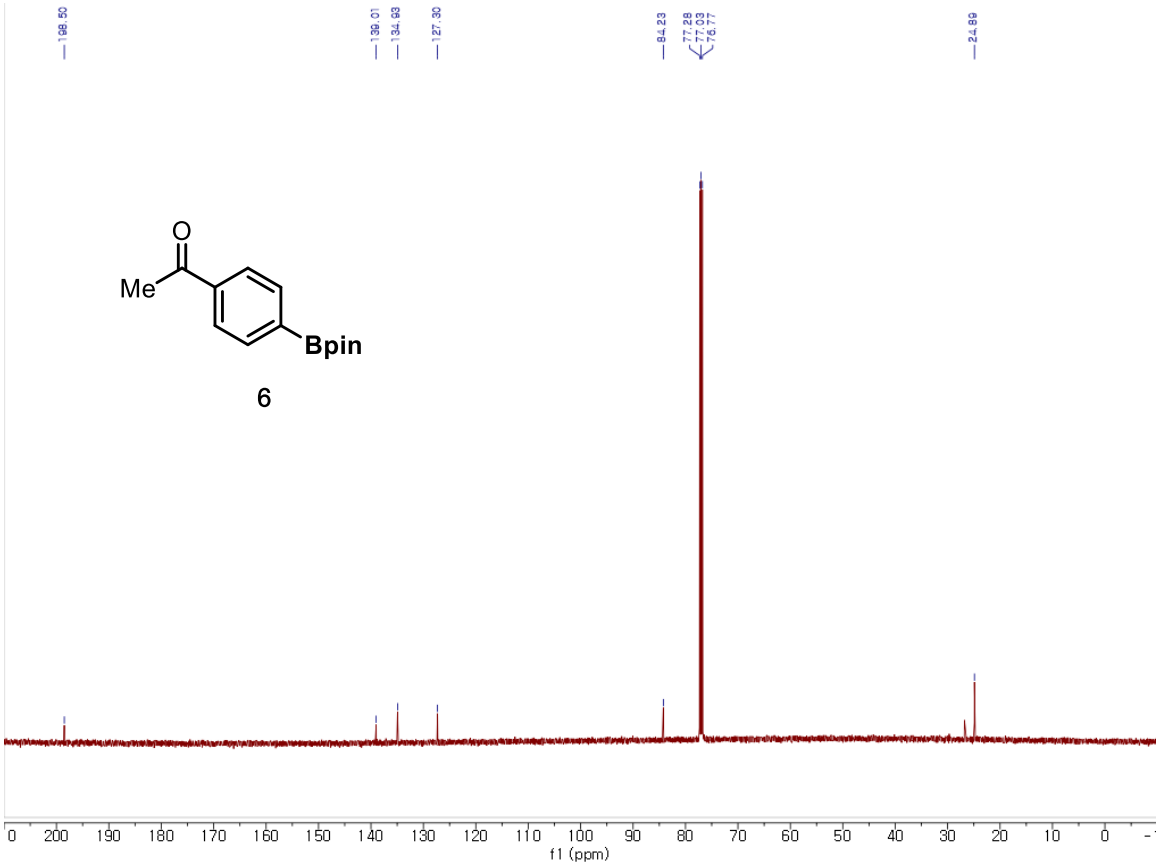
198.50
138.01
134.93
127.30
84.23
77.28
77.03
76.77
24.89
O
Me
Bpin
6
0 200 190 180 170 160 150 140 130 120 110 100 90 80 70 60 50 40 30 20 10 0
f1 (ppm)

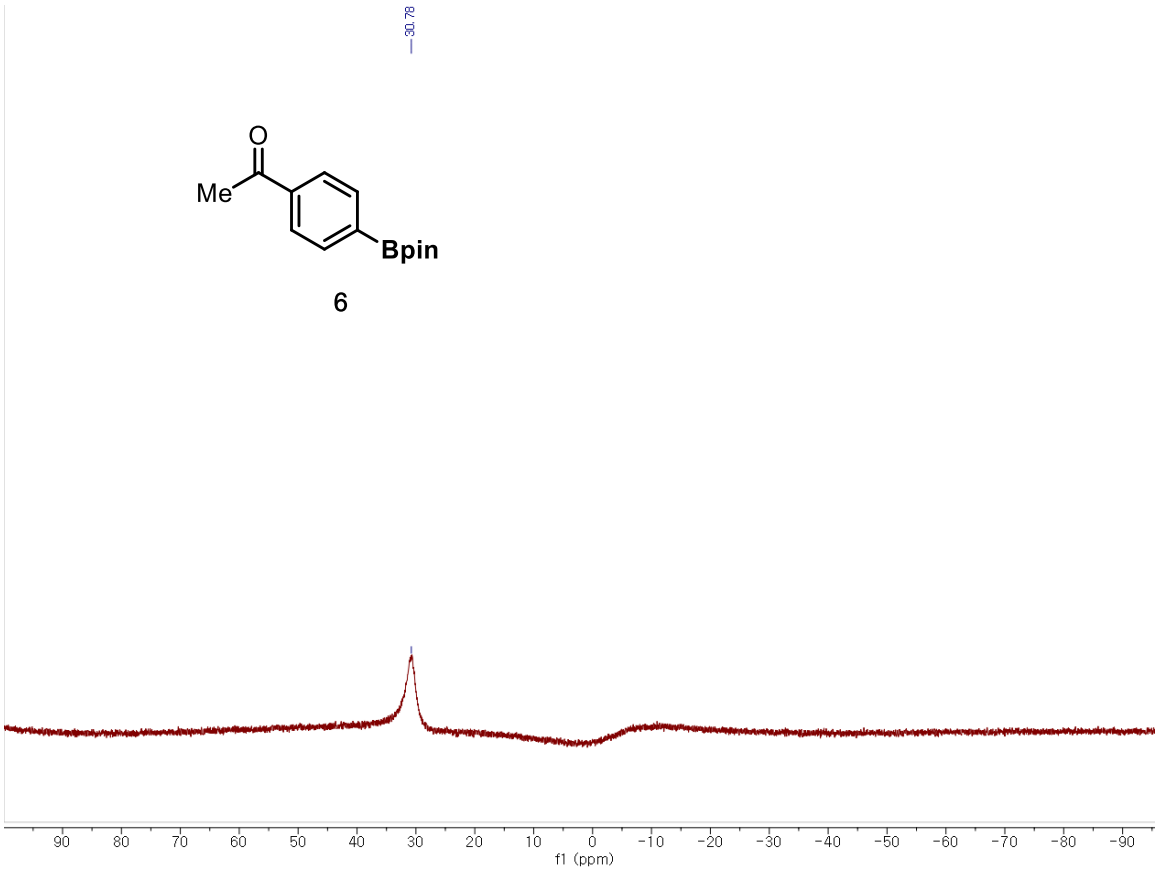
30.78
O
Me
Bpin
6
90
80
70
60
50
40
30
20
10
0
-10
-20
-30
-40
-50
-60
-70
-80
-90
f1 (ppm)

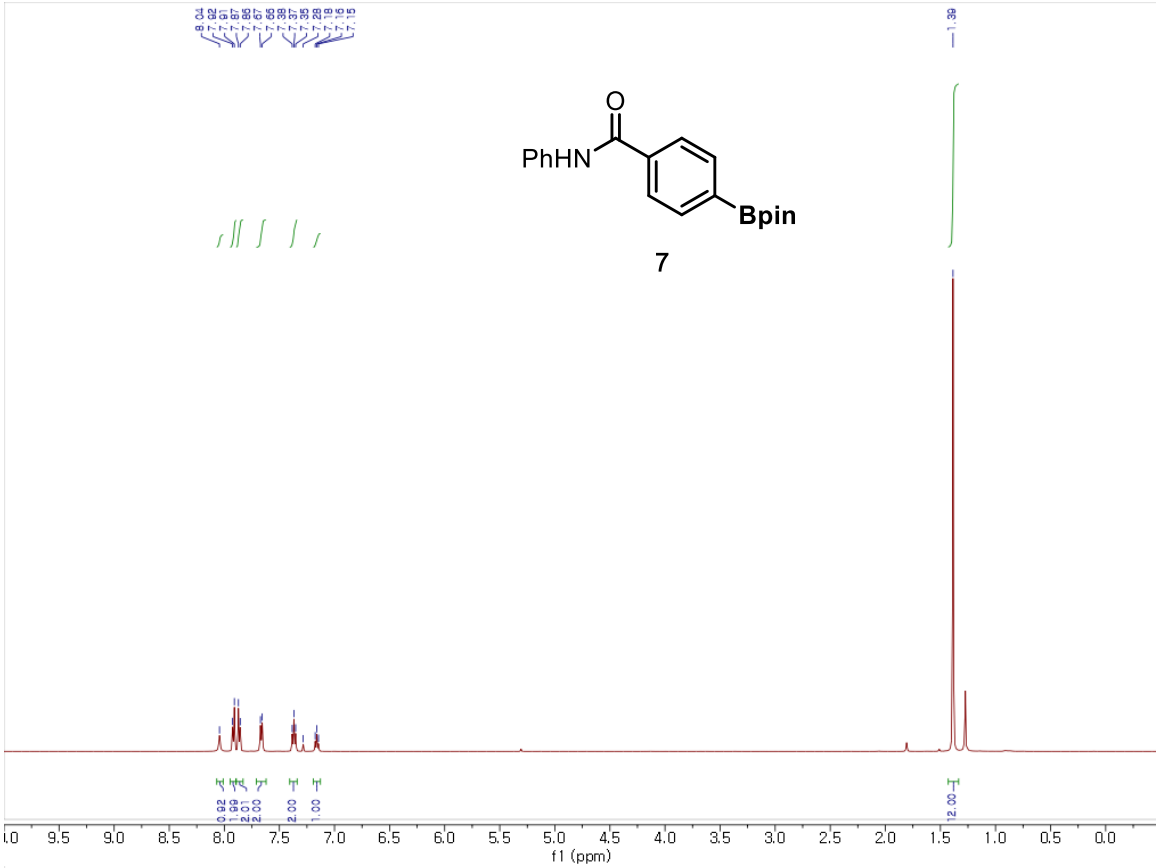
PhHN
O
Bpin
7
f1 (ppm)

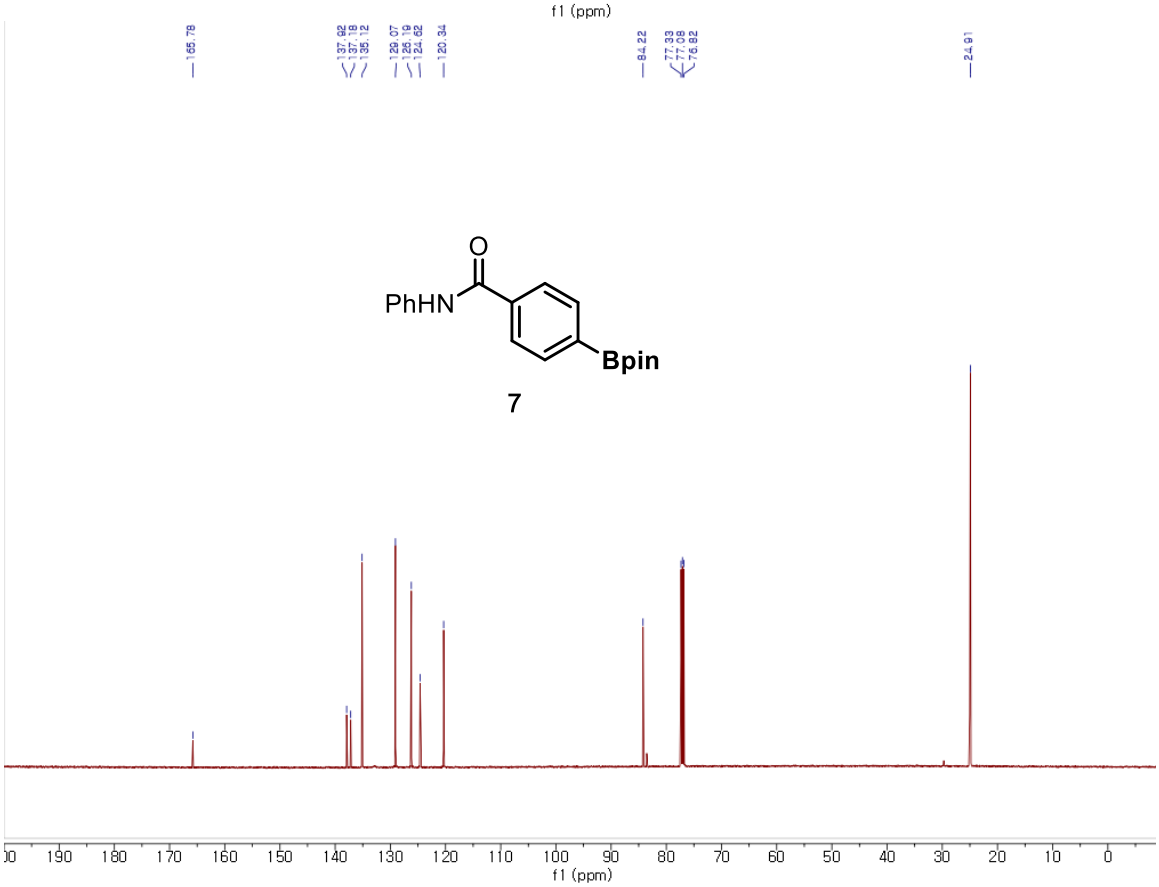
PhHN
O
Bpin
7
f1 (ppm)

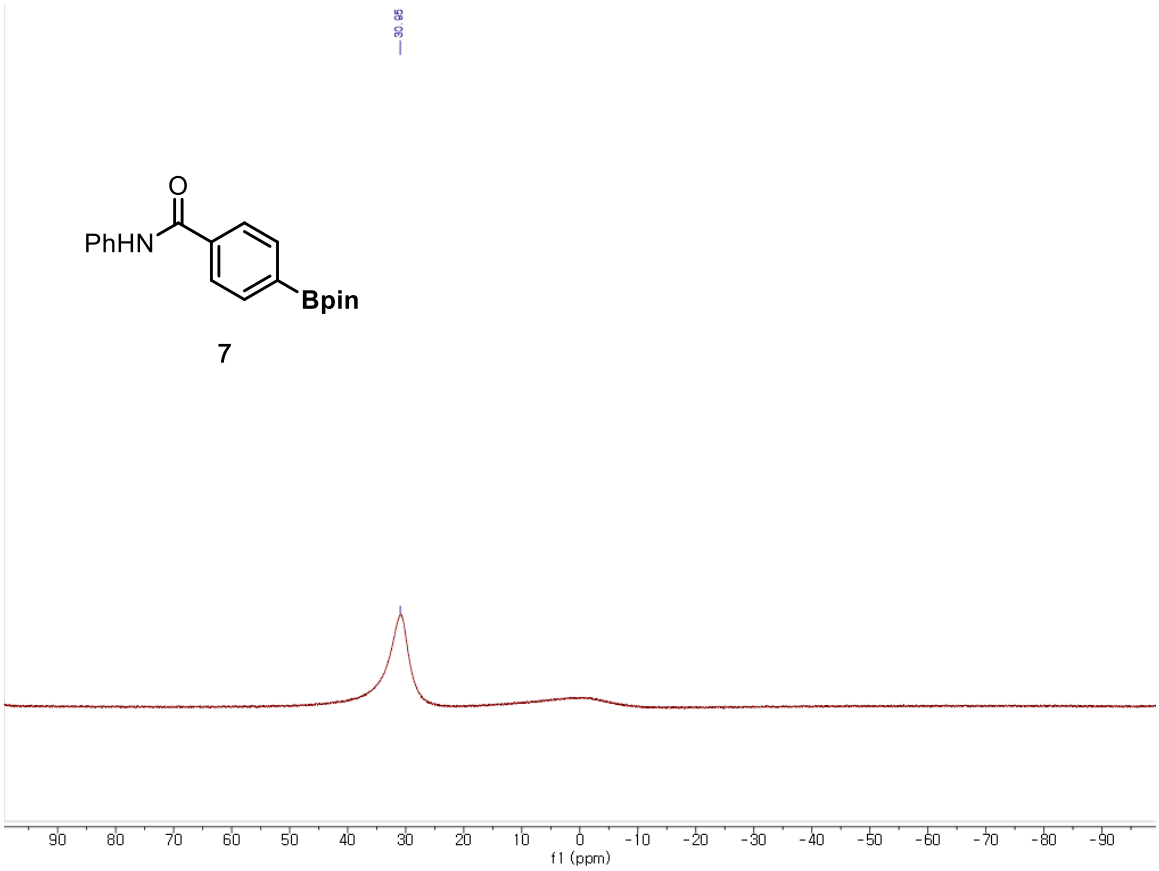
30.95
O
PhHN
Bpin
7
90
80
70
60
50
40
30
20
10
0
-10
-20
-30
-40
-50
-60
-70
-80
-90
f1 (ppm)

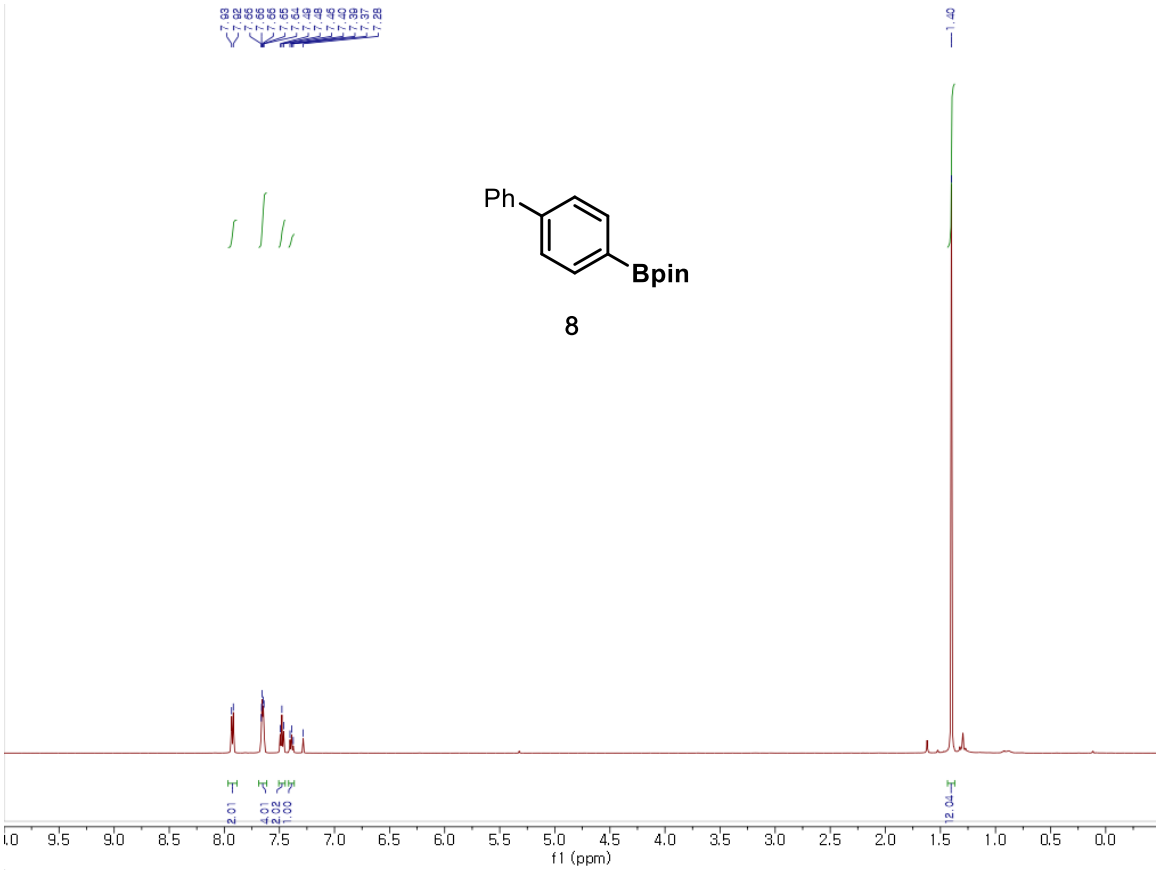
Ph
Bpin
8
f1 (ppm)

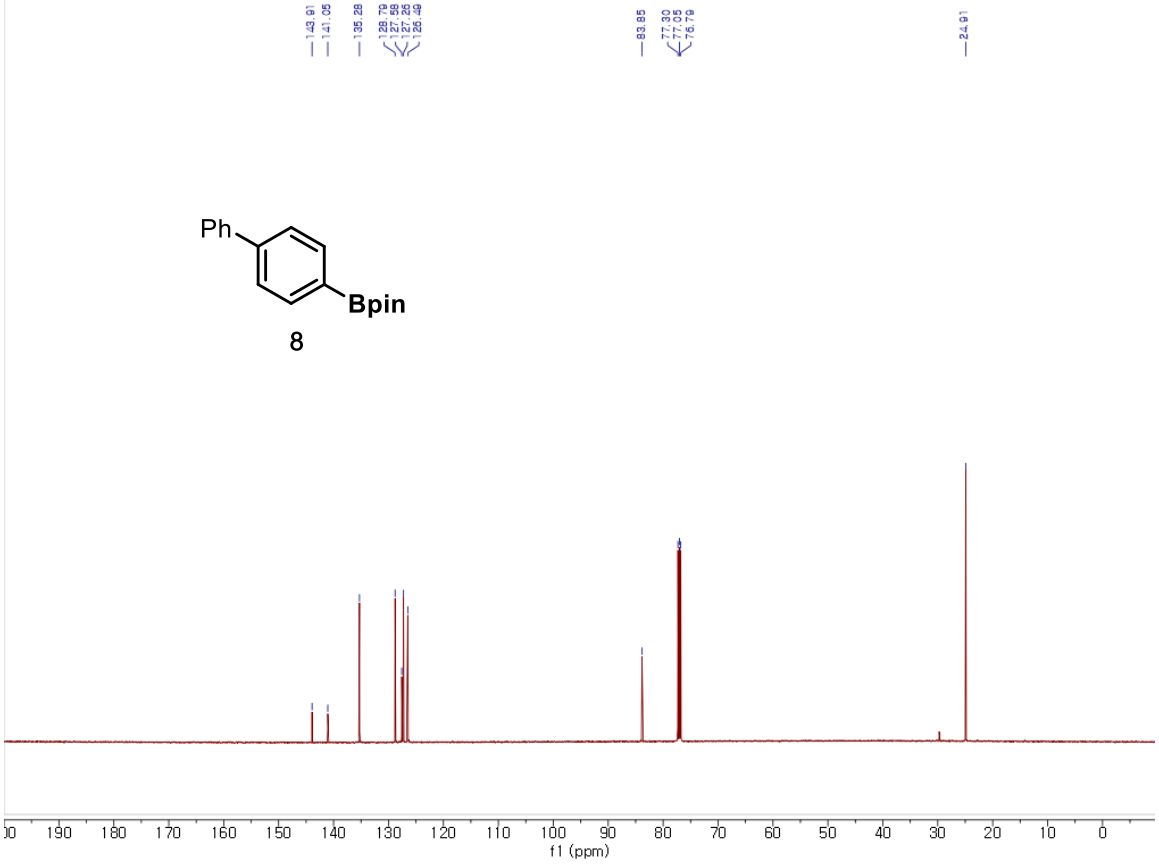
Ph
Bpin
8
f1 (ppm)

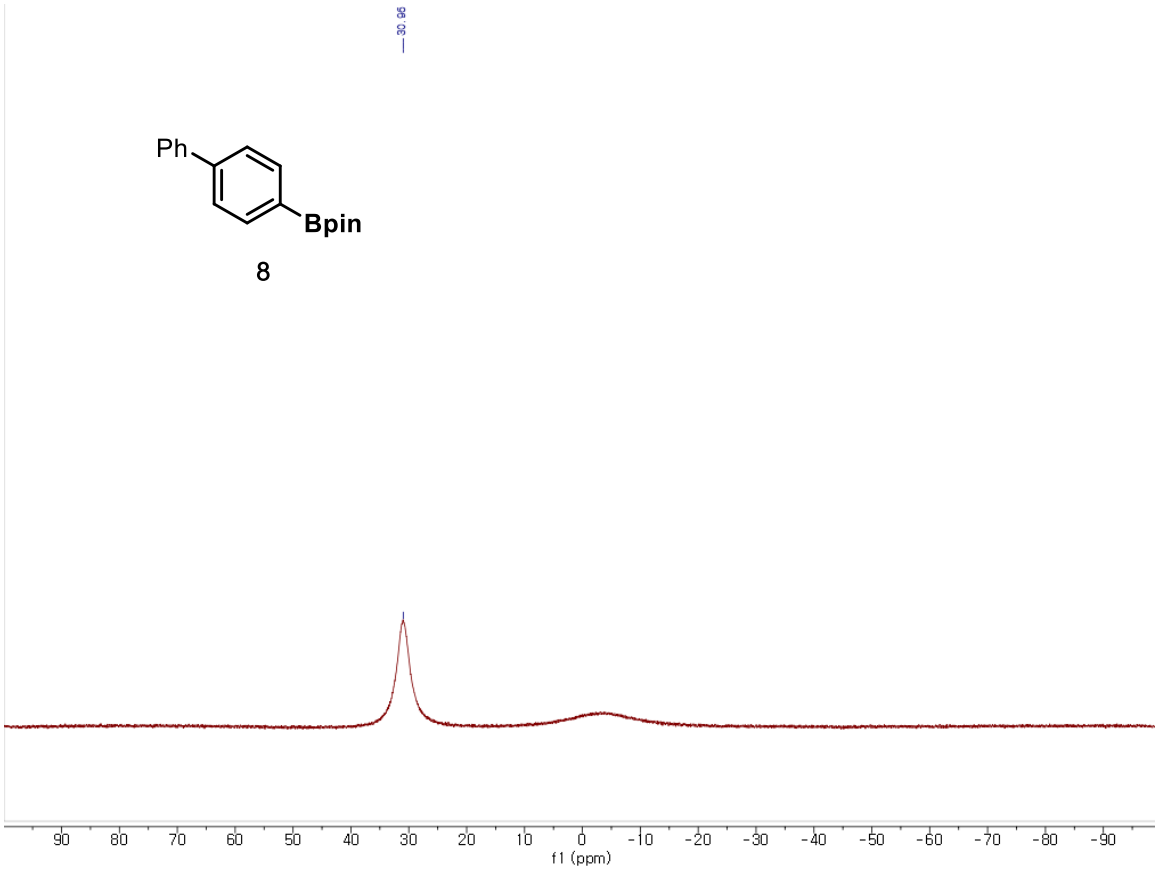
30.96
Ph
Bpin
8
90 80 70 60 50 40 30 20 10 0 -10 -20 -30 -40 -50 -60 -70 -80 -90
f1 (ppm)

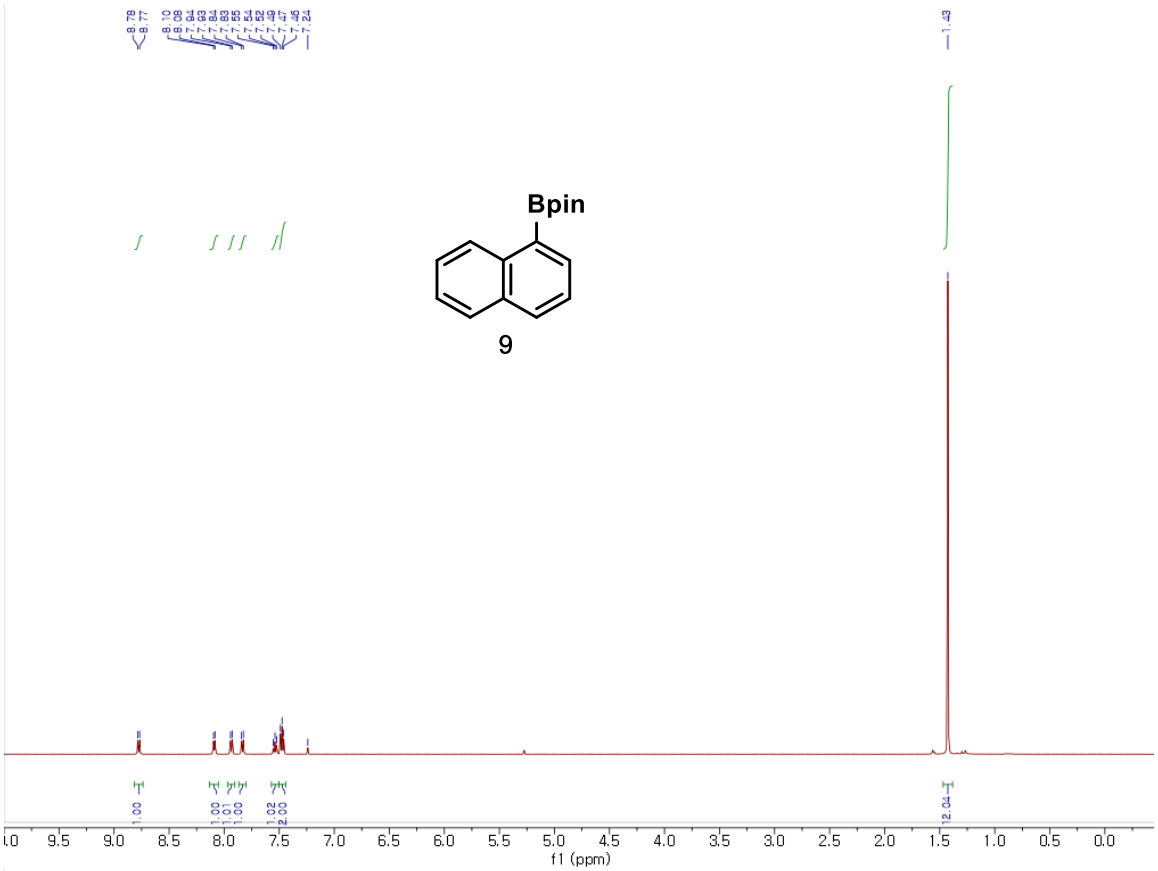
Bpin
9
f1 (ppm)

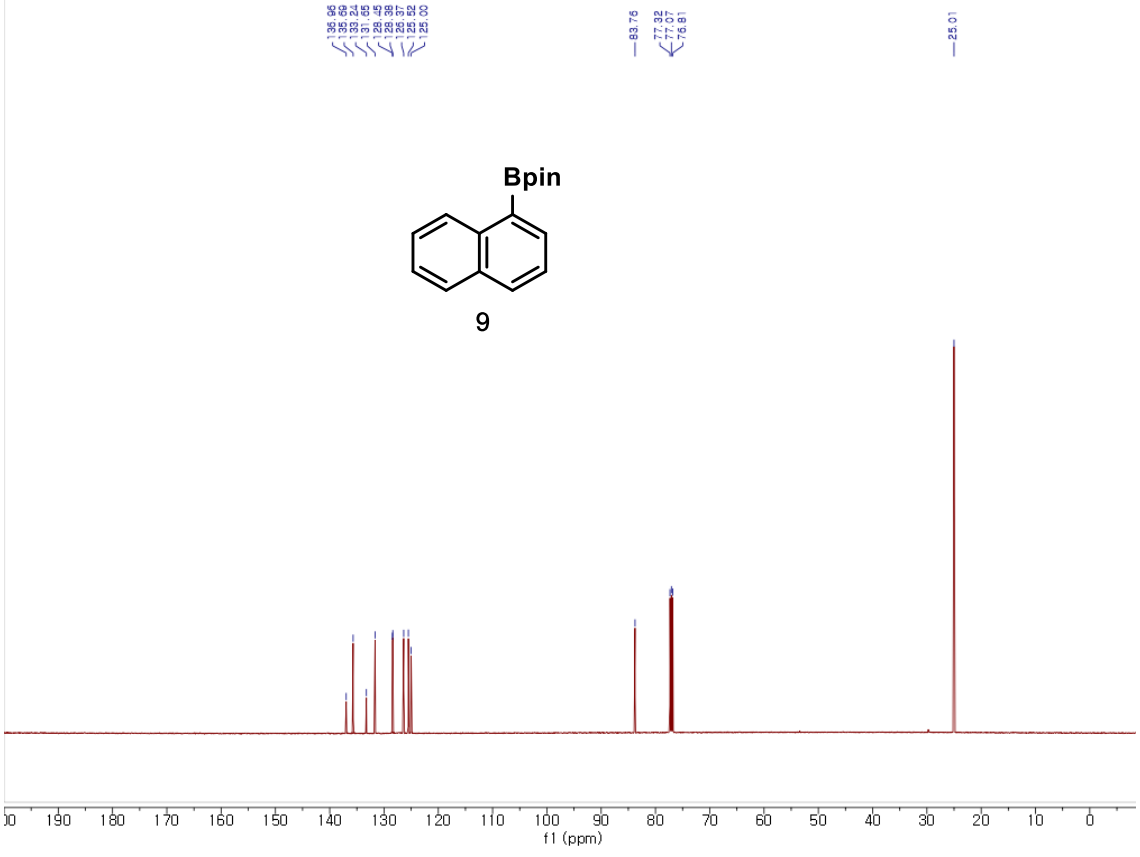
Bpin
9
f1 (ppm)

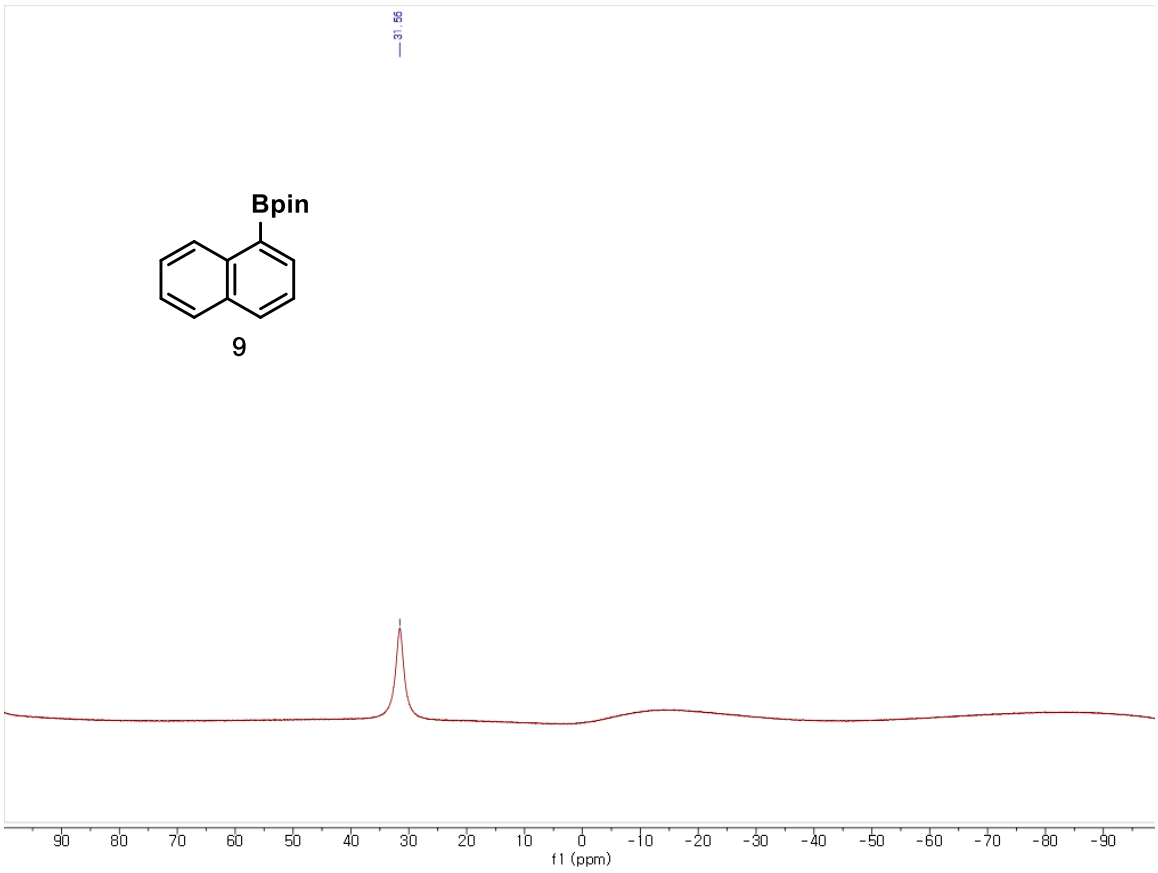
31.66
Bpin
9
90
80
70
60
50
40
30
20
10
0
-10
-20
-30
-40
-50
-60
-70
-80
-90
f1 (ppm)

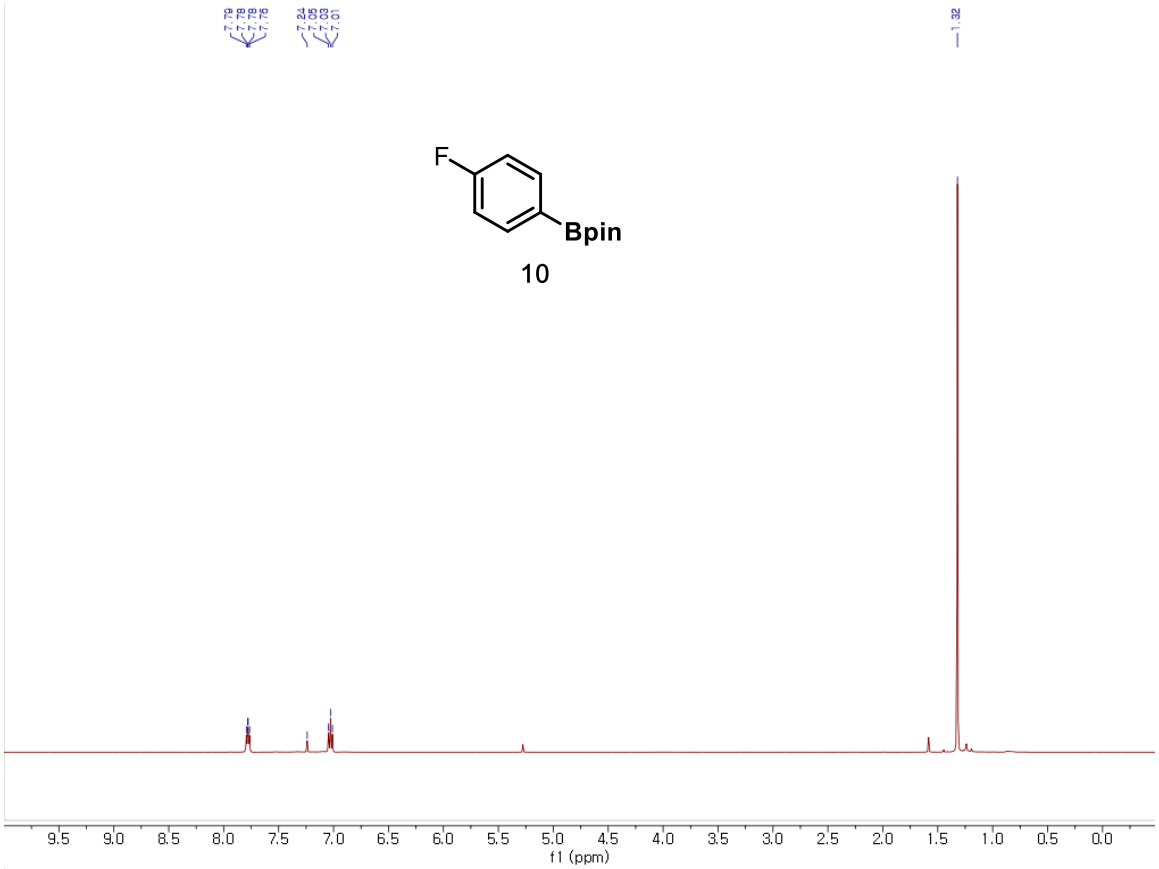
F
Bpin
10
f1 (ppm)

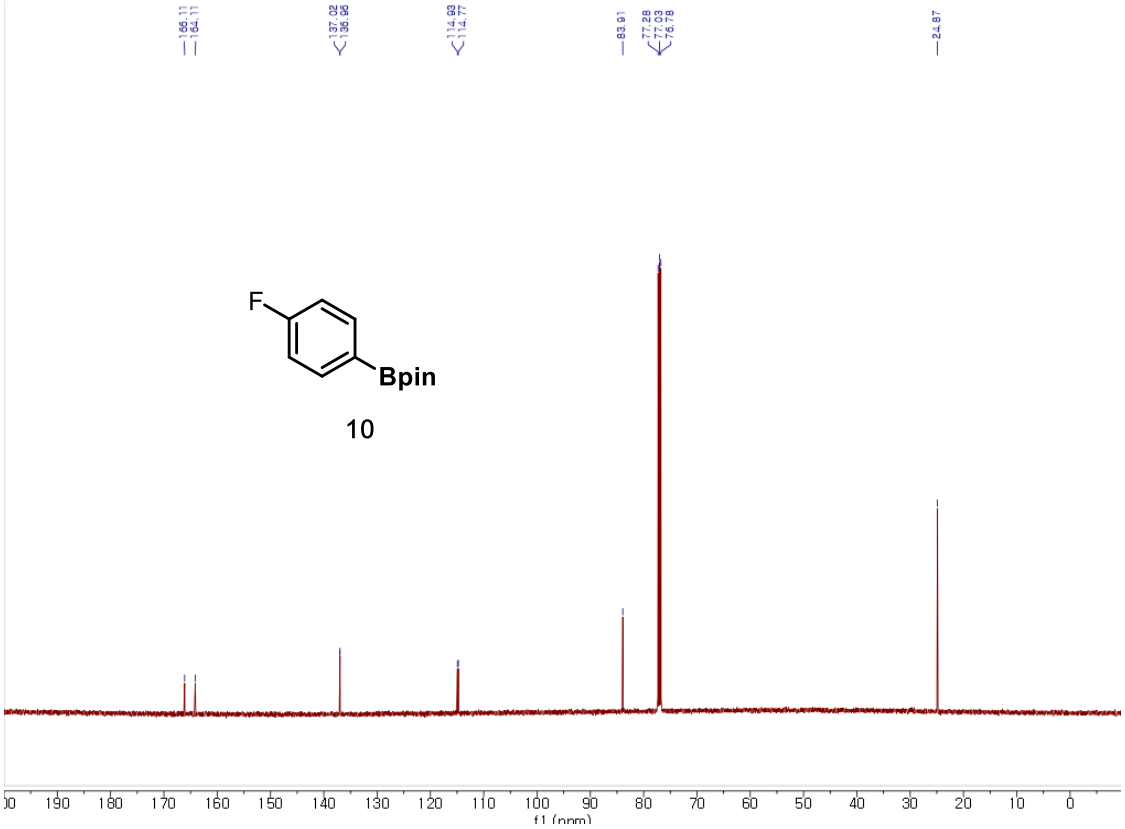
F
Bpin
10
f1 (ppm)

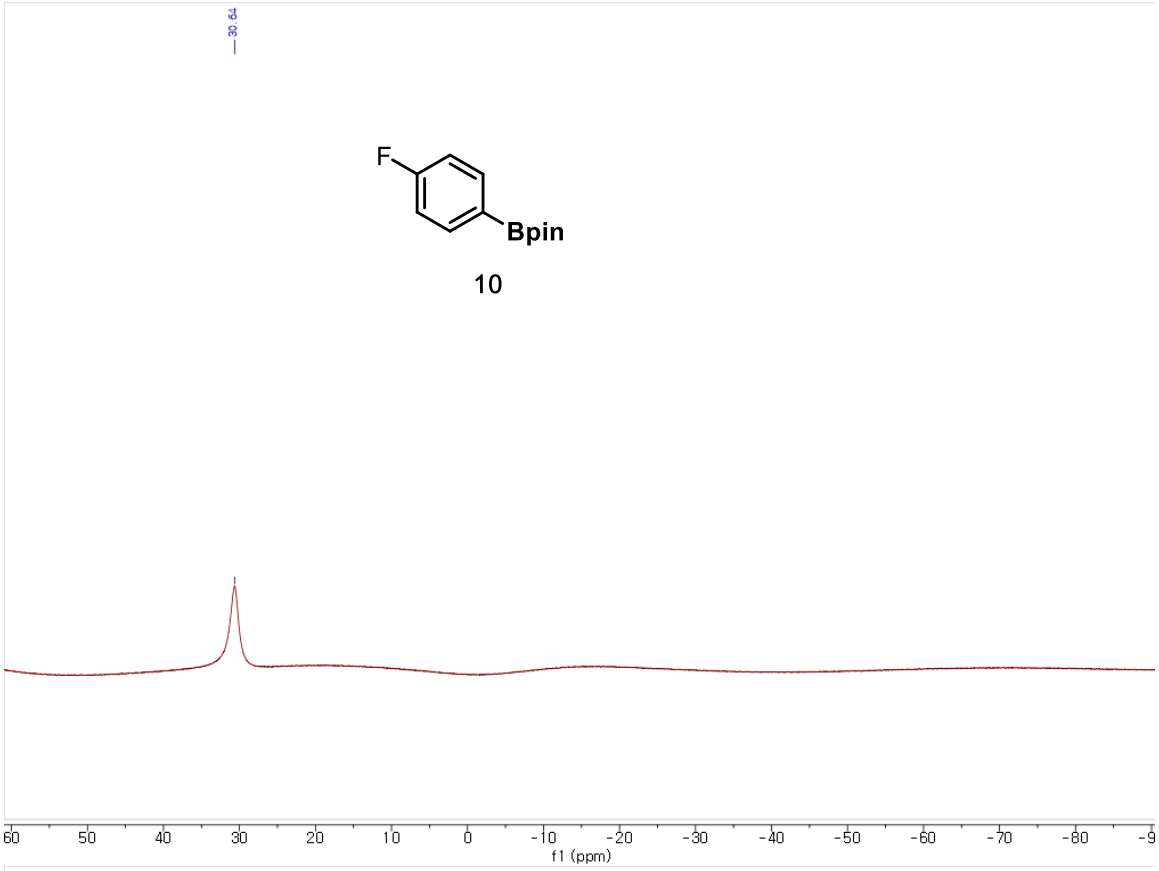
30.64
F
Bpin
10
60 50 40 30 20 10 0 -10 -20 -30 -40 -50 -60 -70 -80 -9
f1 (ppm)

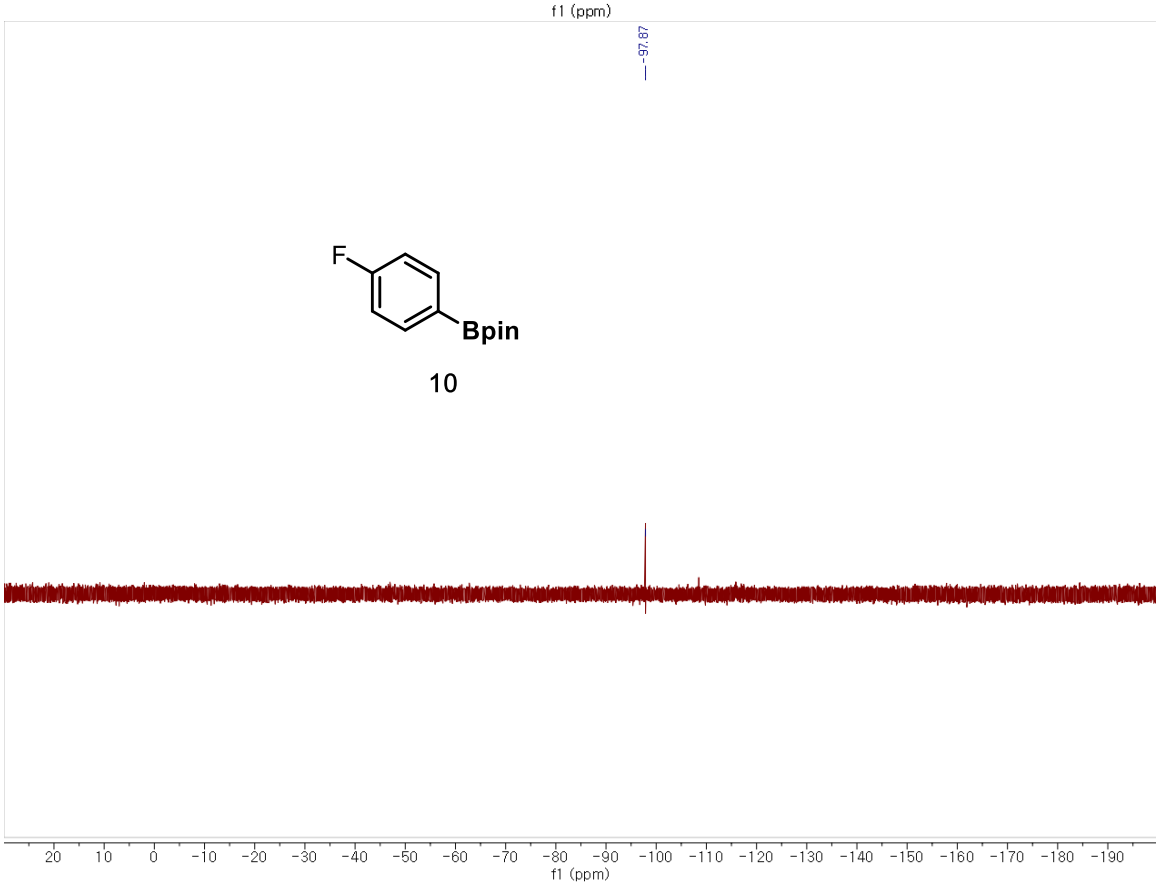
-97.87
F
Bpin
10
20 10 0 -10 -20 -30 -40 -50 -60 -70 -80 -90 -100 -110 -120 -130 -140 -150 -160 -170 -180 -190
f1 (ppm)

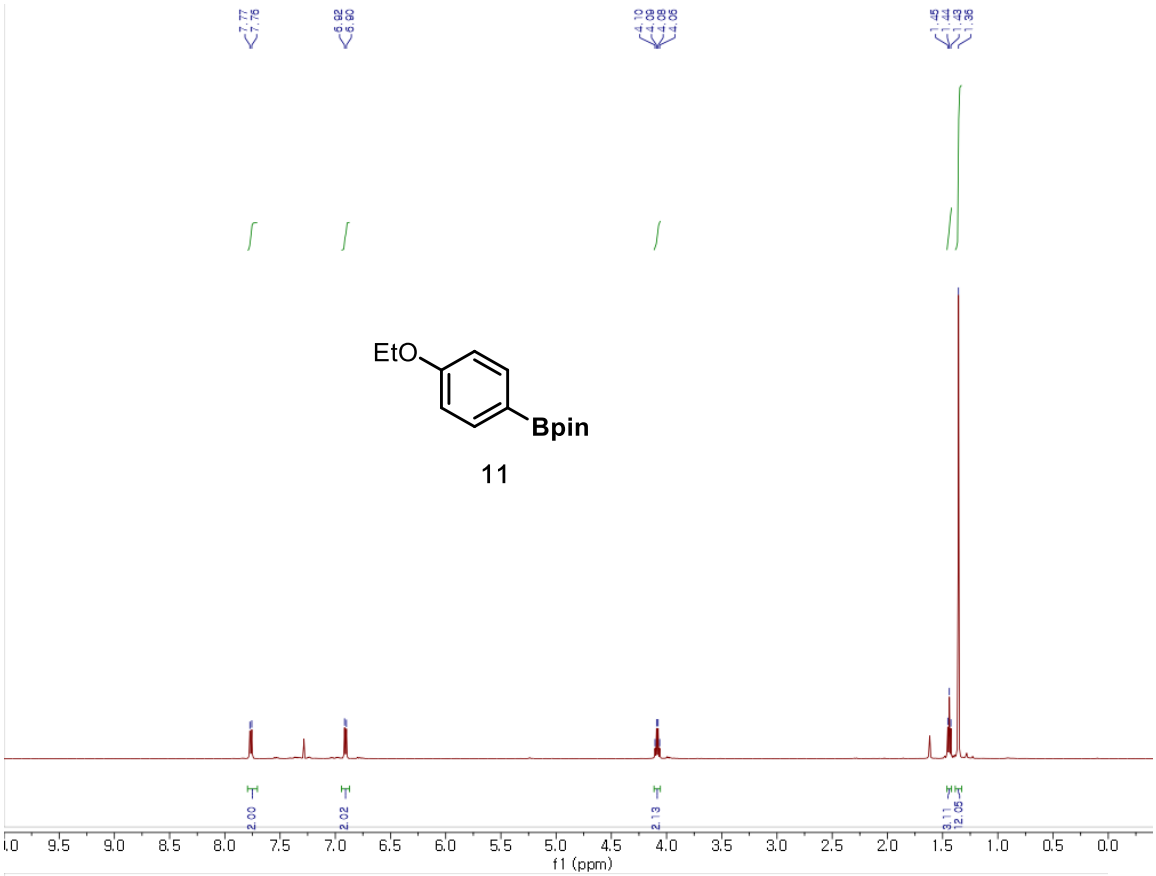
7.77
7.76
6.92
6.90
4.10
4.09
4.08
4.06
1.45
1.44
1.43
1.36
EtO
Bpin
2.00
2.02
2.13
3.11
12.05
f1 (ppm)

11

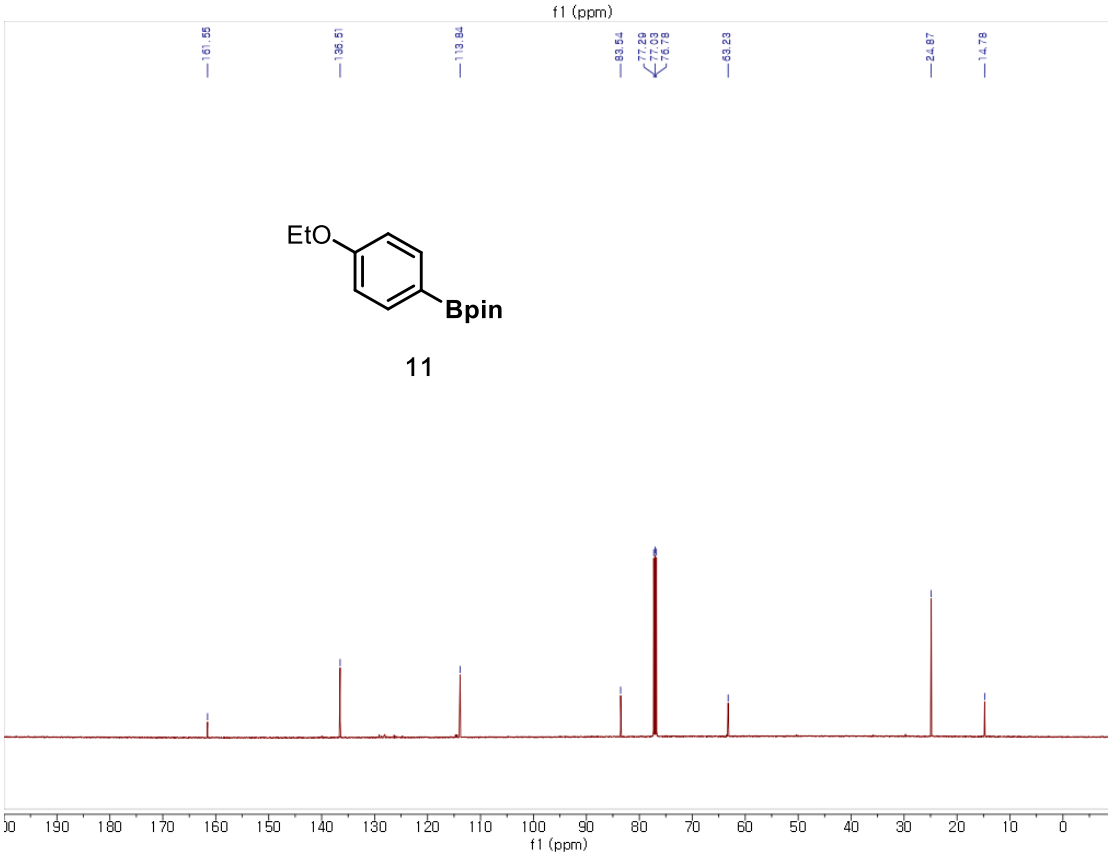
161.55
136.51
113.84
83.54
77.29
77.03
76.78
63.23
24.87
14.78
EtO
Bpin
f1 (ppm)

11

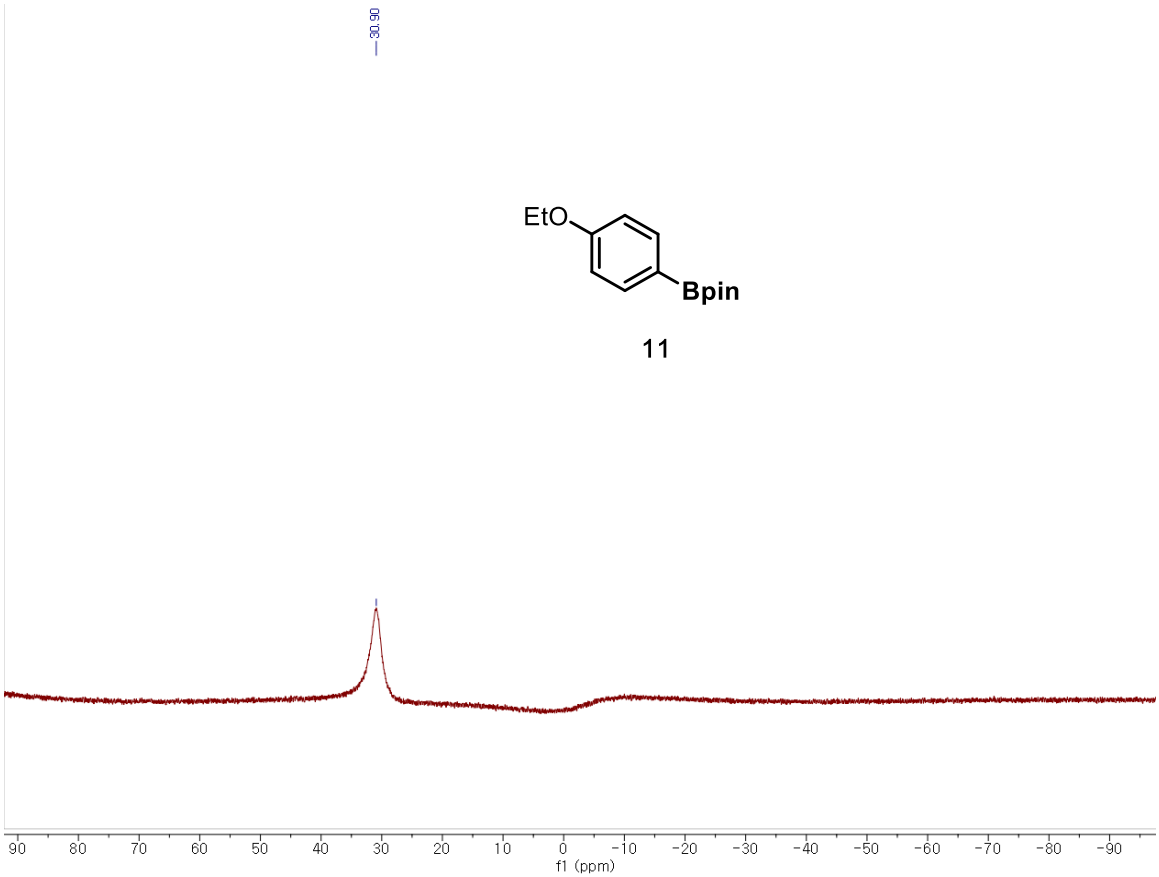
30.90
EtO
Bpin
11
90
80
70
60
50
40
30
20
10
0
-10
-20
-30
-40
-50
-60
-70
-80
-90
f1 (ppm)

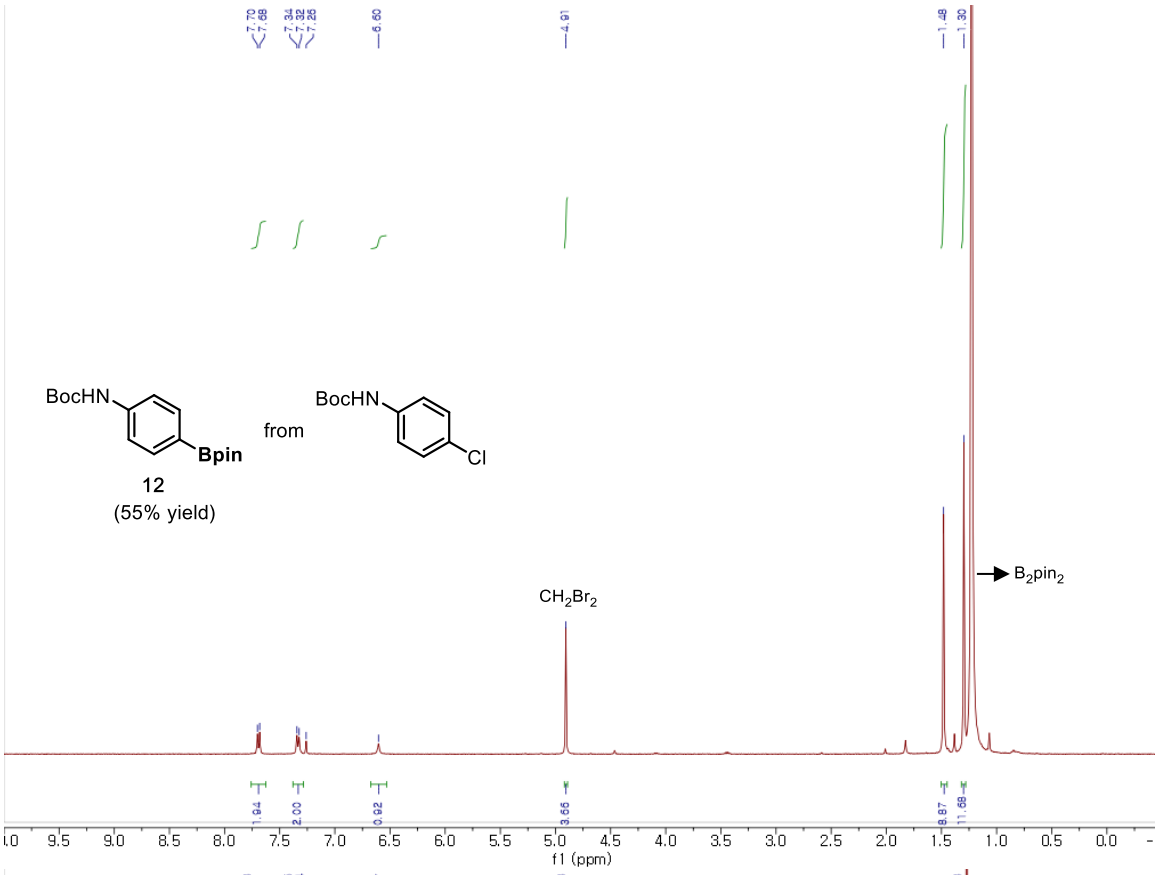
BocHN
Bpin
12
(55% yield)
from
BocHN
Cl
CH_2Br_2
B_2pin_2
f1 (ppm)

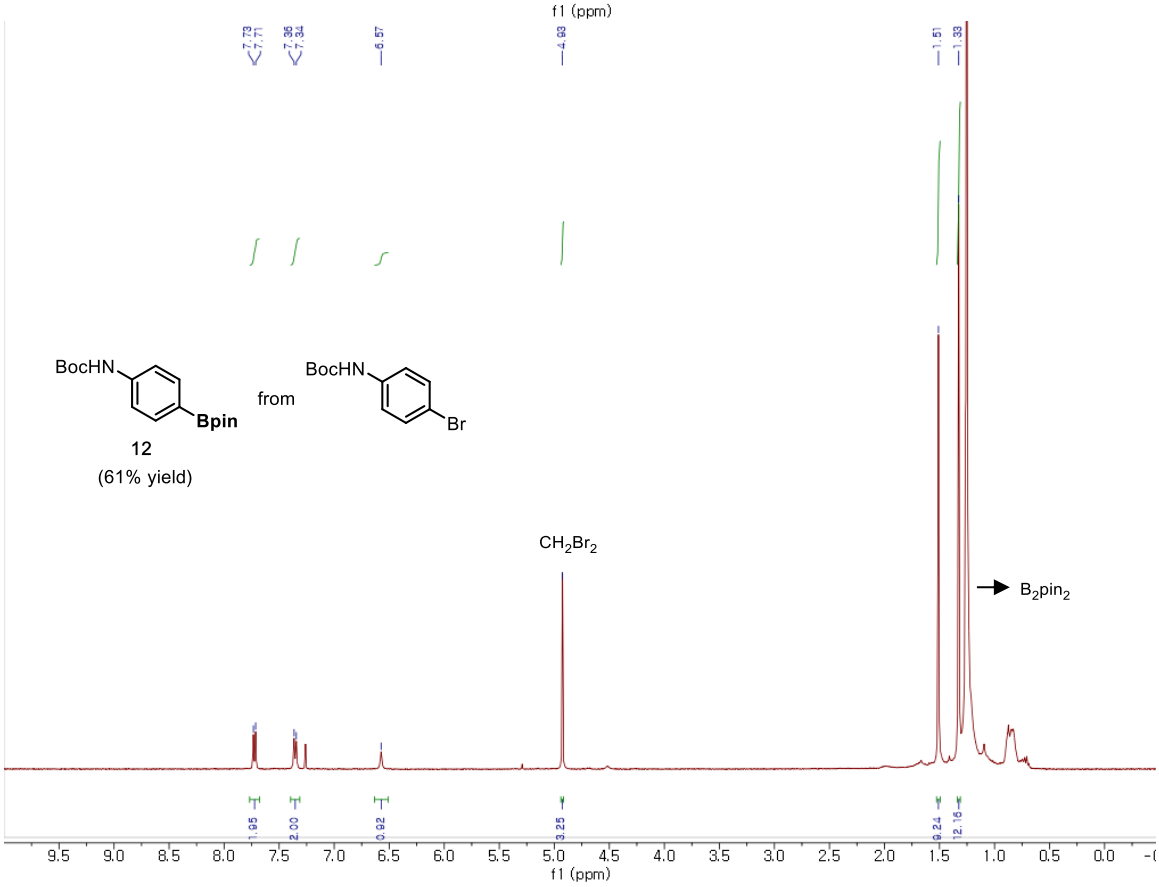
BocHN
Bpin
12
(61% yield)
from
BocHN
Br
CH_2Br_2
B_2pin_2
f1 (ppm)

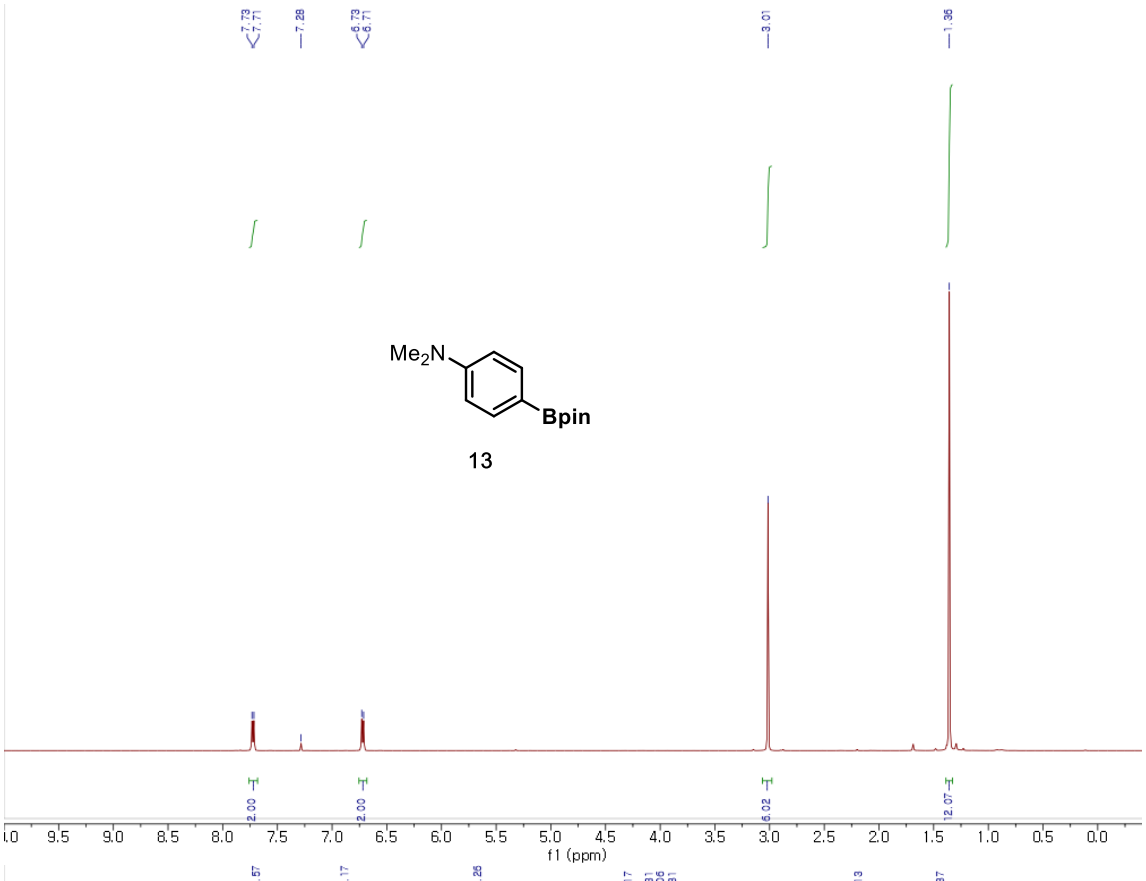
7.73
7.71
7.28
6.73
6.71
3.01
1.36
Me2N
Bpin
2.00
2.00
6.02
12.07
f1 (ppm)

13

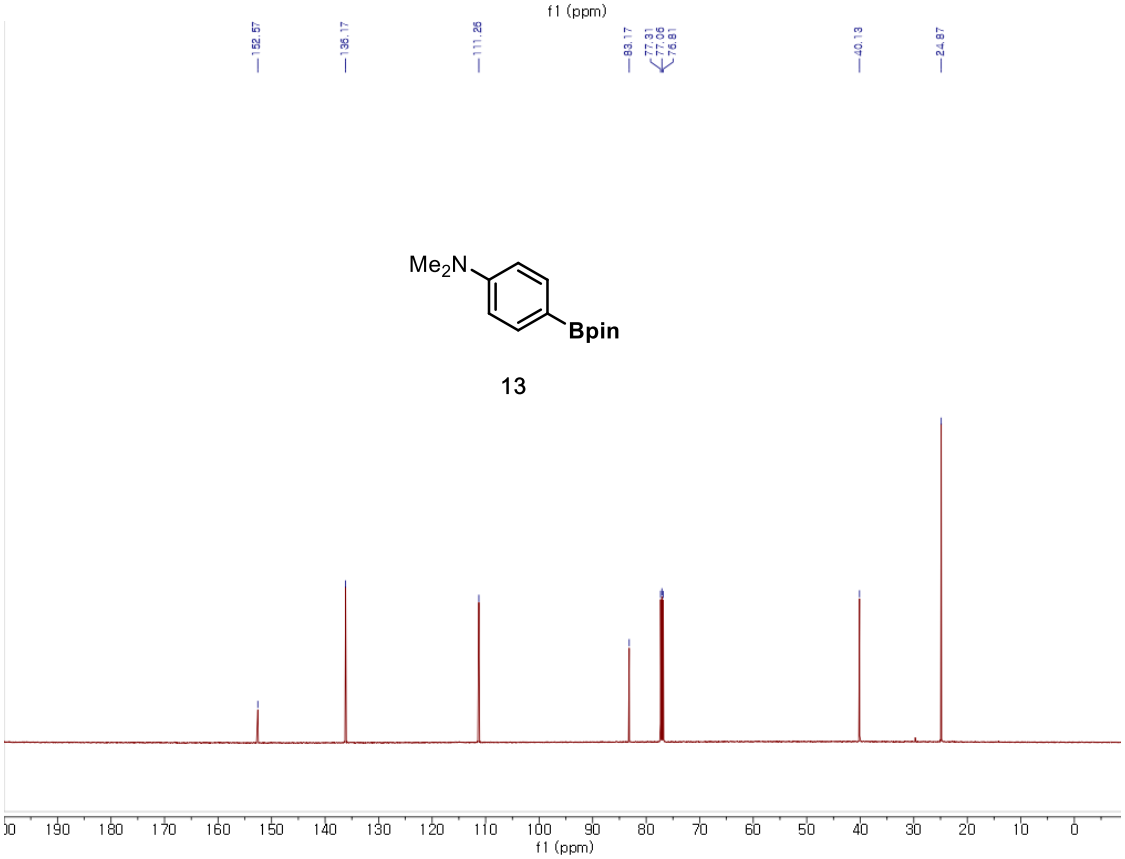
152.57
136.17
111.28
83.17
77.31
77.06
76.81
40.13
24.87
Me2N
Bpin
f1 (ppm)

13

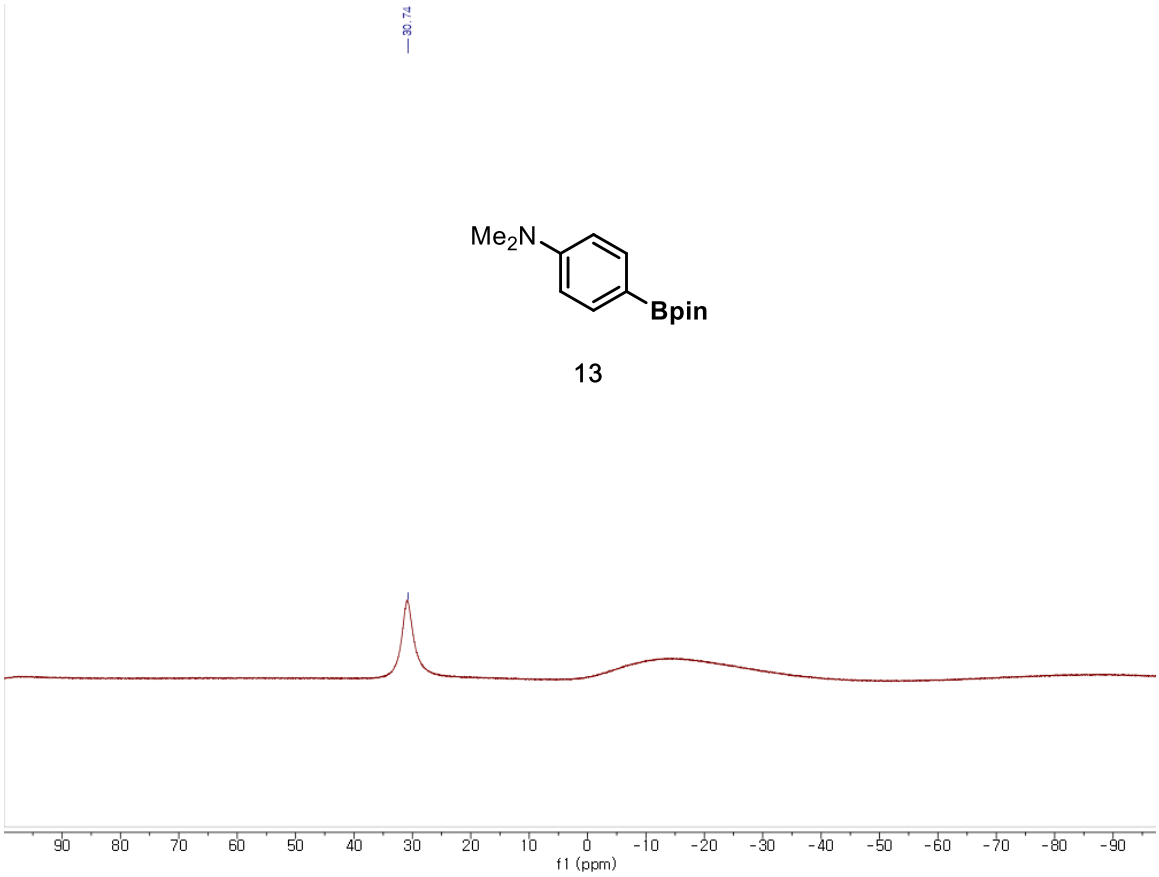
30.74
Me2N
Bpin
13
90 80 70 60 50 40 30 20 10 0 -10 -20 -30 -40 -50 -60 -70 -80 -90
f1 (ppm)

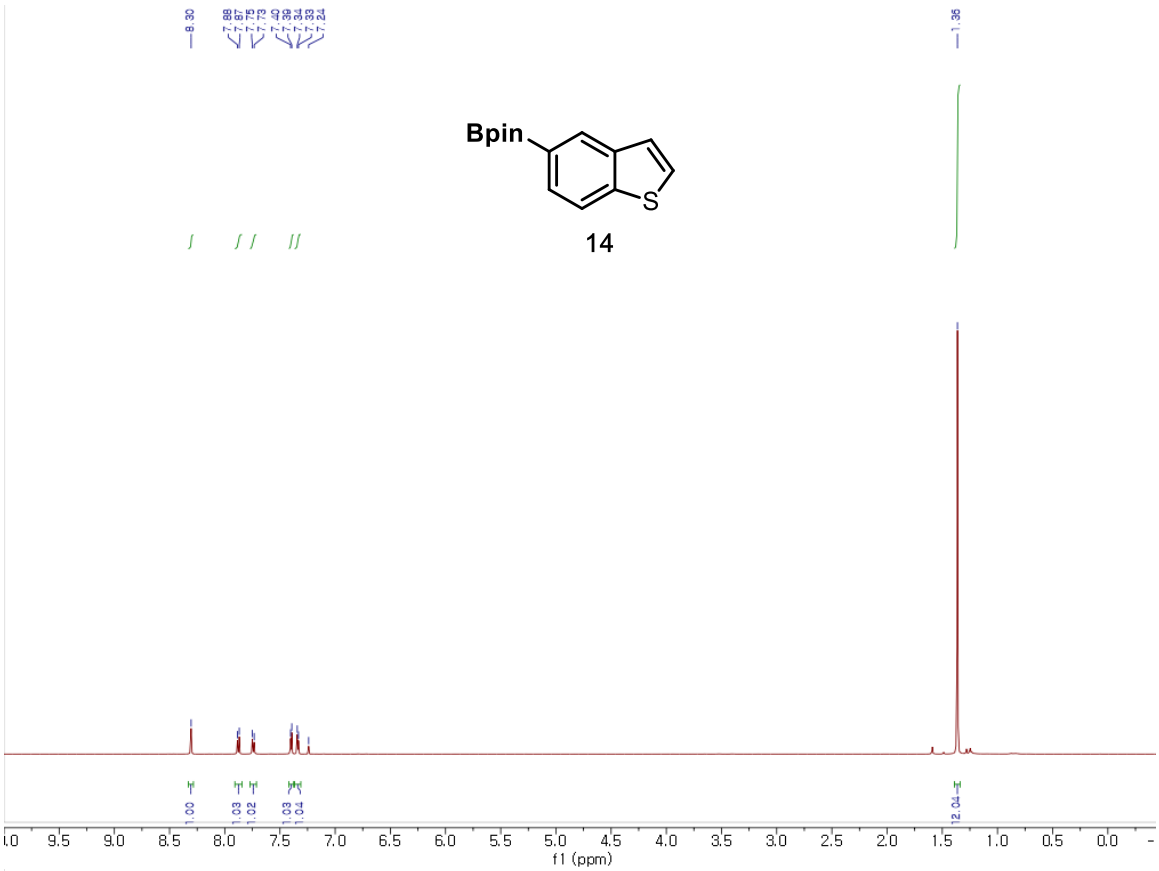
8.30
7.88
7.85
7.75
7.73
7.40
7.38
7.34
7.33
7.24
1.36
Bpin
S
14
1.00
1.03
1.02
1.03
1.04
12.04
f1 (ppm)

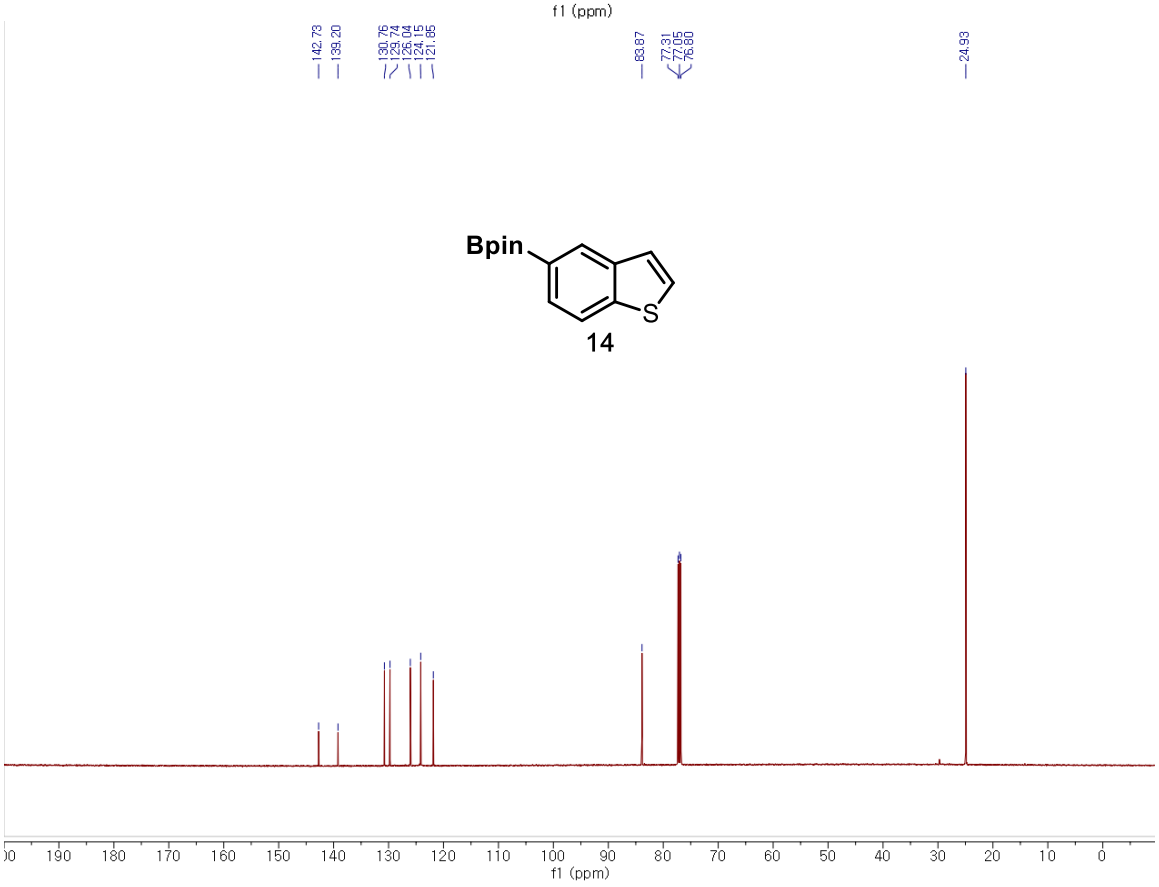
142.73
139.20
130.76
129.74
126.04
124.15
121.85
83.87
77.31
77.05
76.80
24.93
Bpin
S
14
f1 (ppm)

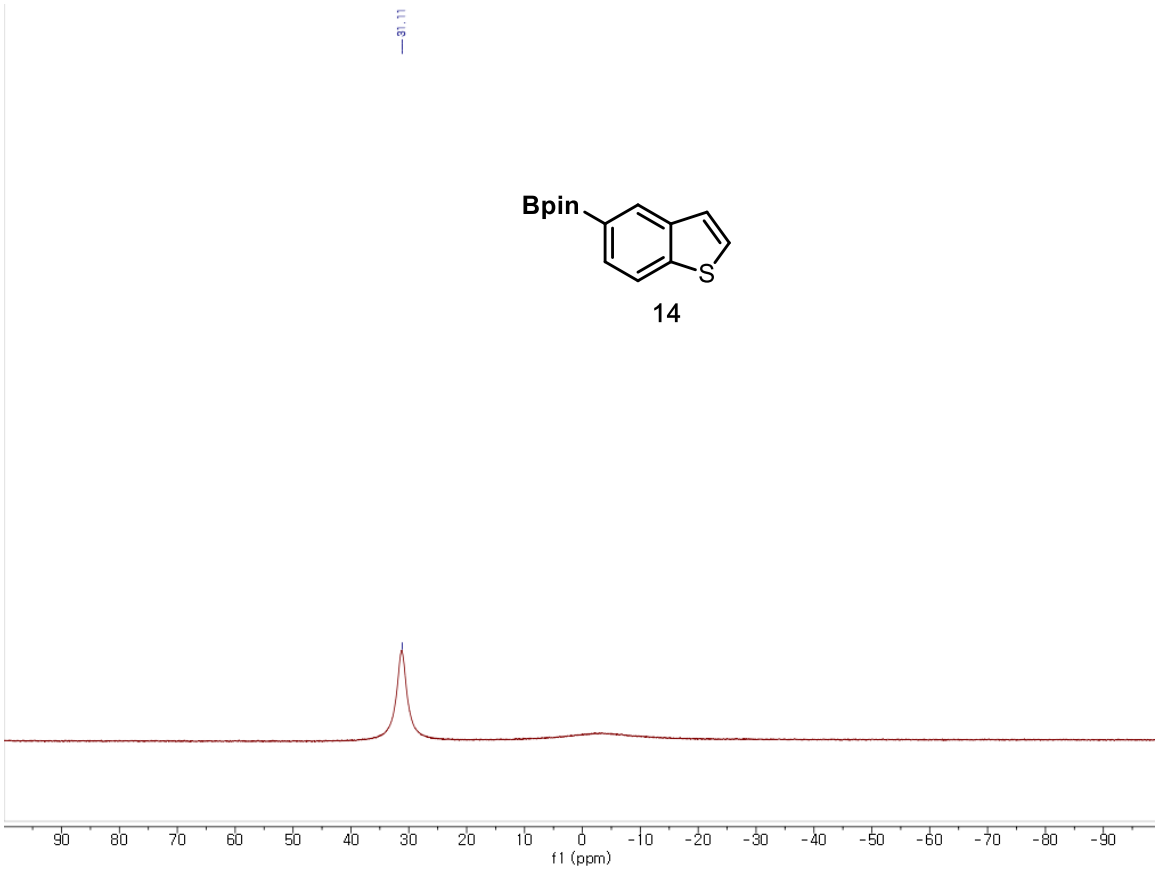
31.11
Bpin
S
14
90
80
70
60
50
40
30
20
10
0
-10
-20
-30
-40
-50
-60
-70
-80
-90
f1 (ppm)

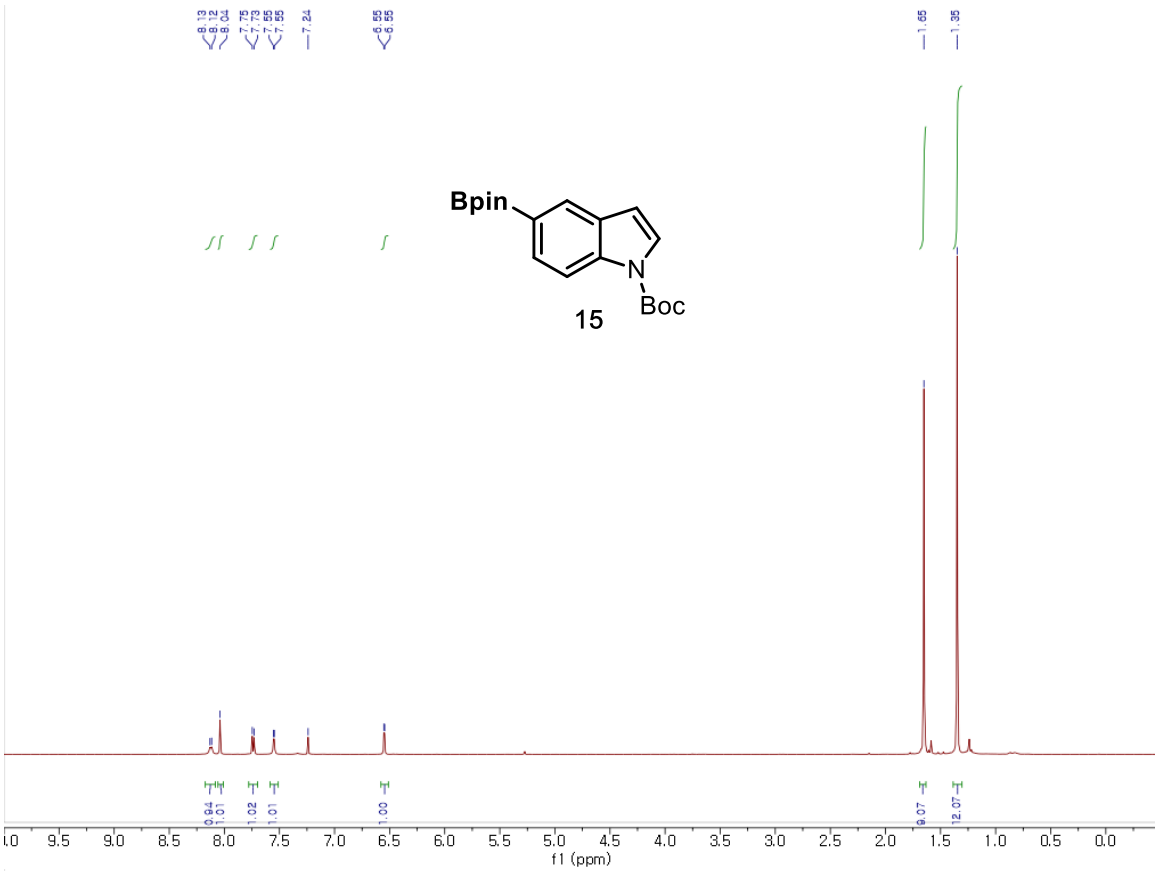
Bpin
N
Boc
15
f1 (ppm)

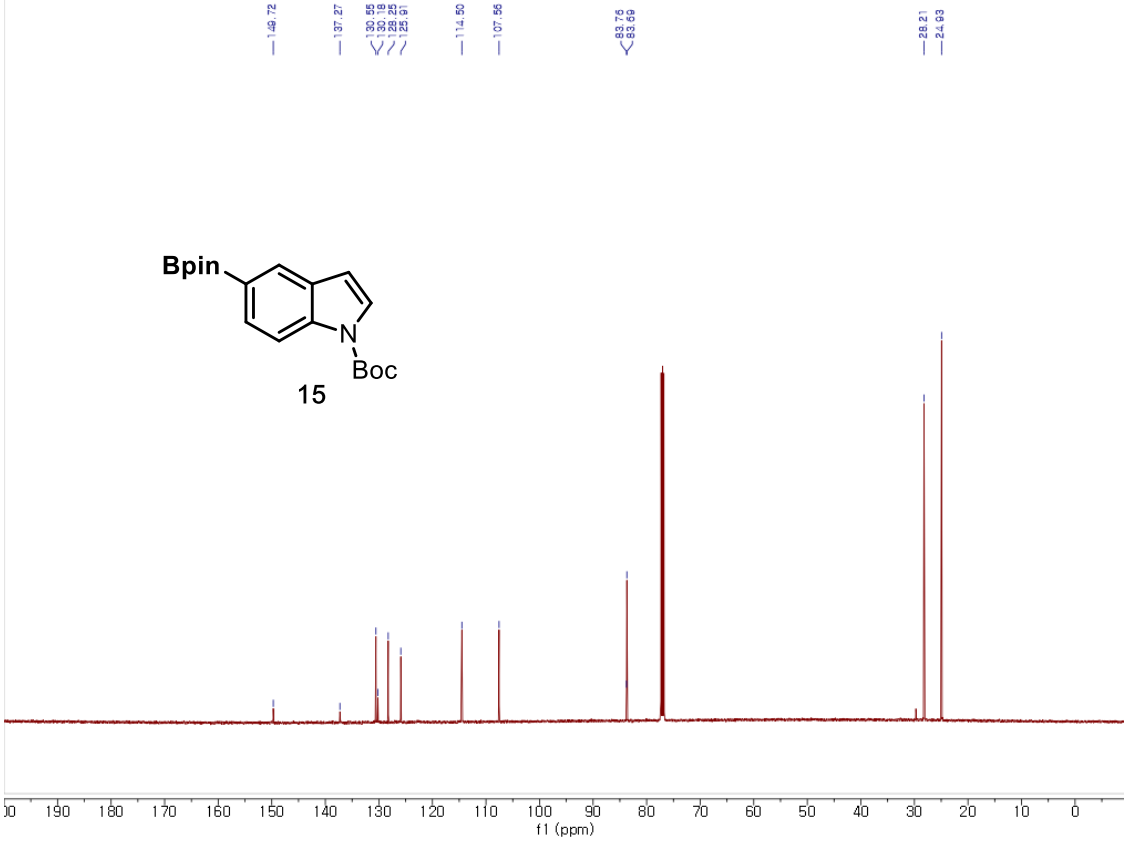
Bpin
N
Boc
15
f1 (ppm)

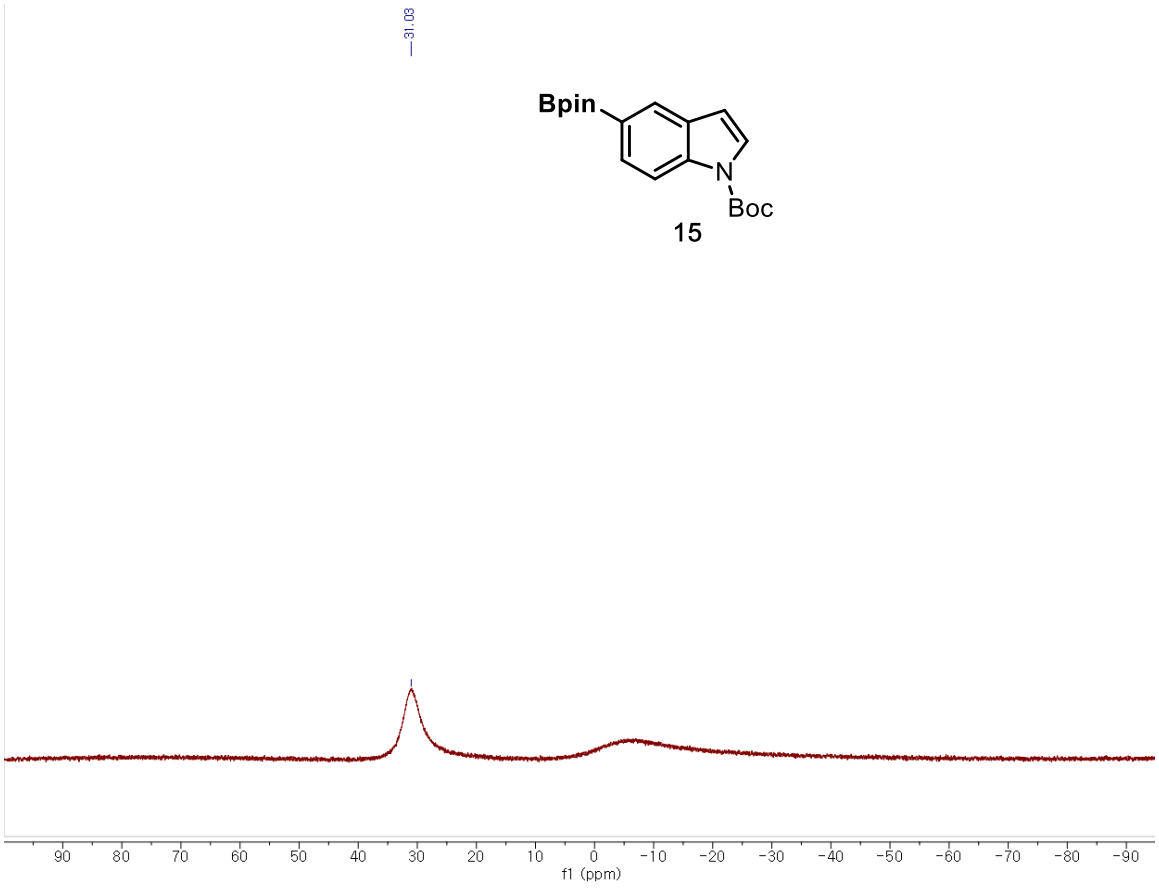
31.03
Bpin
N
Boc
15
90
80
70
60
50
40
30
20
10
0
-10
-20
-30
-40
-50
-60
-70
-80
-90
f1 (ppm)

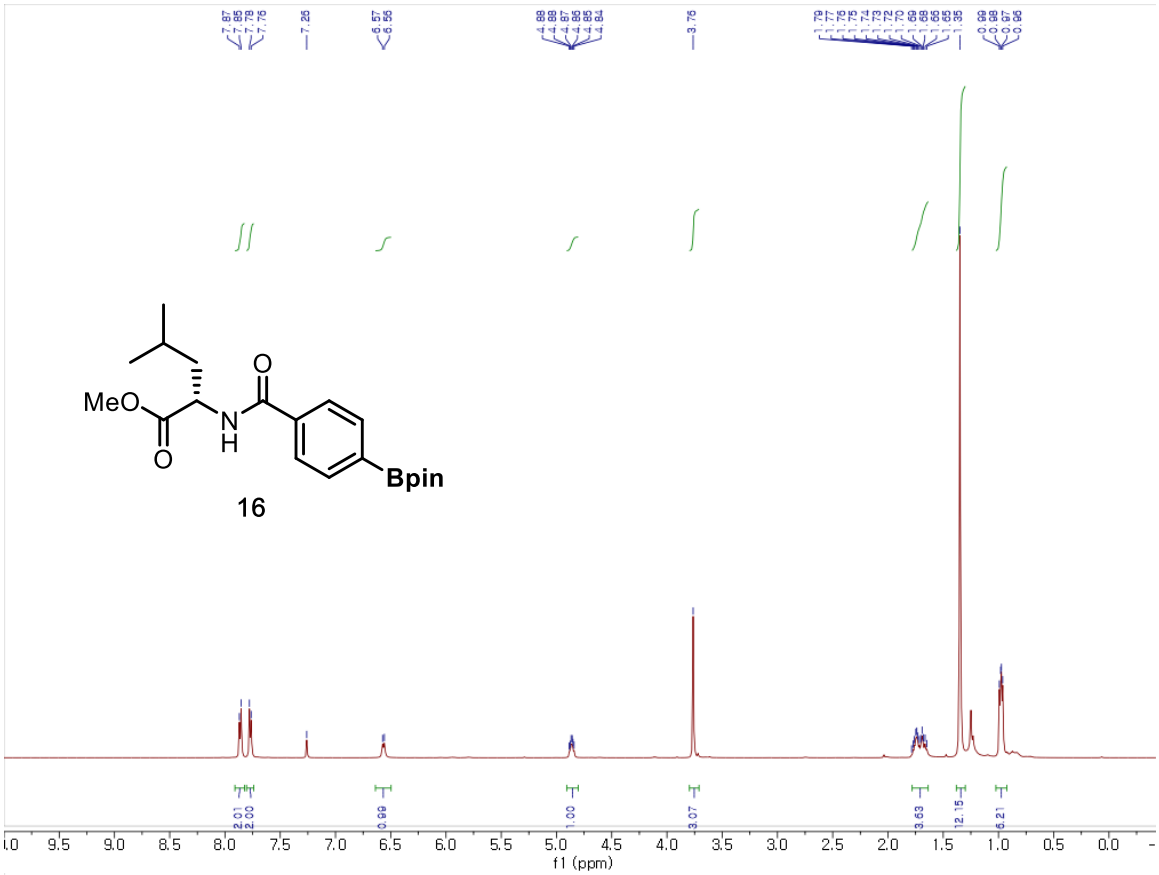
MeO
O
N
H
O
Bpin
16
f1 (ppm)

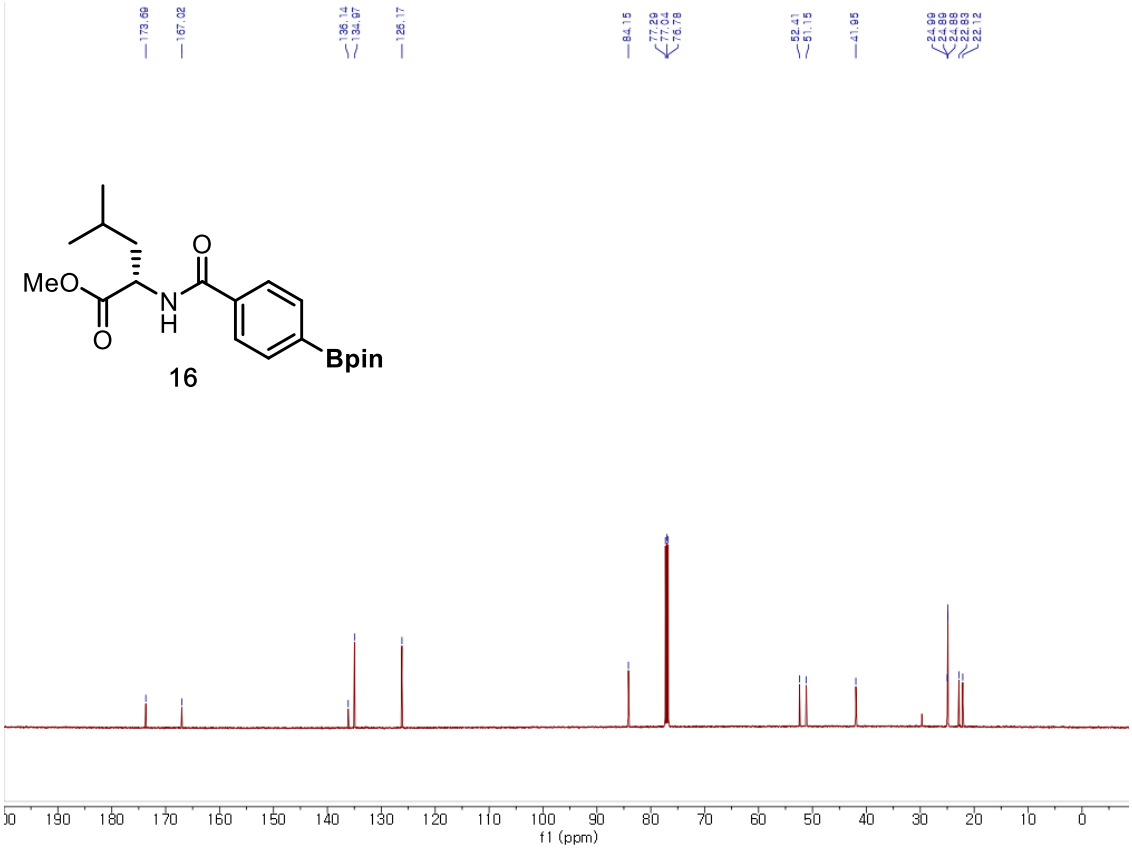
MeO
O
N
H
O
Bpin
16
f1 (ppm)

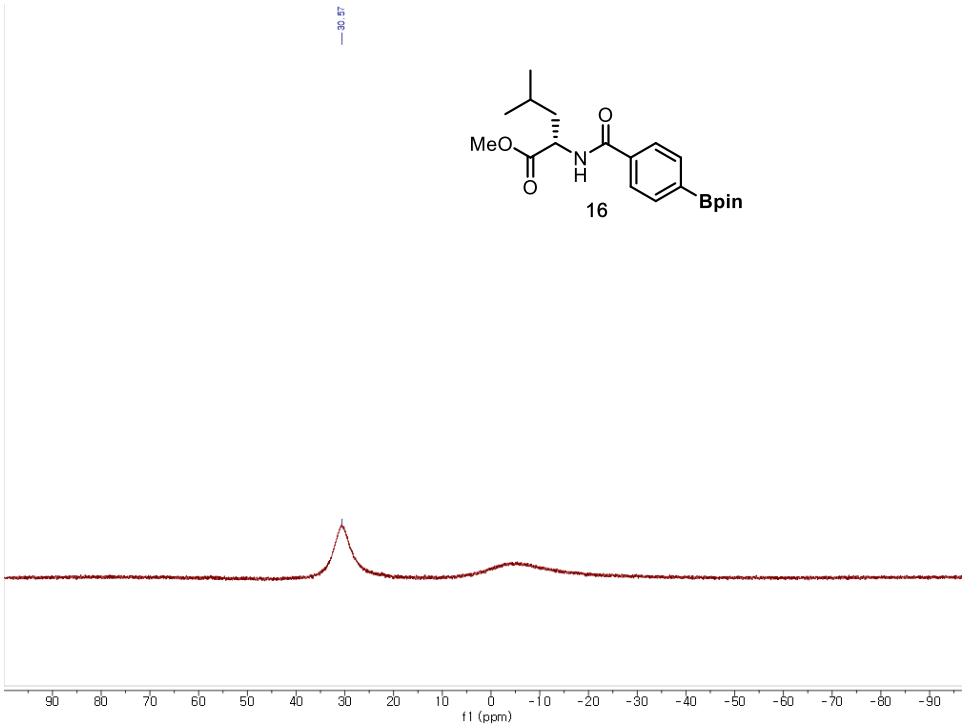

HPLC Data for (rac)-**16** [IA, Hex/*i*PrOH = 95/5, 1.0 mL/min, t_1 = 12.453 min (R), t_2 = 16.083 min (S)]

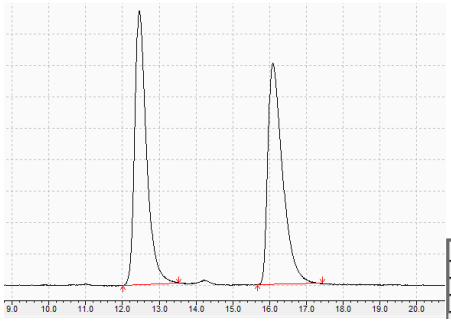

Peak#	Peak Start	Peak End	Ret. Time	Area	Height	Area%
1	12.011	13.525	12.453	4877653	217947	49.950
2	15.669	17.429	16.083	4887425	175633	50.050
Total				9765079	393580	100.000

HPLC Data for (S)-**16** [IA, Hex/*i*PrOH = 95/5, 1.0 mL/min, t_1 = 12.542 min (R), t_2 = 15.949 min (S)]

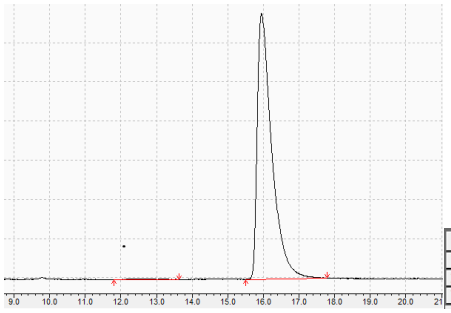

Peak#	Peak Start	Peak End	Ret. Time	Area	Height	Area%
1	11.808	13.632	12.542	40683	812	0.421
2	15.499	17.792	15.949	9617477	339569	99.579
Total				9658160	340382	100.000

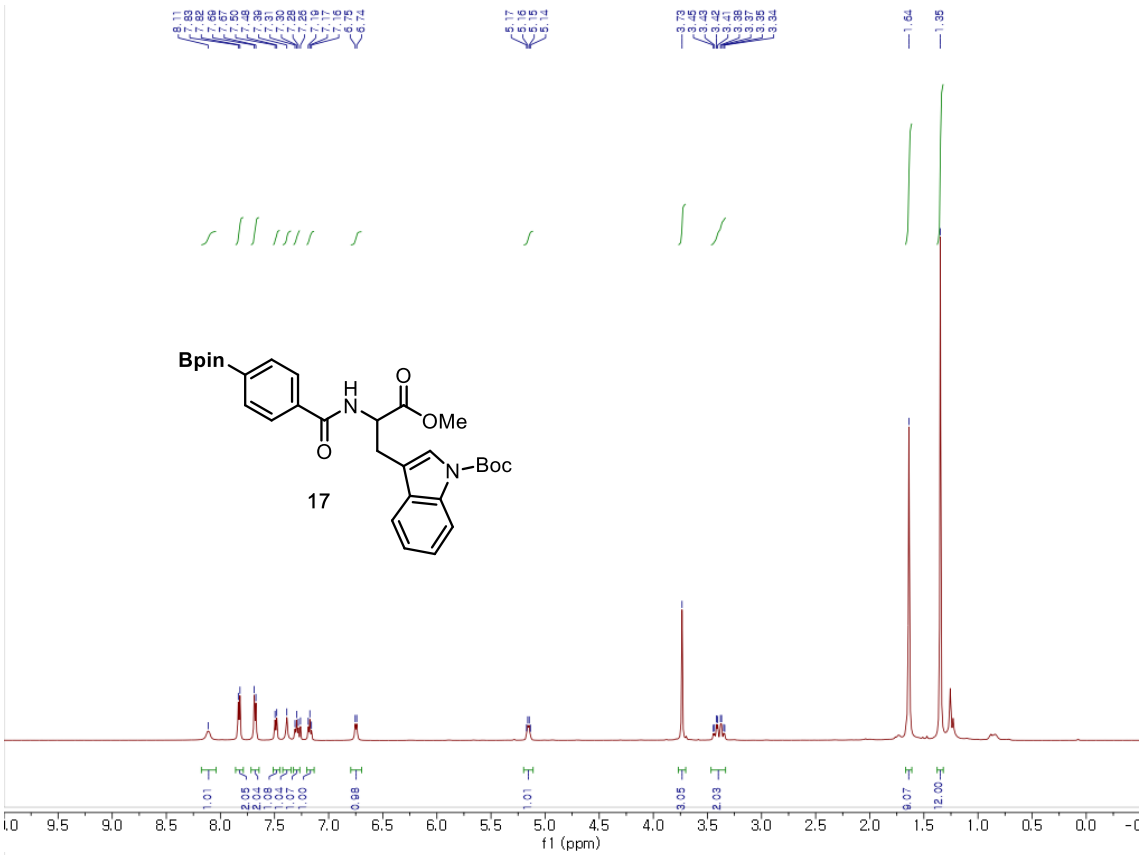
Bpin
H
N
O
OMe
O
N–Boc
17
f1 (ppm)

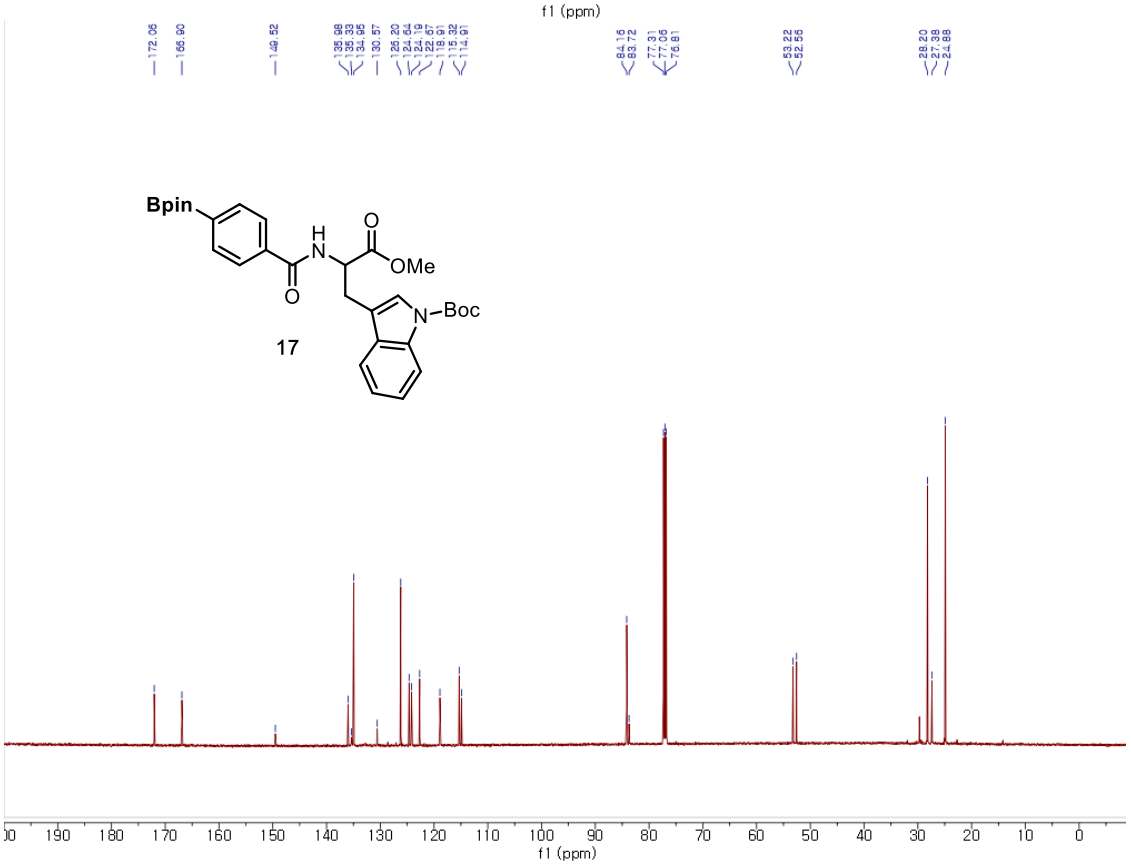
Bpin
H
N
O
OMe
O
N–Boc
17
f1 (ppm)

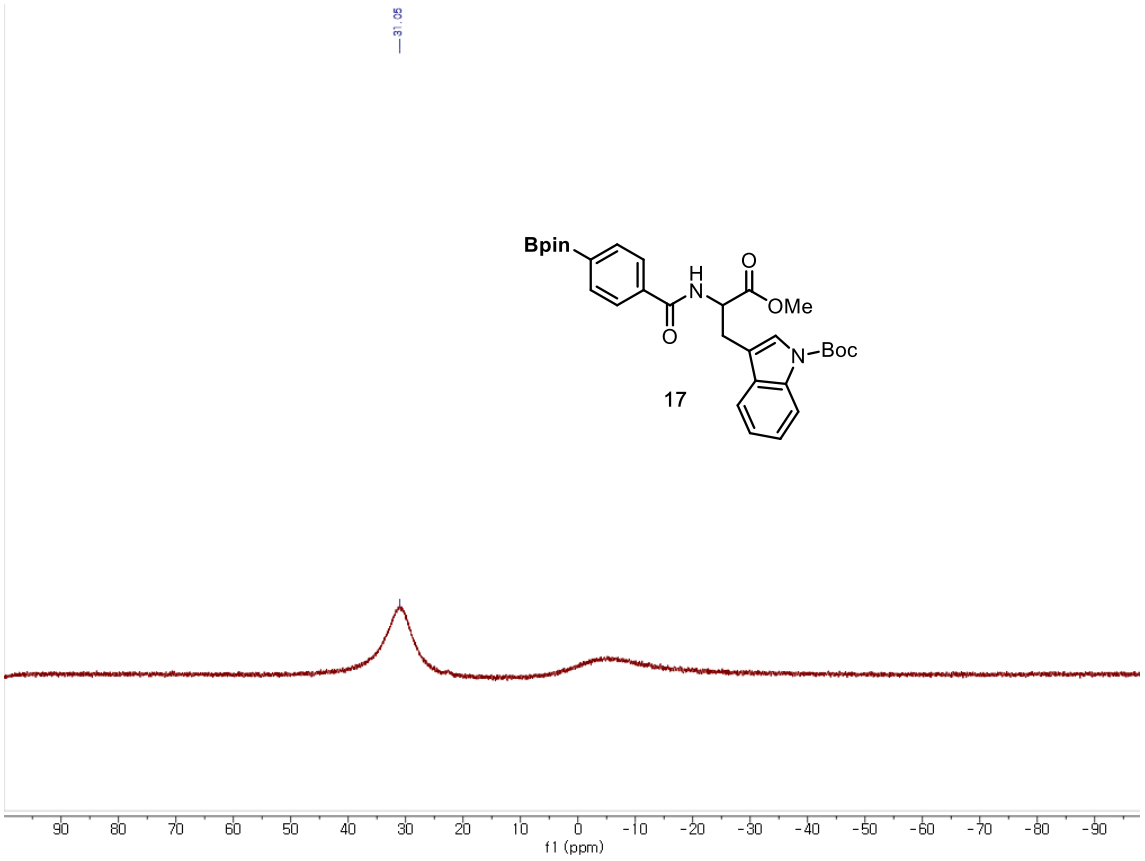
31.05
Bpin
H
N
O
O
OMe
O
N–Boc
17
90
80
70
60
50
40
30
20
10
0
-10
-20
-30
-40
-50
-60
-70
-80
-90
f1 (ppm)

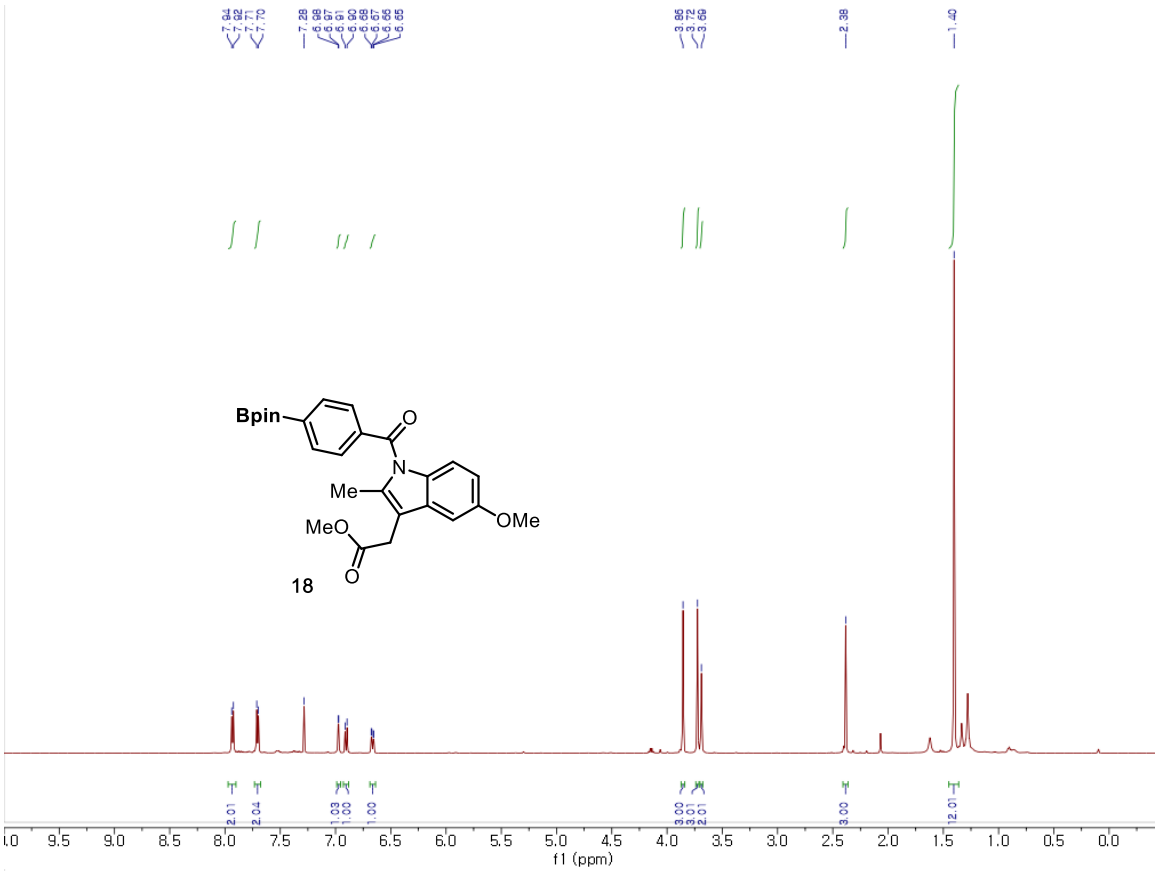
Bpin
O
N
Me
MeO
OMe
O
18
f1 (ppm)

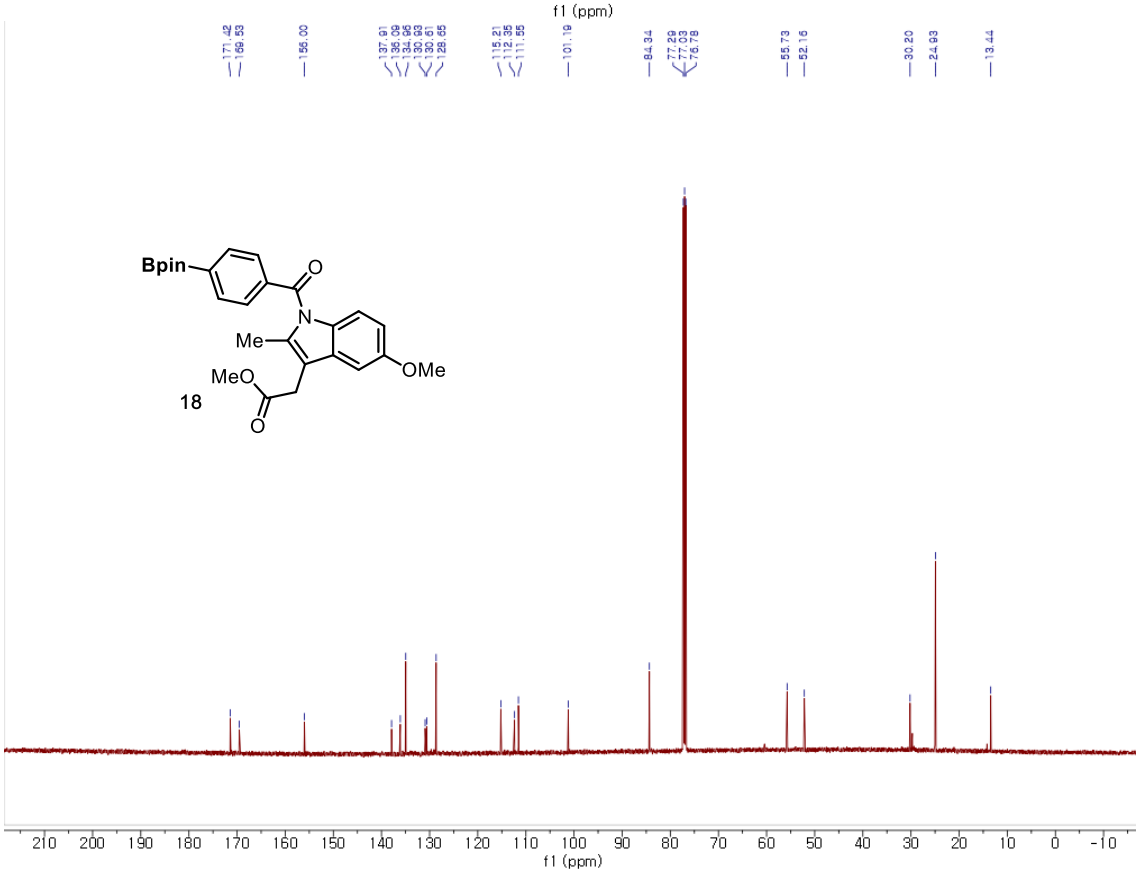
Bpin
O
N
Me
MeO
OMe
O
18
f1 (ppm)

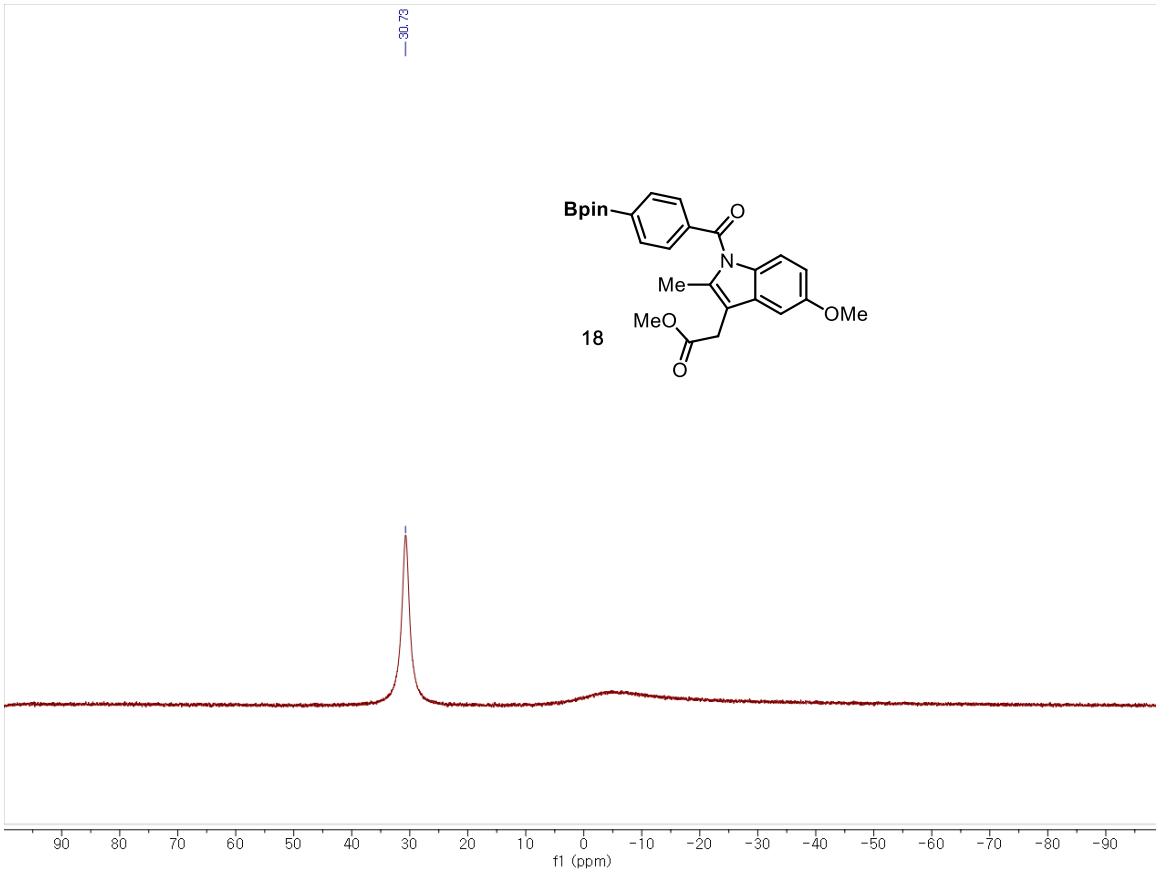
30.73
Bpin
O
N
Me
MeO
OMe
O
18
90
80
70
60
50
40
30
20
10
0
-10
-20
-30
-40
-50
-60
-70
-80
-90
f1 (ppm)

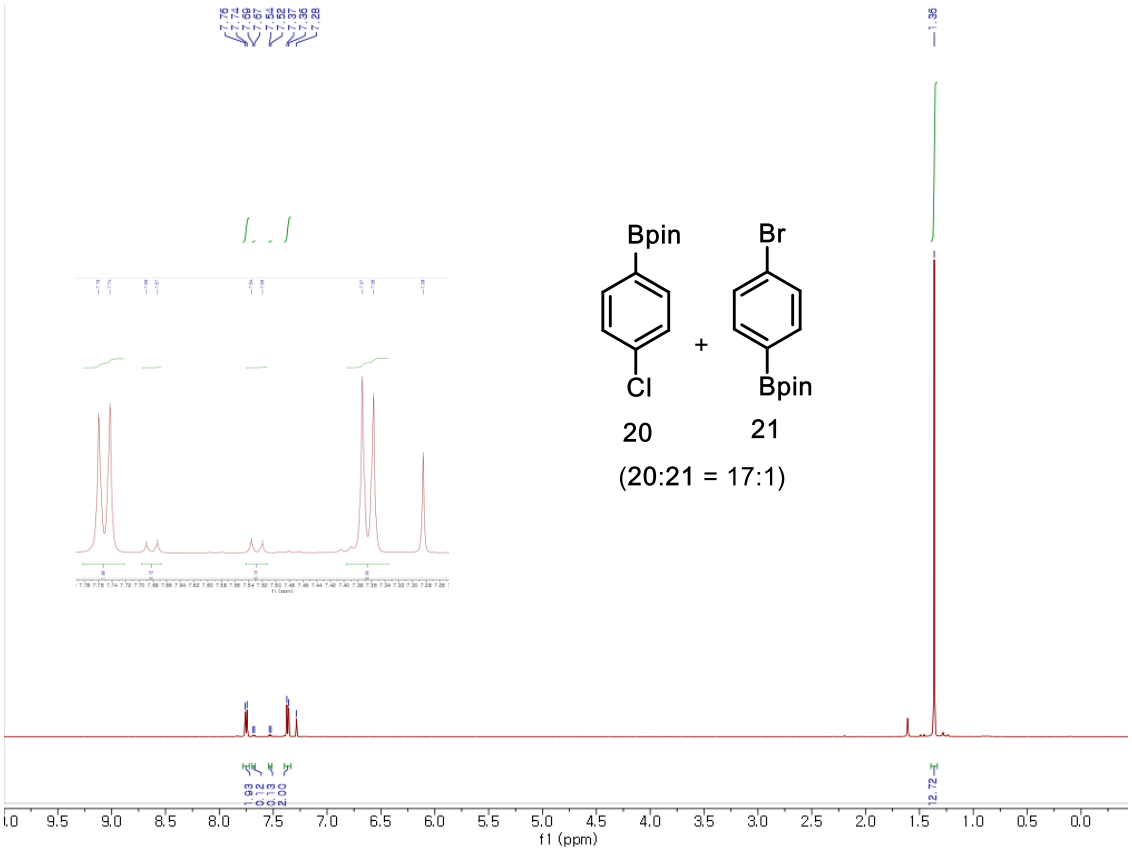
Bpin
Br
Cl
Bpin
20
21
(20:21 = 17:1)
f1 (ppm)

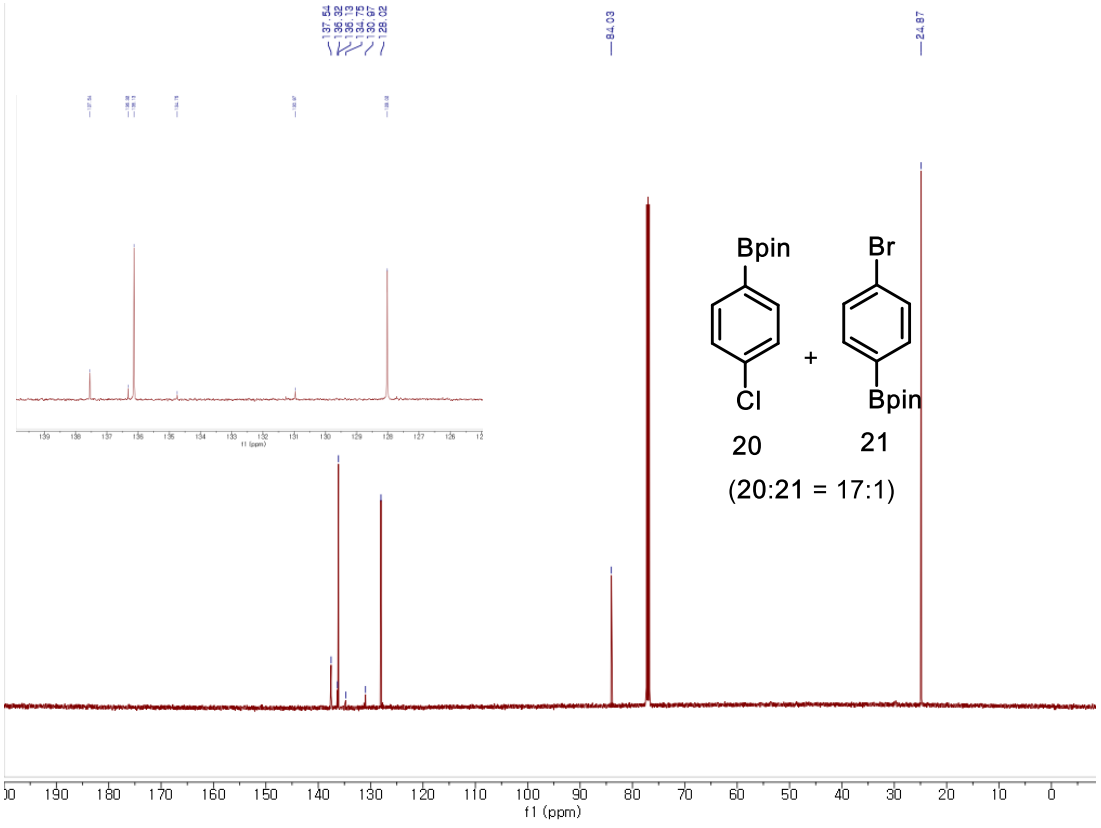
Bpin
Br
Cl
Bpin
20
21
(20:21 = 17:1)
f1 (ppm)

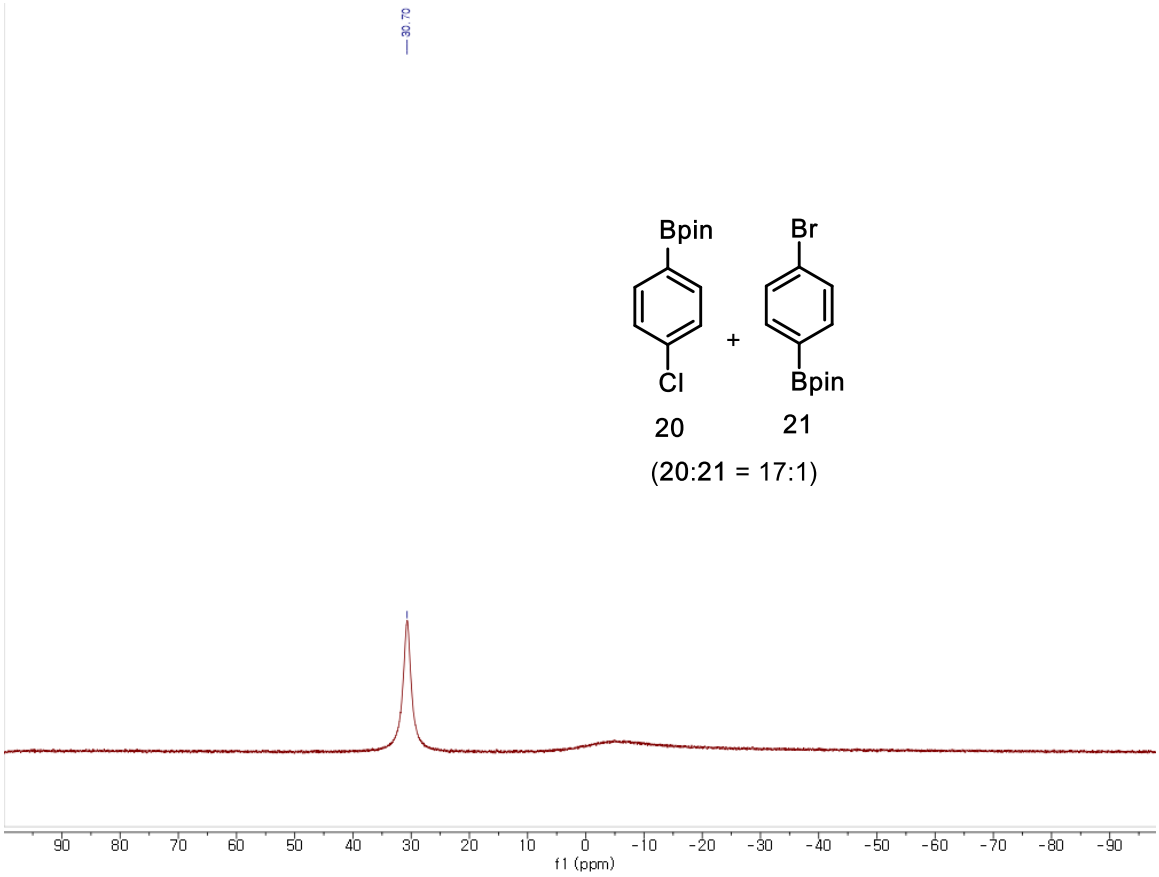
30.70
Bpin
Cl
+
Br
Bpin
20
21
(20:21 = 17:1)
90 80 70 60 50 40 30 20 10 0 -10 -20 -30 -40 -50 -60 -70 -80 -90
f1 (ppm)

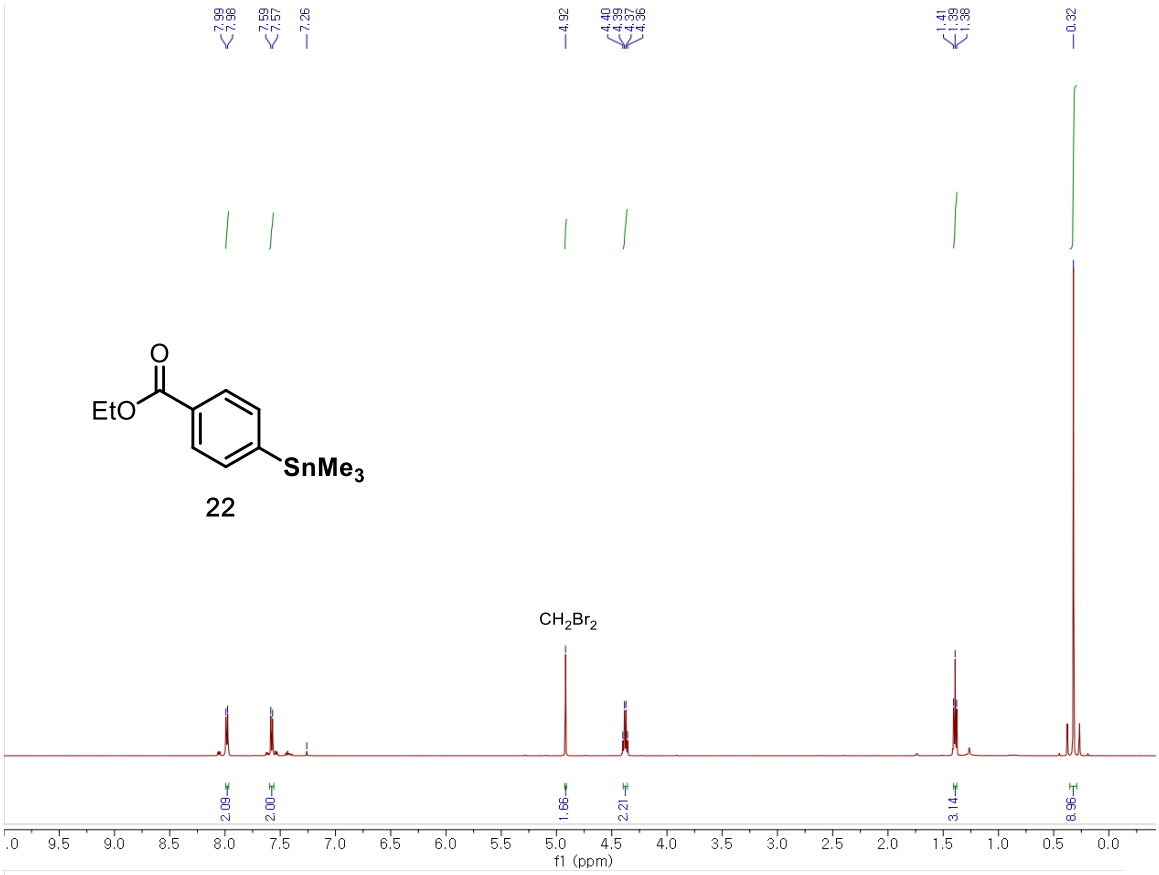
7.99
7.98
7.59
7.57
7.26
4.92
4.40
4.39
4.37
4.36
1.41
1.39
1.38
0.32
EtO
O
SnMe3
22
CH2Br2
2.09
2.00
1.66
2.21
3.14
8.96
f1 (ppm)

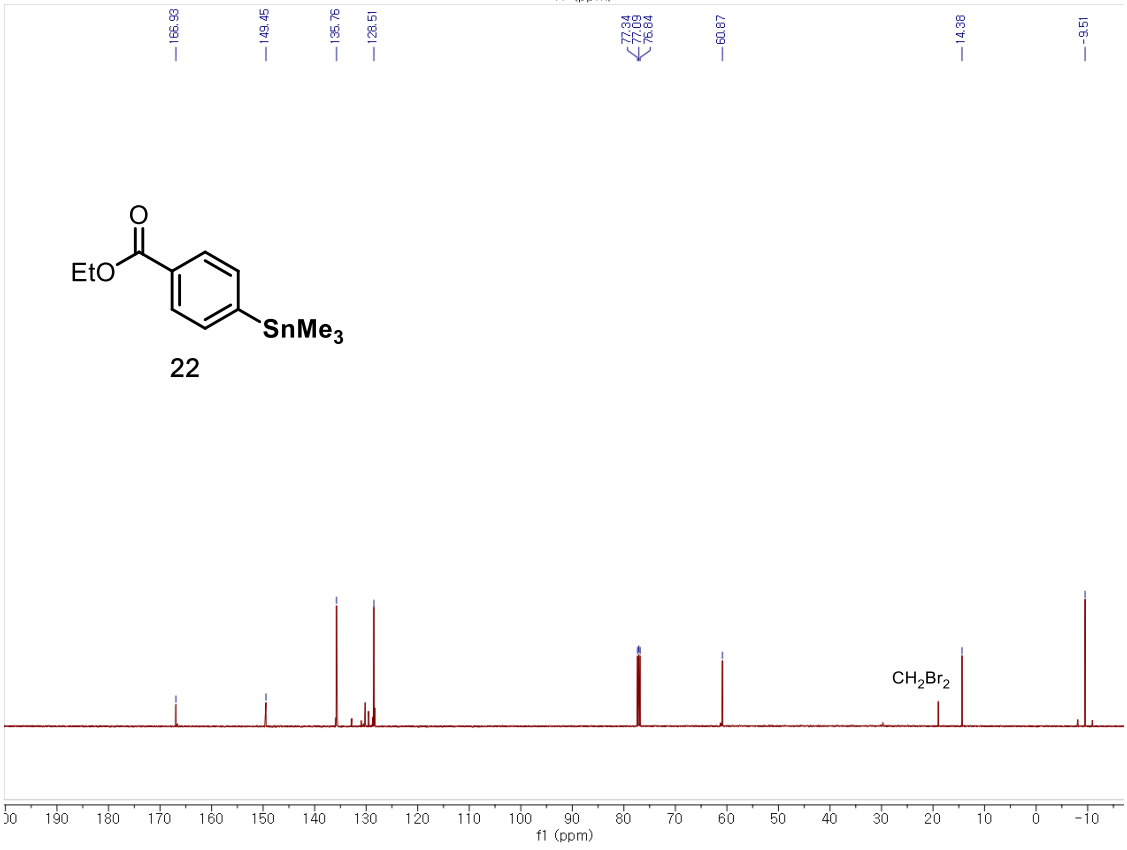
166.93
149.45
135.76
128.51
77.34
77.09
76.84
60.87
14.38
-9.51
EtO
O
SnMe3
22
CH2Br2
f1 (ppm)

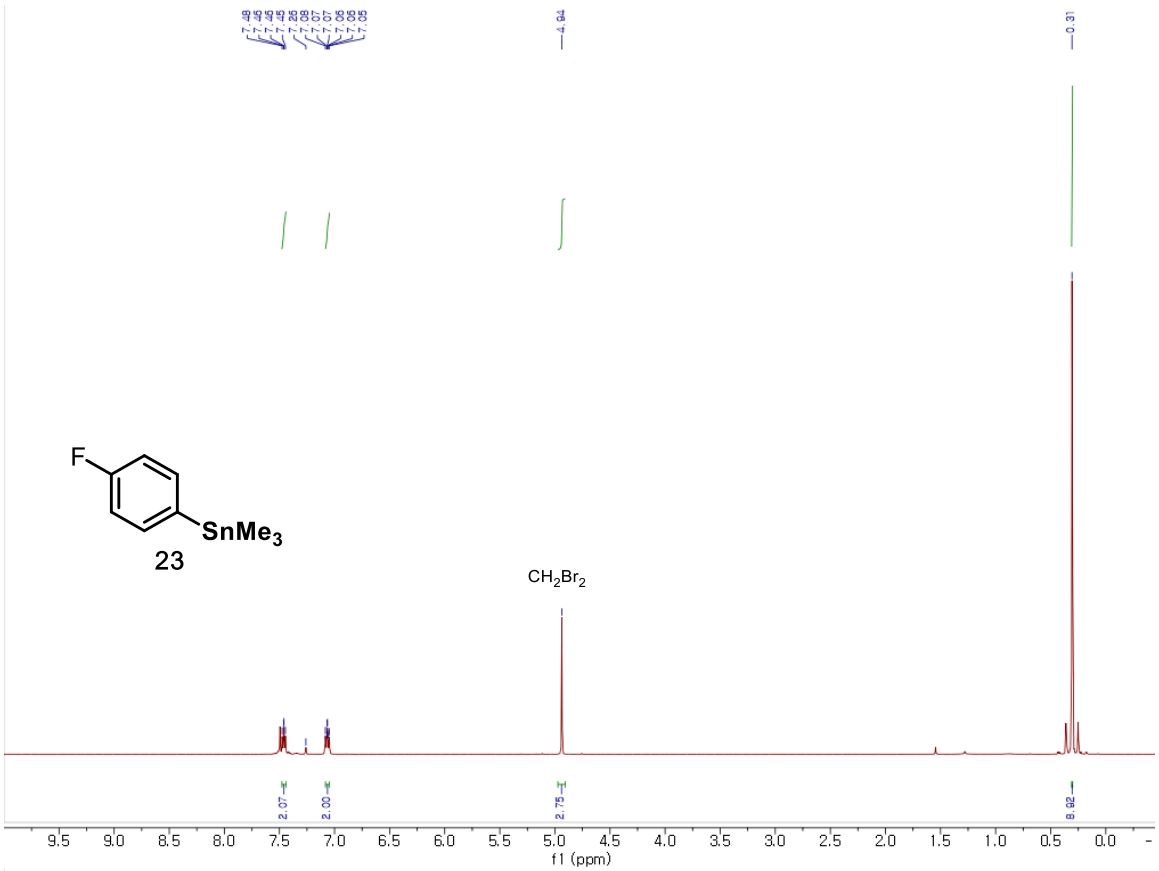
F
SnMe3
23
CH2Br2
f1 (ppm)

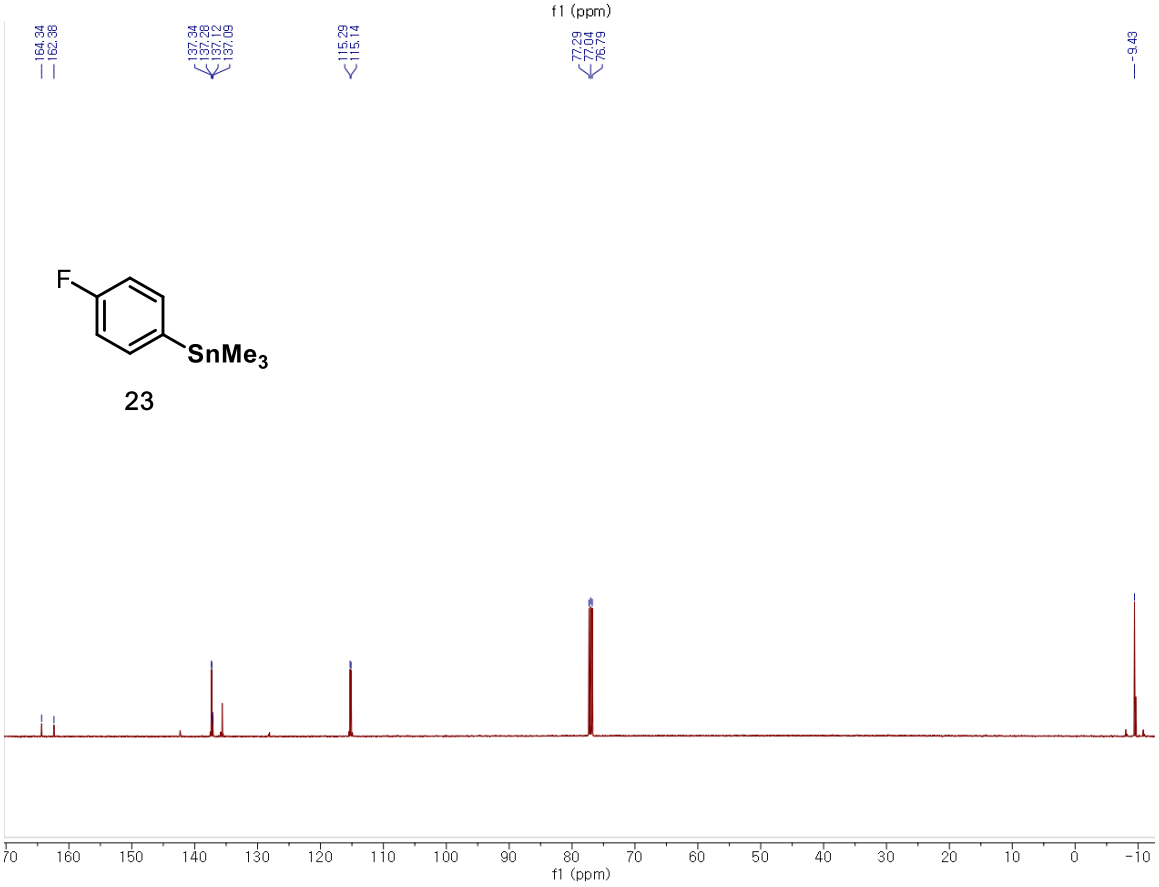
F
SnMe3
23
f1 (ppm)

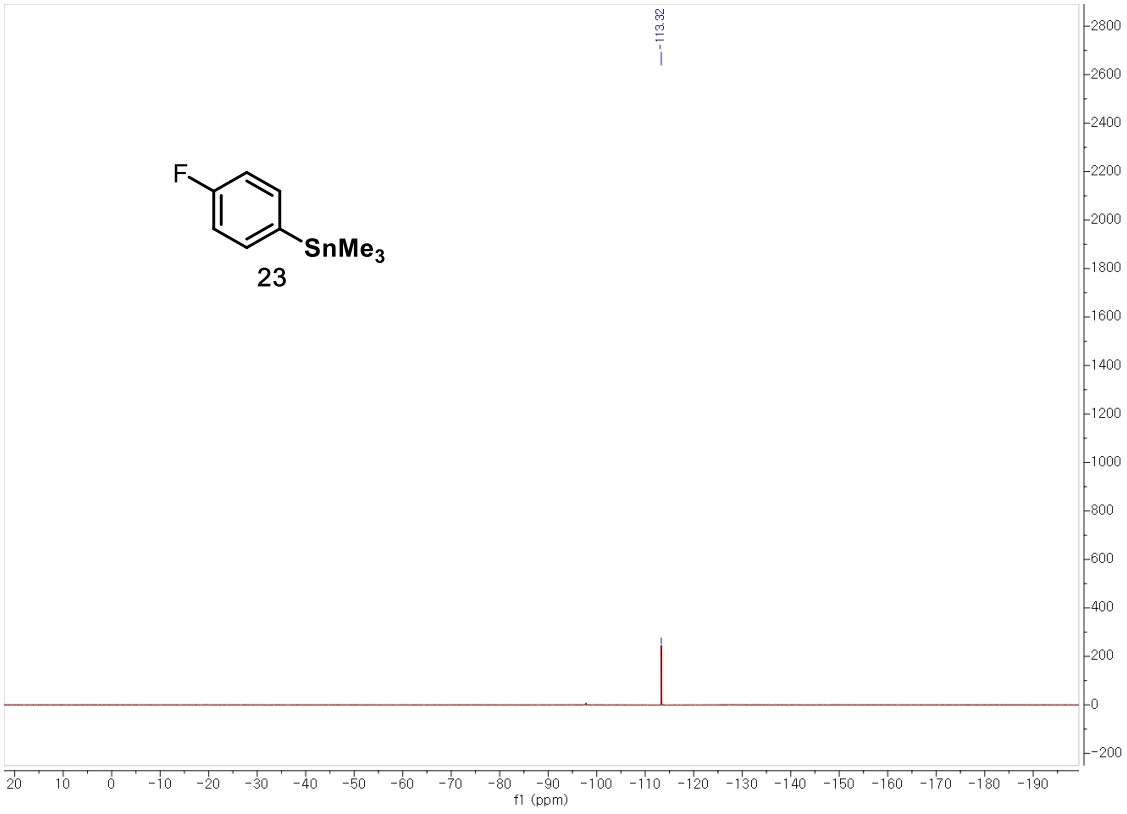
F
SnMe3
23
-113.32
2800
2600
2400
2200
2000
1800
1600
1400
1200
1000
800
600
400
200
0
-200
20 10 0 -10 -20 -30 -40 -50 -60 -70 -80 -90 -100 -110 -120 -130 -140 -150 -160 -170 -180 -190
f1 (ppm)

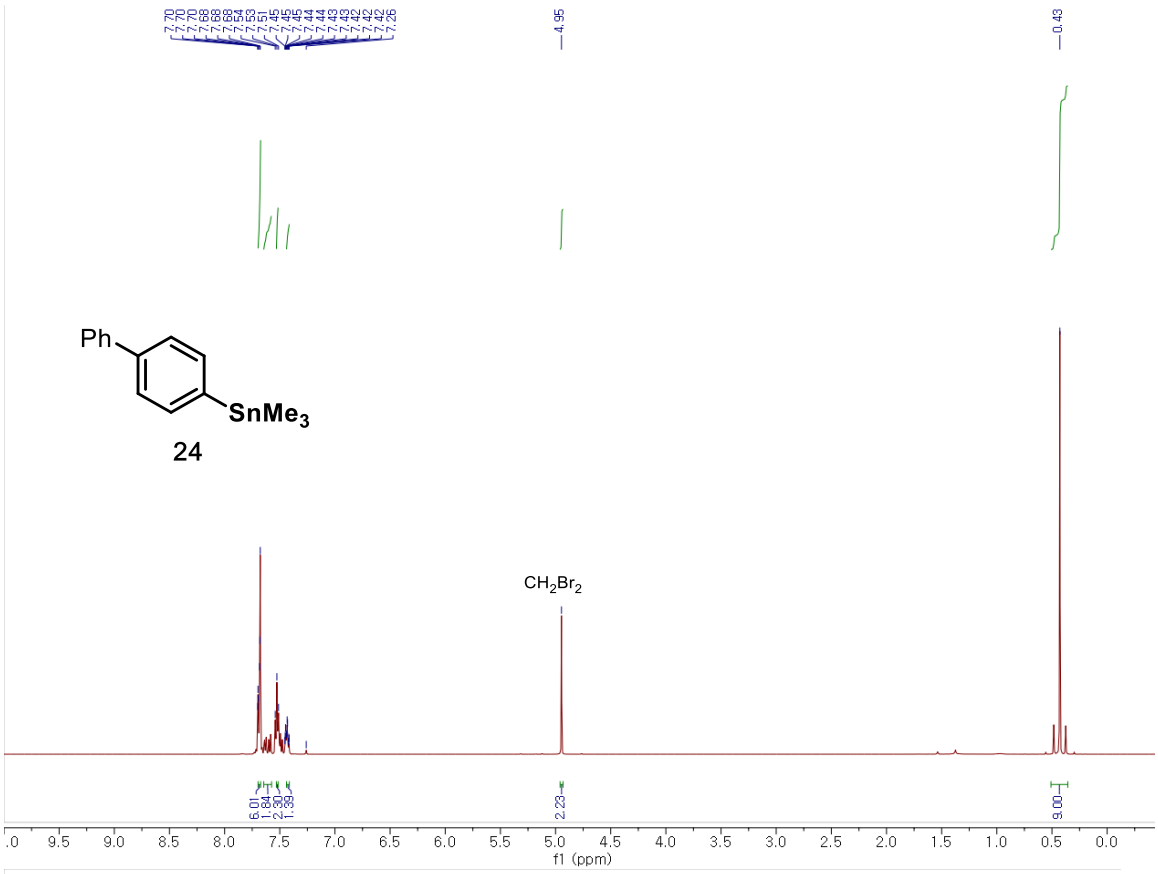
Ph
SnMe3
24
CH2Br2
f1 (ppm)

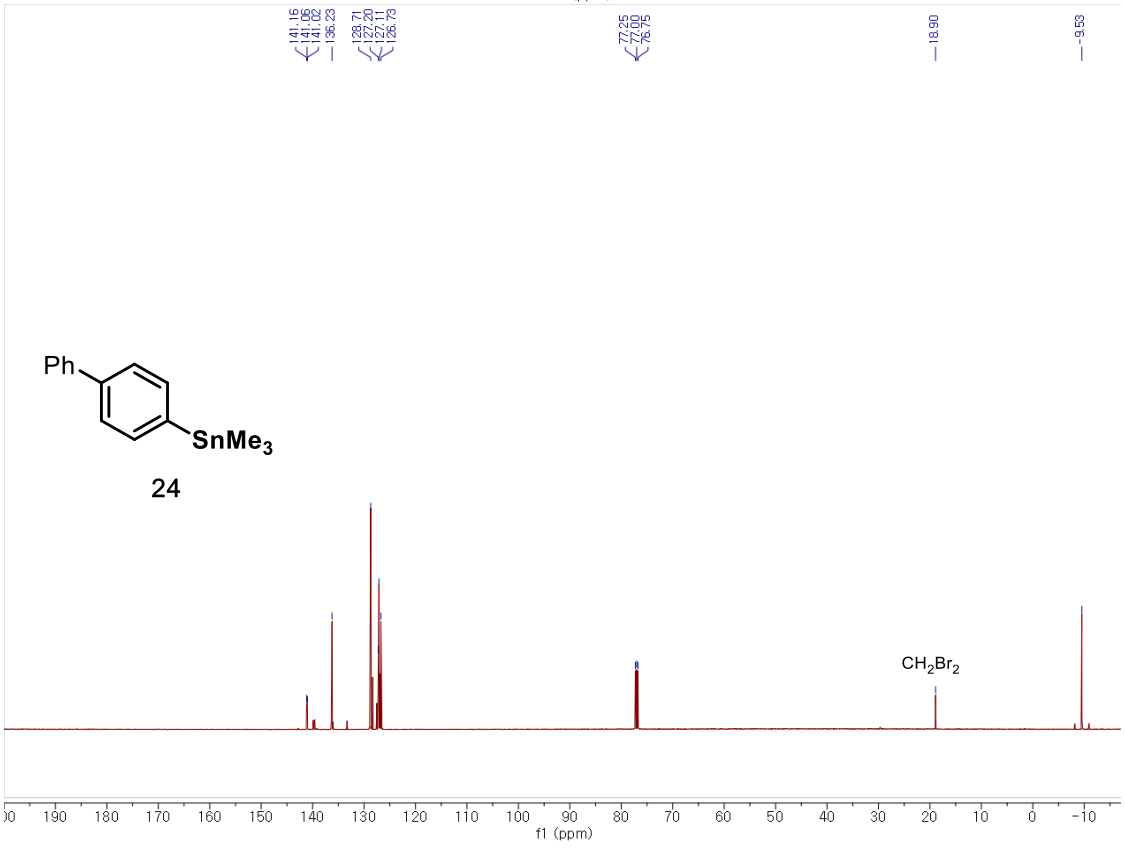
Ph
SnMe3
24
CH2Br2
f1 (ppm)

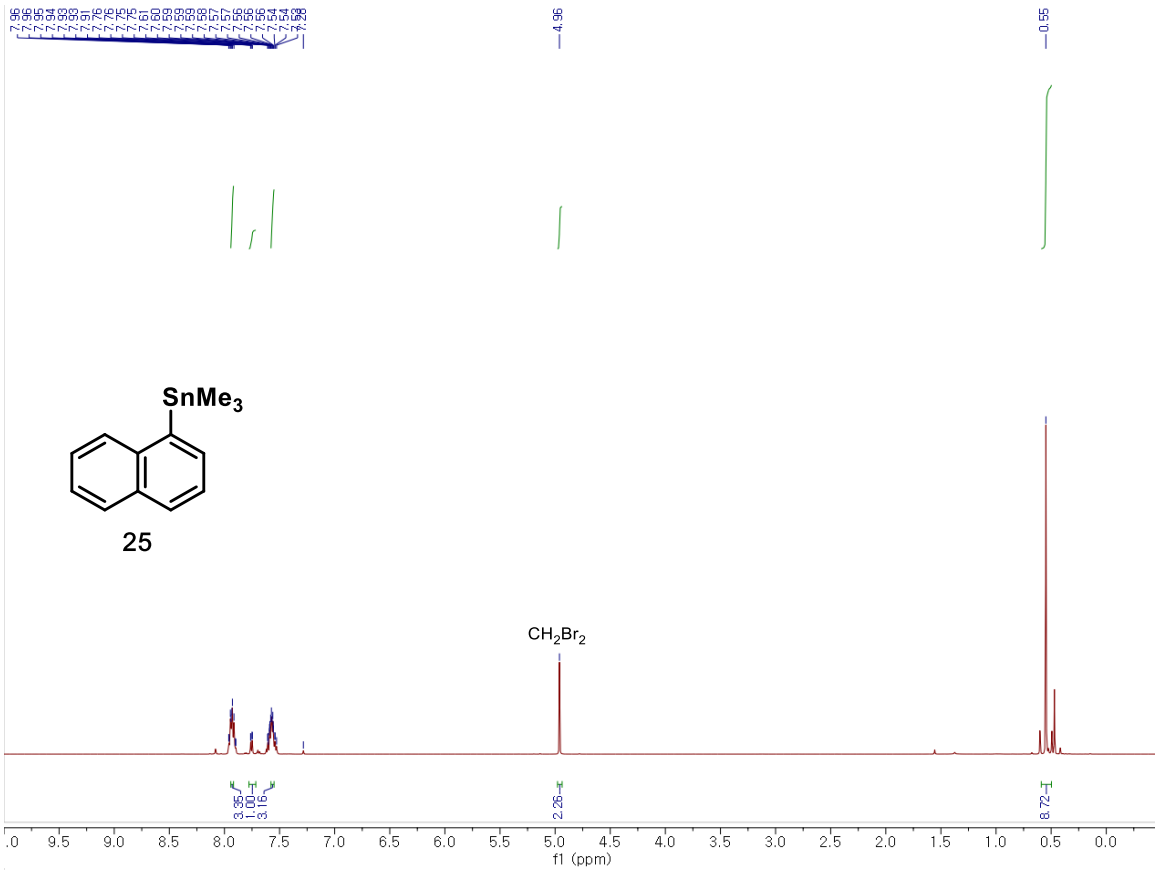
SnMe3
25
CH2Br2
f1 (ppm)

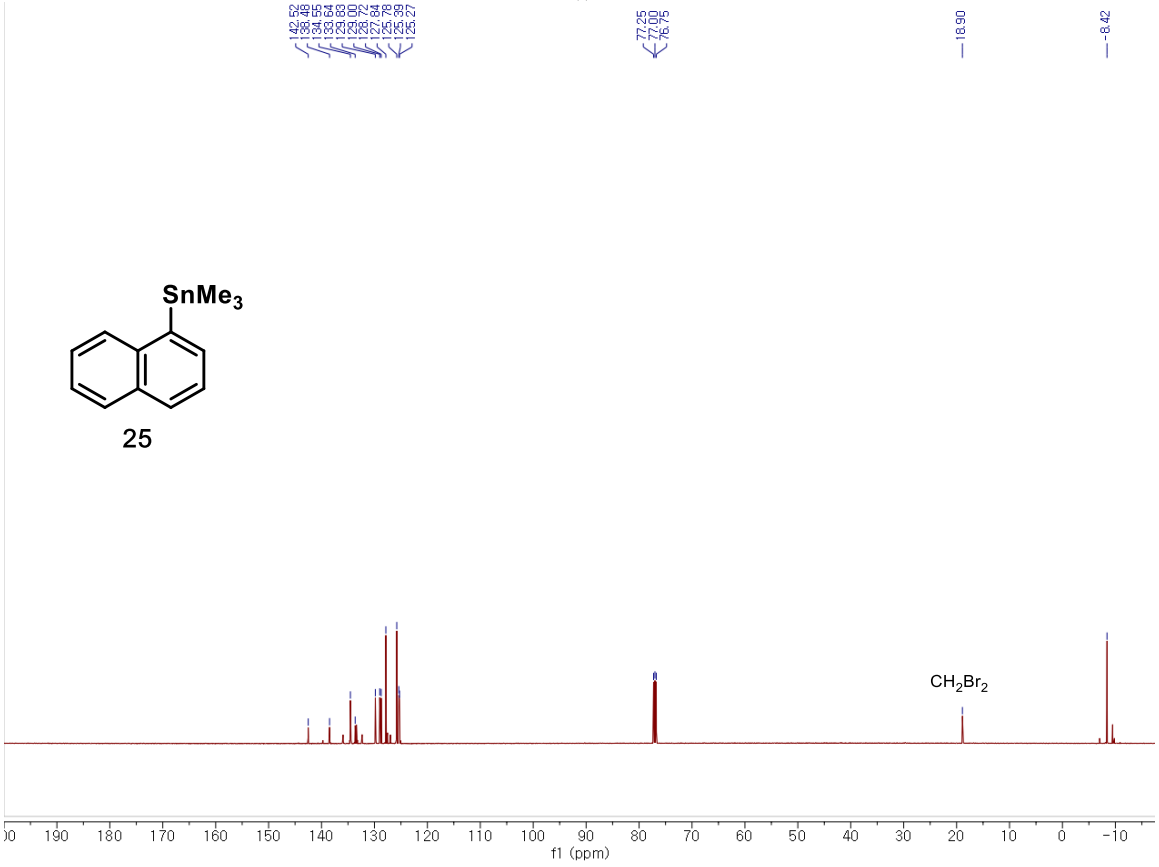
SnMe3
25
CH2Br2
f1 (ppm)

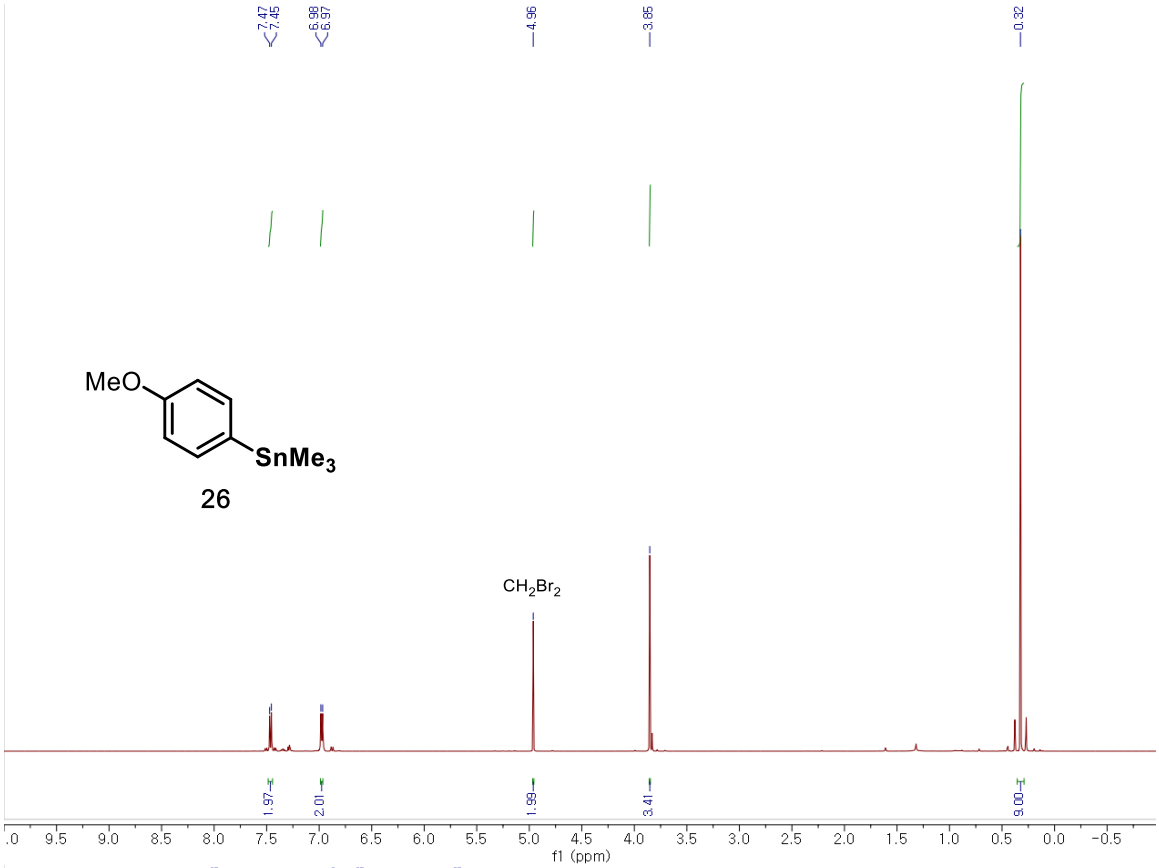
7.47
7.45
6.98
6.97
4.96
3.85
0.32
MeO
SnMe3
26
CH2Br2
1.97
2.01
1.99
3.41
9.00
f1 (ppm)

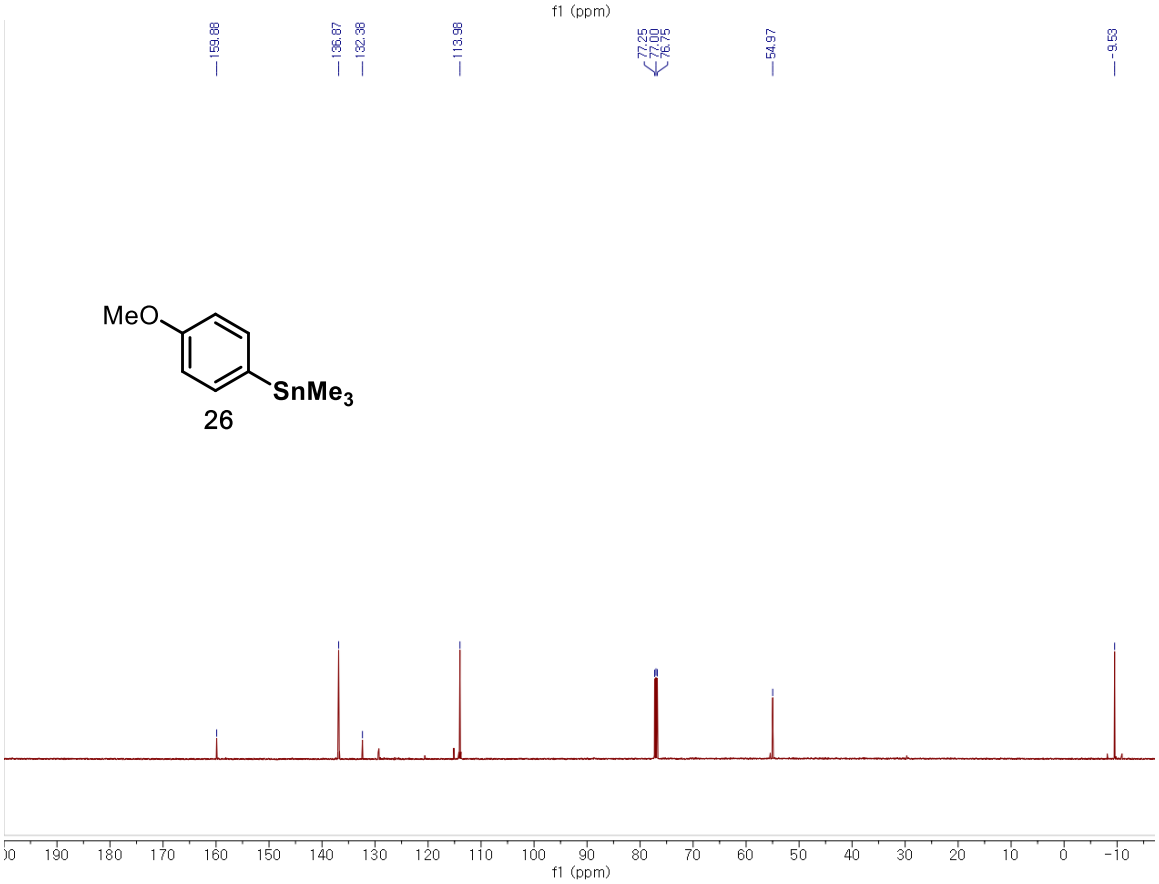
159.88
136.87
132.38
113.98
77.25
77.00
76.75
54.97
-9.53
MeO
SnMe3
26
f1 (ppm)

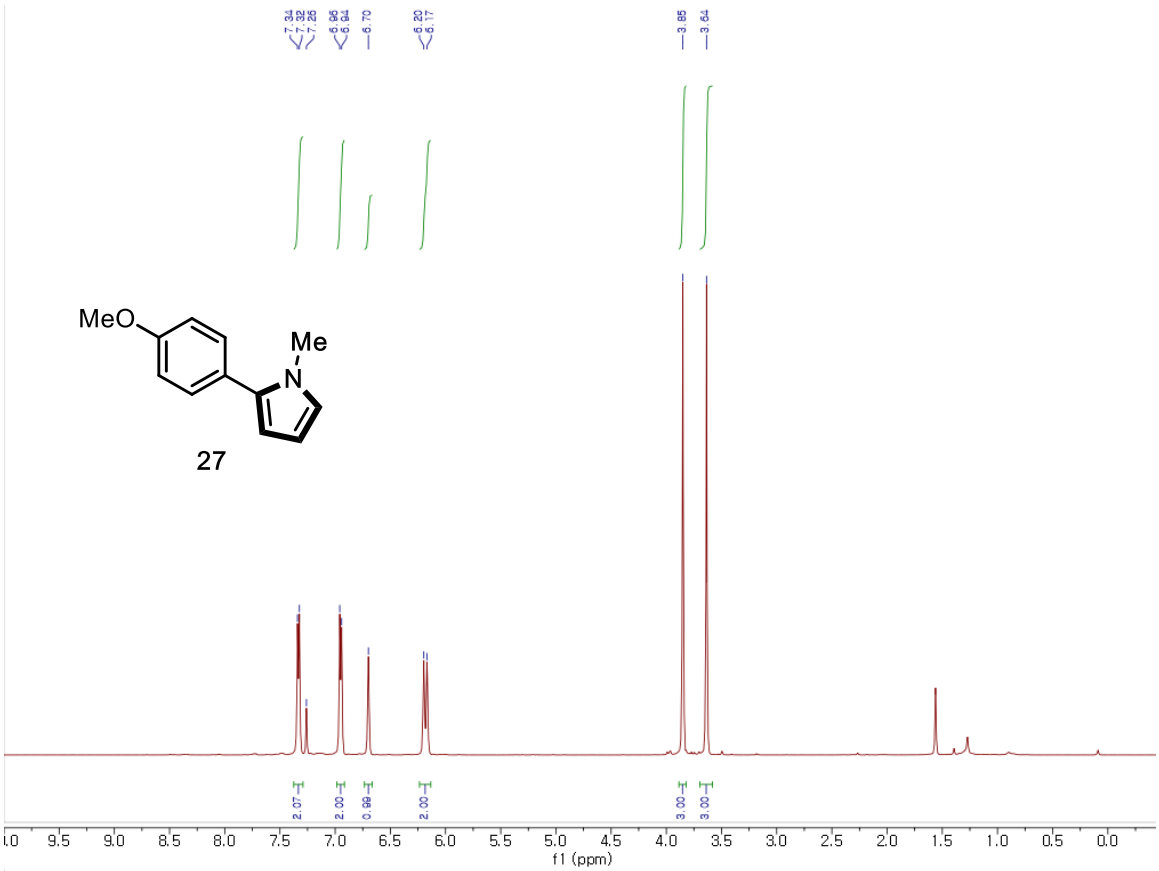
MeO
Me
N
27
f1 (ppm)

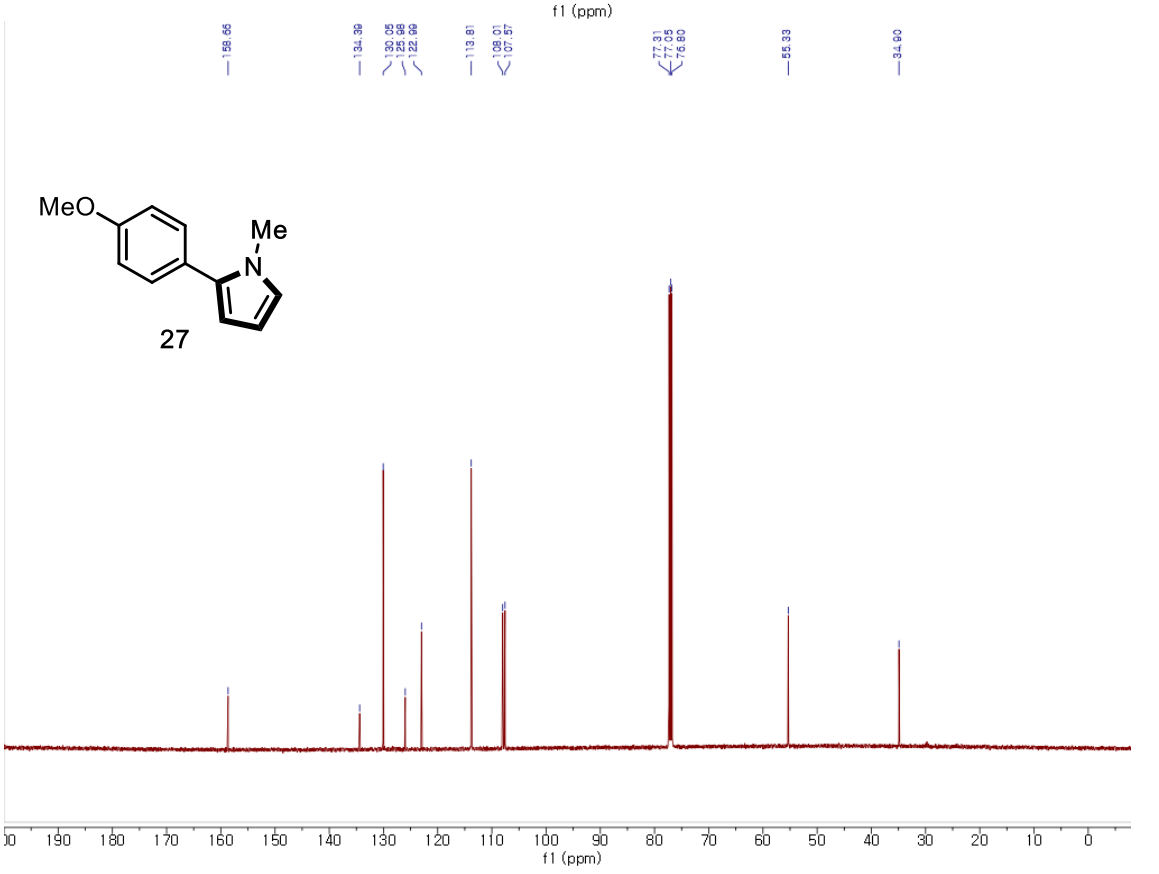
MeO
Me
N
27
f1 (ppm)

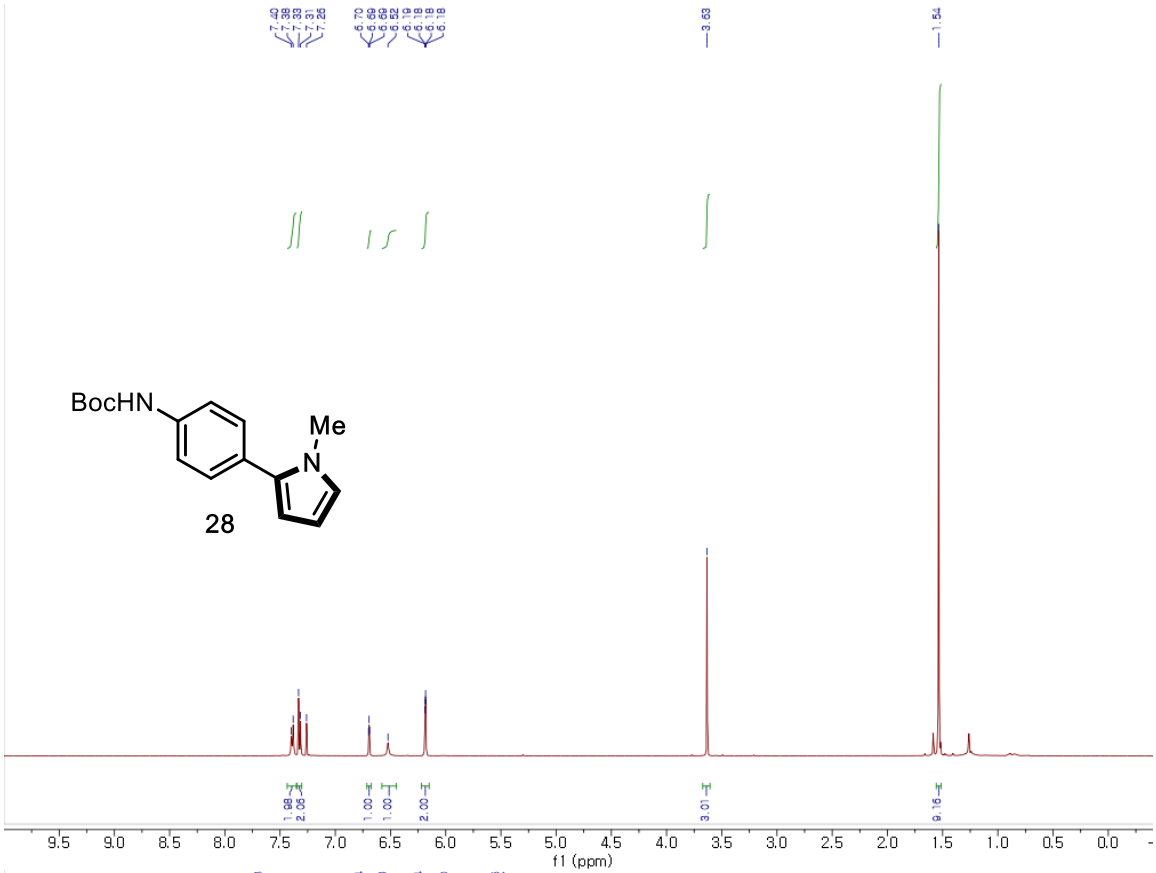
BocHN
Me
N
28
f1 (ppm)

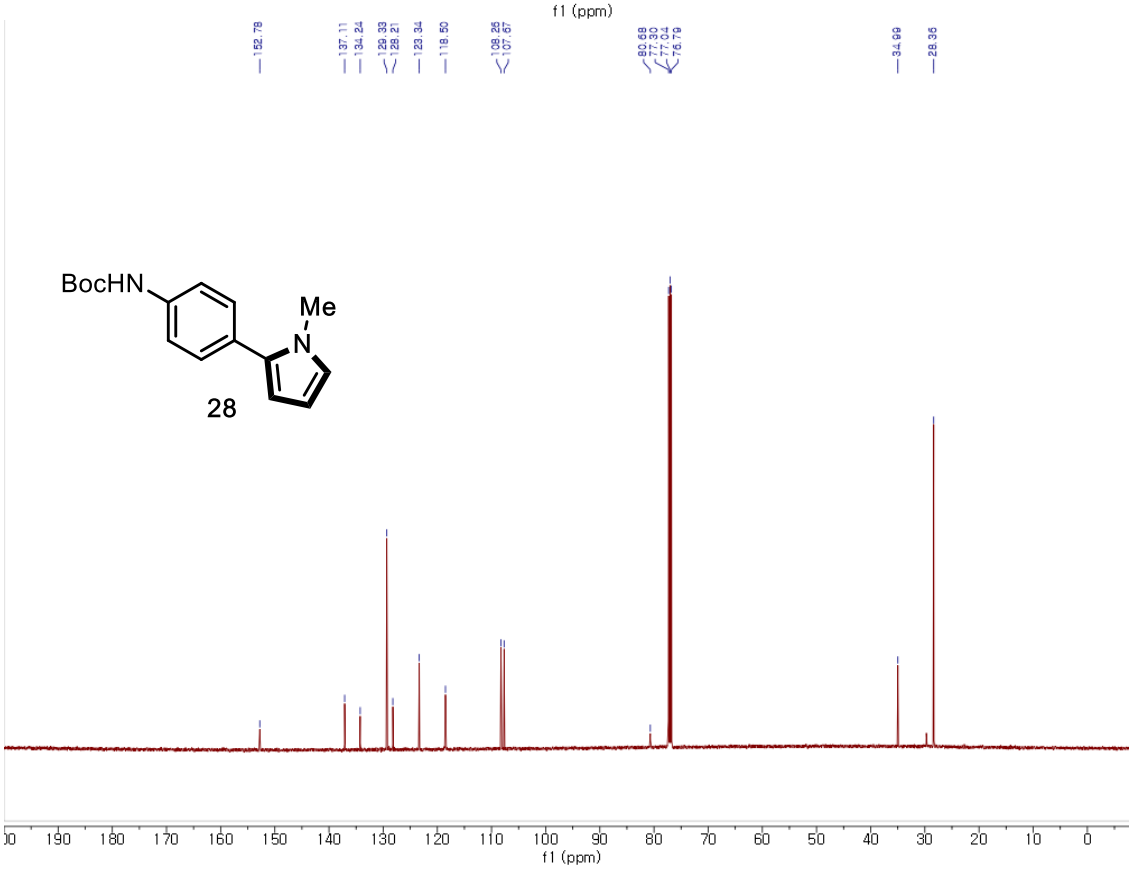
BocHN
Me
N
28
f1 (ppm)

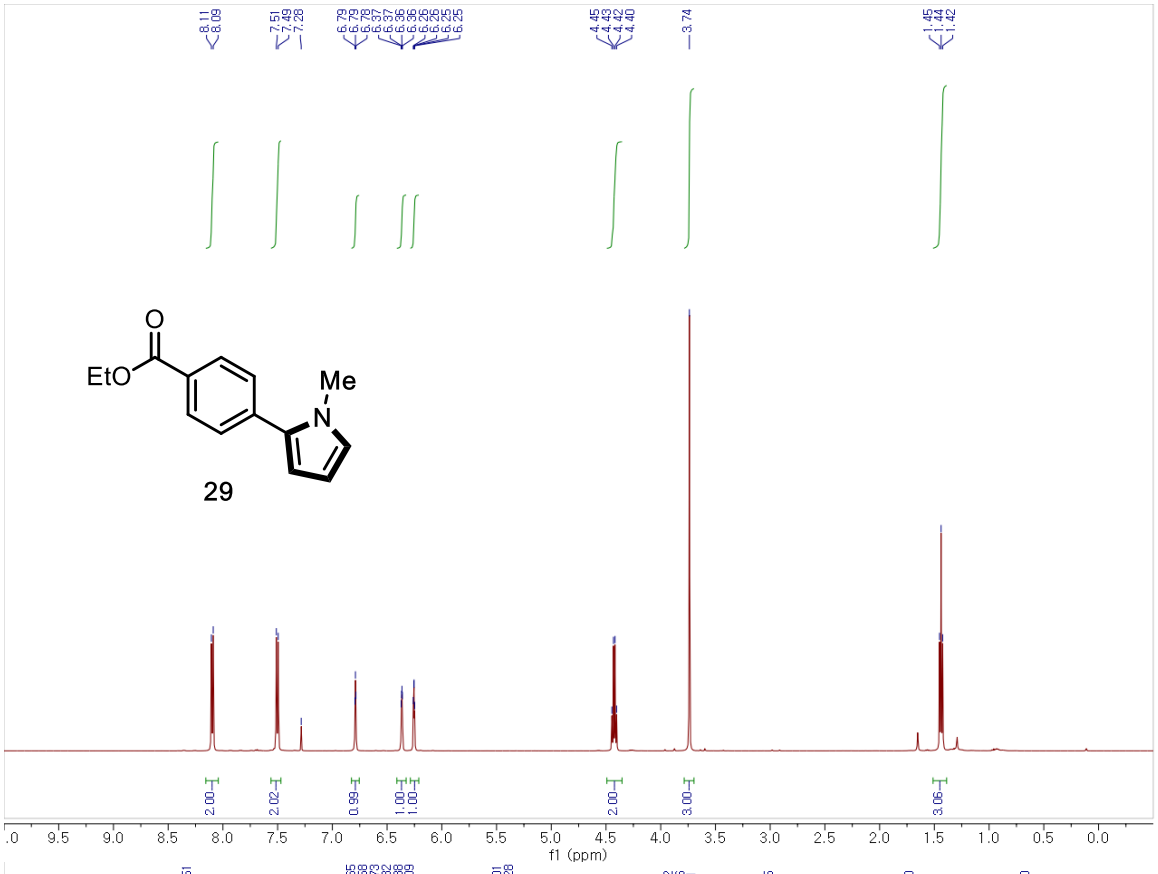
8.11
8.09
7.51
7.49
7.28
6.79
6.79
6.78
6.37
6.36
6.36
6.26
6.26
6.25
6.25
4.45
4.43
4.42
4.40
3.74
1.45
1.44
1.42
O
EtO
Me
N
29
2.00
2.02
0.99
1.00
1.00
2.00
3.00
3.06
f1 (ppm)

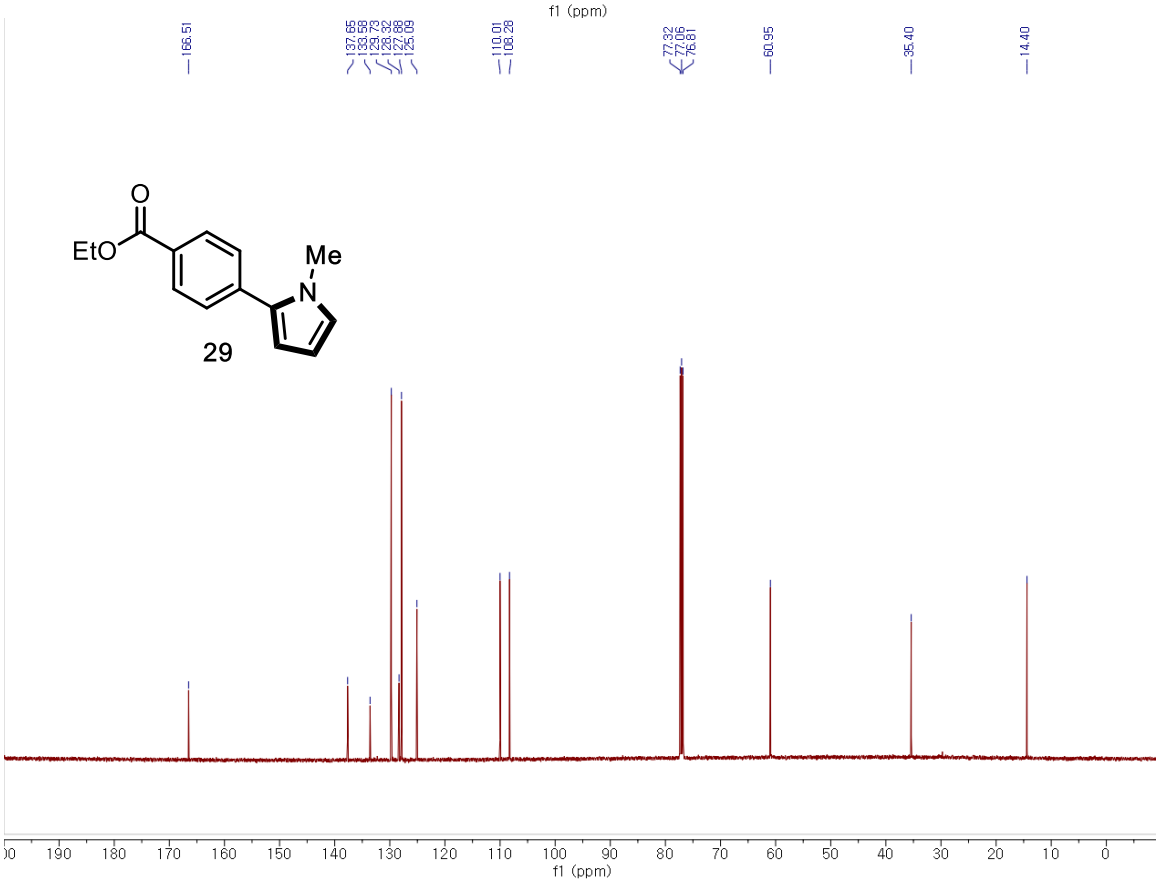
166.51
137.65
130.59
129.73
128.32
127.88
125.09
110.01
108.28
77.32
77.06
76.81
60.95
35.40
14.40
O
EtO
Me
N
29
f1 (ppm)

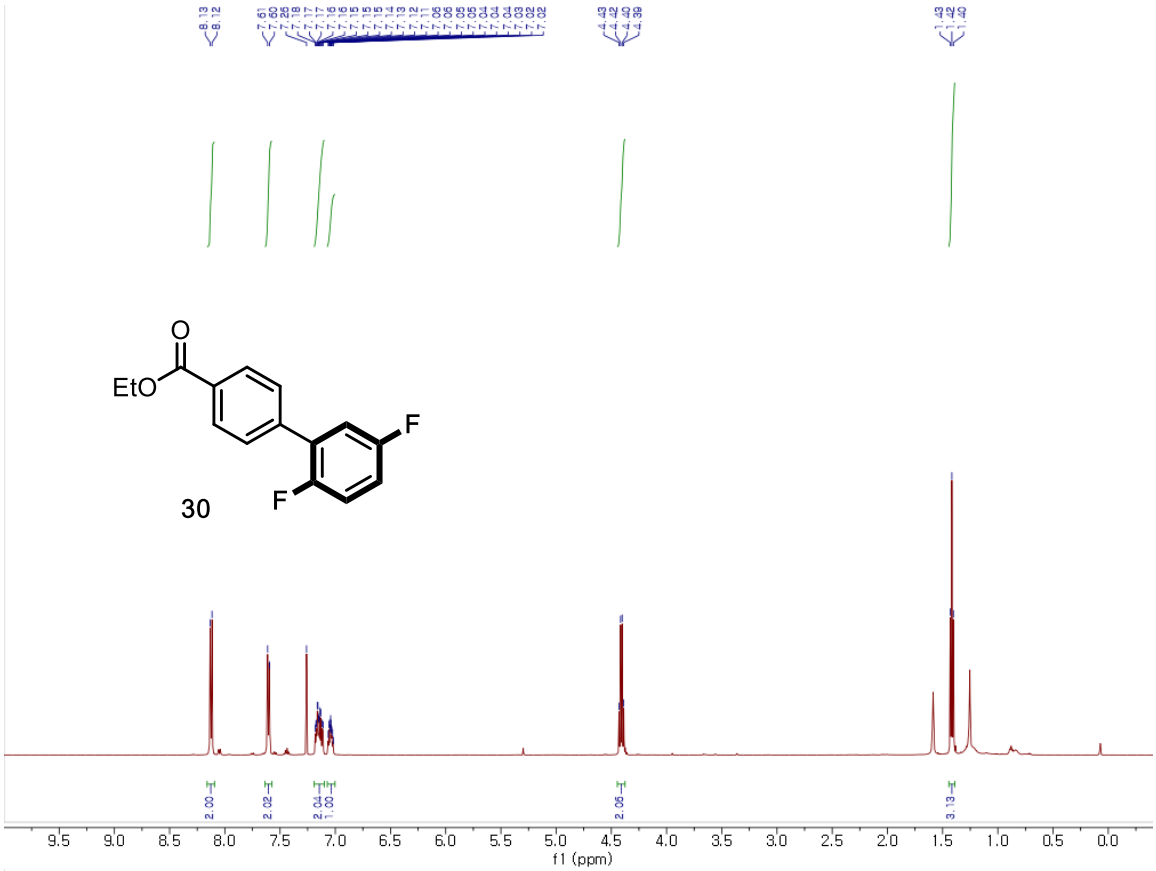
EtO
O
F
F
30
f1 (ppm)

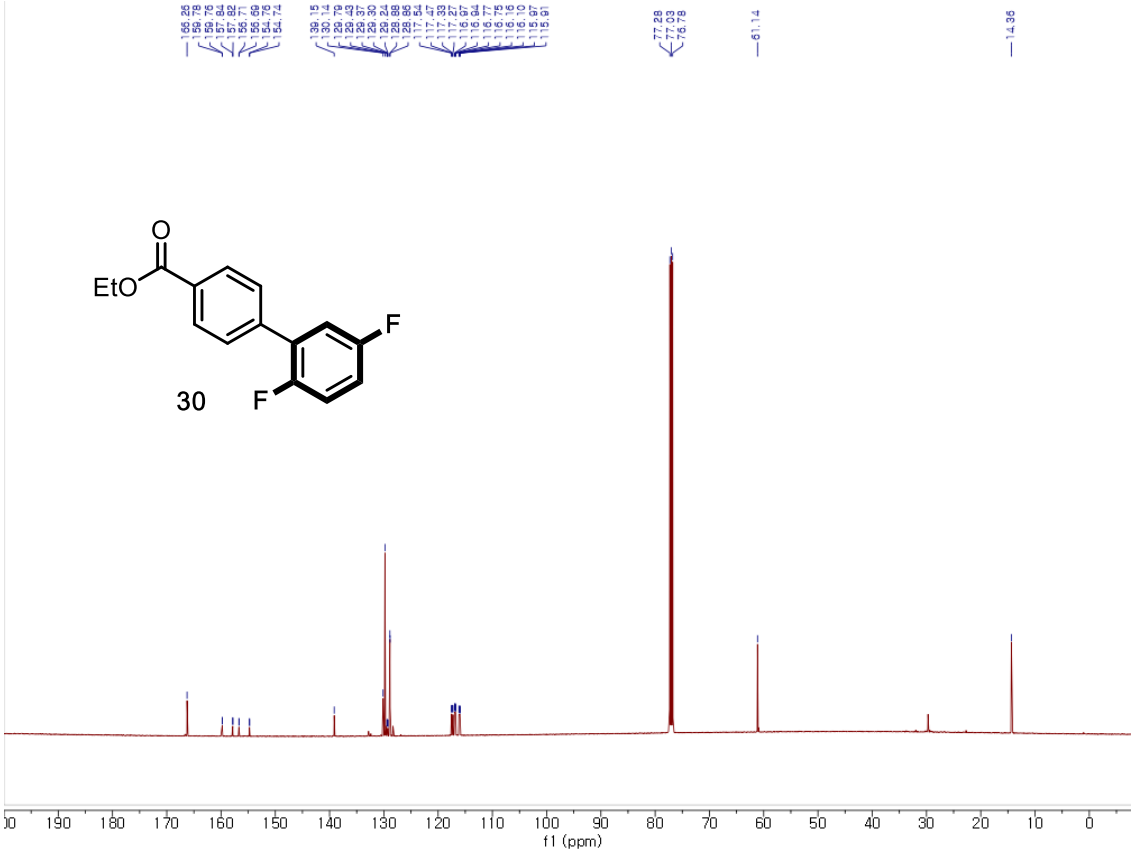
EtO
O
F
F
30
f1 (ppm)

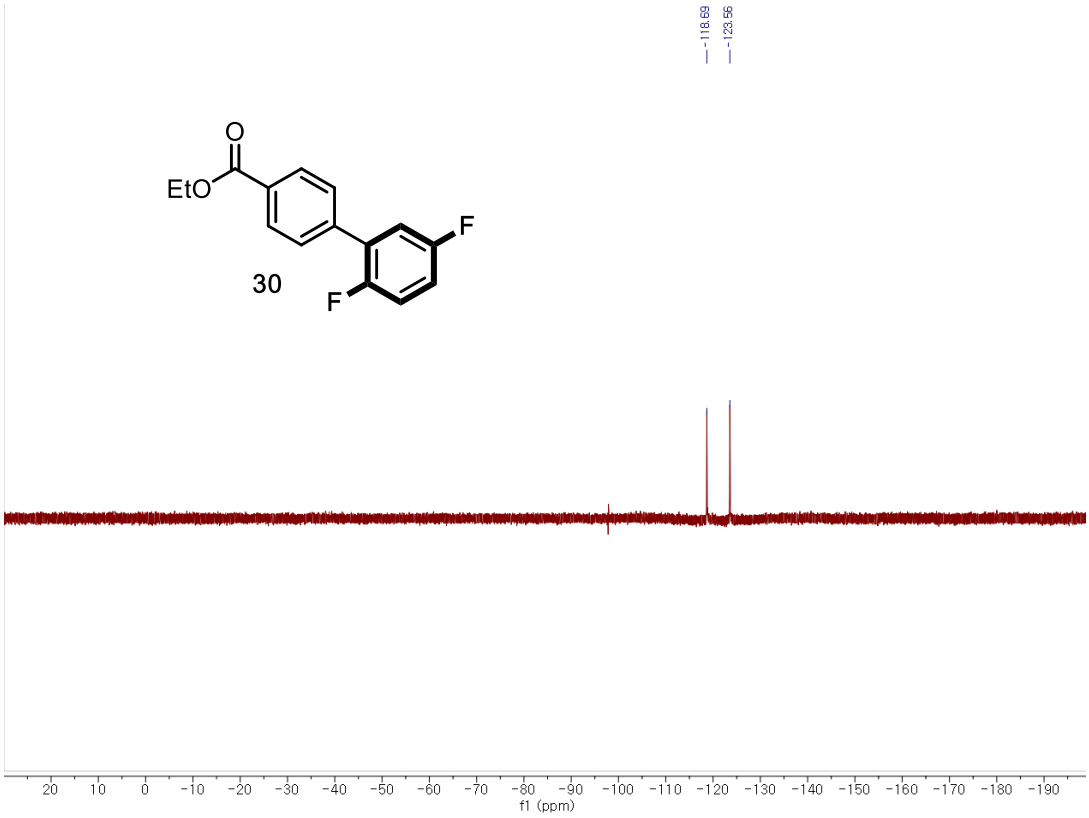
118.69
123.56
O
EtO
F
F
30
20
10
0
-10
-20
-30
-40
-50
-60
-70
-80
-90
-100
-110
-120
-130
-140
-150
-160
-170
-180
-190
f1 (ppm)

Section 7. References

1. Yang, X.-Y.; Zhao, H.-Y.; Mao, S.; Zhang, S.-Q. Copper-Mediated monochlorination of anilines and nitrogen-containing heterocycles. *Synth. Commun.* **2018,** *48*, 2708−2714.

2. Kim, H.; Shin, K.; Chang, S. Iridium-Catalyzed C–H Amination with Anilines at Room Temperature: Compatibility of Iridacycles with External Oxidants. *J. Am. Chem. Soc.* **2014,** *136*, 5904−5907.

3. Painter, T. O.; Wang, L.; Majumder, S.; Xie, X.-Q.; Brummond, K. M. Diverging DOS Strategy Using an Allene-Containing Tryptophan Scaffold and a Library Design that Maximizes Biologically Relevant Chemical Space While Minimizing the Number of Compounds. *ACS Comb. Sci.* **2011,** *13*, 166−174.

4. Svejstrup, T. D.; Ruffoni, A.; Juliá, F.; Aubert, V. M.; Leonori, D. Synthesis of Arylamines via Aminium Radicals. *Angew. Chem. Int. Ed.* **2017,** *56*, 14948−14952.

5. Eriksen, J.; Lund, H.; Nyvad. A. I. Electron-Transfer Fluorescence Quenching of Radical Ions. *Acta Chem. Scand. B.* **1983**, *37*, 459−466.

6. Mo, F.; Jiang, Y.; Qiu, D.; Zhang, Y.; Wang, J. Direct Conversion of Arylamines to Pinacol Boronates: A Metal-Free Borylation Process. *Angew. Chem. Int. Ed.* **2010,** *49*, 1846-1849.

7. Chen, K.; He, P.; Zhang, S.; Li, P. Synthesis of aryl trimethylstannanes from aryl halides: an efficient photochemical method. *Chem. Commun.* **2016,** *52*, 9125−9128.